FUNCTIONAL & STRUCTURAL STUDIES OF STONUSTOXIN (SNTX), A LETHAL FACTOR FROM STONEFISH (*SYNANCEJA HORRIDA*) VENOM

LIEW HUEI CHUN
(*B.Sc. Biomedical Science (Hons)*)

A THESIS SUBMITTED FOR THE DEGREE OF
MASTER OF SCIENCE

Department of Biochemistry
National University of Singapore
2004

ACKNOWLEDGEMENTS

I would like to thank my supervisors, Associate Professor Khoo Hoon Eng and Associate Professor Shabbir Moochhala for their guidance, encouragement and understanding during the course of my project. I am grateful to my supervisors for giving me this precious opportunity to do this project, from which I have furthered my insight as a scientist. In addition, I would also like to show my appreciation to Professor Philip Moore from the Department of Pharmacology for allowing me to use his facilities and for his invaluable tips and advices. I am also thankful to Associate Professor Tan Chee Hong and Foong Har for allowing me to use their equipment and also for their friendship.

To Yin Hoe, Meiling, Kian Chye, Shirhan and Zhongjing, I would like to thank them for imparting to me invaluable techniques and sharing with me insightful knowledge during the period of my studies. To Lili and Julie as well as others in DMERI, I thank you for your invaluable assistance during the course of my work. In addition, I am grateful to my friends Wanping, Yoke Yin and Hui Voon for their encouragements.

Importantly, I would also like to thank Defence Science & Technology Agency for the award of the project grant to oversee the experiments.

Lastly, I would like to thank my parents and brothers for their love and support.

TABLE OF CONTENTS

CONTENTS **PAGE**

SUMMARY

Stonustoxin (*Sto*nefish *N*ational *U*niversity of *S*ingapore, SNTX) is a 148kDa, dimeric lethal factor isolated from stonefish *Synanceja horrida* venom that exhibits a multitude of activity including species-specific haemolysis and platelet aggregation, edema-induction, hypotension, endothelium-dependent vasorelaxation, and inhibition of neuromuscular function in the mouse hemidiaphragm and chick biventer cervicis muscle (Low *et al*., 1993; Khoo *et al*., 1995; Chen *et al*., 1997; Sung *et al*., 2002). In this thesis, the potent vasorelaxing effect of SNTX that leads to marked hypotension and death in victims was investigated.

SNTX was purified according to the method of Poh *et al*., 1991 with a change in the column size and flow-rate used for the anion-exchange chromatography part of the purification process that led to a decrease in purification time. Organ bath studies with 2mm, endothelium-intact, precontracted rat thoracic aortic rings showed that SNTX (10-640ng/ml) progressively causes vasorelaxation that was inhibited by L-N^G-nitro arginine methyl ester (L-NAME). This confirmed findings by Low *et al*., 1993 and Sung *et al*., 2002 that nitric oxide (NO) is a gaseous mediator of SNTX-induced vasorelaxation.

The involvement of hydrogen sulfide (H_2S) working in synergy with NO in SNTX-induced vasorelaxation was examined. H_2S, a well known toxic gas associated with many industrial fatalities (Burnett *et al*., 1977; Guidotti, 1994; Sydner *et al*., 1995) was found to be an endogenously generated smooth muscle relaxant that may work in synergy with

NO (Hosoki *et al*., 1997). Since SNTX causes vasorelaxation, H_2S could possibly be a mediator of SNTX's effect. Using D, L-proparglyglycine (PAG) and β-cyano-L-alanine (BCA), both inhibitors of cystathionine-γ-lyase (CSE) which is the main enzyme responsible for H_2S production in the vascular system showed that H_2S has a role in SNTX-induced vasorelaxation of precontracted aortic rings. Use of L-NAME in conjuction with PAG or BCA showed a greater inhibitory effect than when each inhibitor was used individually thus suggesting that H_2S may possibly work synergistically with NO to bring about SNTX-induced vasorelaxation. To date, this is the first report on the involvement of H_2S working together with NO to mediate a toxin's biological effect. Interestingly, as an attempt to reverse the inhibitory effect of PAG or BCA on SNTX-induced vasorelaxation, an unexpected transient increase in tone of resting rat thoracic aortic rings was observed with 1mM L-cysteine.

The role of the SNTX B30.2 domains in SNTX-induced vasorelaxation was also investigated. SNTX shows no significant homology to other proteins except that it possesses a novel B30.2 domain in each of its subunit that is present in a rapidly growing family of proteins with diverse functions and cellular locations (Henry *et al*., 1998). Currently, little is known about the structure and function of this domain. Expression and purification of recombinant Glutathione-S-transferase fusion proteins from *E. coli* BL21 was met with co-expression of chaperonin GroEL and aggregation of fusion proteins as inclusion bodies. In future, more work can be done to improve protein yields and purity in addition to screening the B30.2 domains for other biological functions that SNTX possesses.

LIST OF FIGURES & TABLES

ABBREVIATIONS AND SYMBOLS USED

Ach	Acetylcholine chloride
AFP	Acid finger protein
AMT-HCl	2-amino-5,6-dihydro-6-methyl-4H-1,3-thiazine
ATP	Adenosine triphosphate
BoNT	Botulinum toxin
BTN	Bovine butyrophilin
cGMP	Cyclic guanylyl monophosphate
CBS	cystathionine β-synthase
CSE	cystathionine γ-lyase
COMT	Catechol-O-methyltransferase
efp	Estrogen finger protein
FPLC	Fast Performance Liquid Chromatography
GST	Glutathionse-S-transferase
GST-αB30.2	Fusion protein of GST with the B30.2 domain of SNTX-α
GST-βB30.2	Fusion protein of GST with the B30.2 domain of SNTX-β
H_2S	Hydrogen sulfide
IPTG	Isopropyl-β-D-thiogalactopyranoside
iNOS	Inducible nitric oxide synthase
LD_{50}	Lethal dose 50
L-NAME	L-NG-nitro arginine methyl ester
NA	Noradrenaline

NATB	N-acetyl-L-tryptophan-3, 5-bis (trifluromethyl)-benzyl ester
NO	Nitric oxide
PBS	Phosphate buffered saline
PE	L-phenylephrine hydrochloride
PVDF	Polyvinylidene difluoride
PwA33	Pleurodeles waltl
RFB30	RING finger B30 protein
rfp	Ret finger protein
SDS	Sodium dodecyl sulfate
SNTX	Stonustoxin
SP	Substance P
SSA/Ro	Sjogren's syndrome nuclear antigen A/Ro
Staf50	Transcription regulator Staf-50 protein
SNAP	Synaptosomal-associated protein
TEA	Tetraethylammonium chloride
xnf7	Xenopus nuclear factor 7
XO	Xanthine oxidase
SNTX-α	Stonustoxin alpha subunit
SNTX-β	Stonustoxin beta subunit

CHAPTER ONE

INTRODUCTION

1.1 GENERAL INTRODUCTION

Different life forms on this earth are constantly evolving to enhance their survival. From bacteria and flagellates to plants and animals in vastly different habitats, many have developed specialized structures that produce venoms and toxins that function as defensive and/or offensive tools against predators and preys (Figure 1). These chemical tools are highly effective, i.e. in the pharmacological sense; they possess very rapid, potent and specific mechanisms of action. Throughout history, fatalities associated with such poisonings have created an interest in toxin research. Scientists hoped that by finding out the mechanisms of action of toxins, they will be able to elucidate a cure for poisonings and envenomations. In the process, it was discovered that toxins can also be useful in therapeutics and scientific research (Table 1). Botulinum toxin has been used clinically for cosmetic purposes to reduce wrinkles. In addition, cholera toxin has also been useful in the understanding of the mechanism of adenylate cyclase activation and the role of cyclic AMP as a second messenger.

Figure 1. Pictures of poisonous and venomous organisms. (a) Rattlesnake, (b) Platypus, (c) Honey bee, (d) Tarantula, (e) Poison dart frog, (f) Box jellyfish, (g) Puffer fish, (h) Foxglove

(a) 

(b) 

(c) 

(d) 

(e) 

(f) 

(g) 

(h) 

Table 1. Toxins from various organisms - Mechanisms of actions and therapeutic and scientific uses.

Organism	**Habitat**	**Mode of Transmission**	**Toxin**	**Clinical Manifestations**	**Pharmacological Action**	**Therapeutics / Tools for Scientific Research**	**References**
Clostridium botulinum	Soil and marine sediments	Consumption of contaminated food and infection of wound by spores and bacteria	Botulinum toxin, BoNT/A-G	Botulism	Toxin produced by bacteria binds to receptors on presynaptic membrane of motor neurons associated with peripheral nervous system. Proteolysis of target proteins in these neurons inhibits the release of acetylcholine, thereby preventing muscle contraction. BoNT/A and E target synaptosomal-associated protein SNAP-25. BoNTs/B, D, F, and G cleave vesicle associated membrane protein and synaptobrevin. BoNT/C hydrolyzes syntaxin and SNAP-25.	BoNT/A – Used for Blepharospams, Strabismus and also cosmetically to reduce deep wrinkles caused by contraction of facial muscles.	Singh *et al*., 1995; Schiavo *et al*., 1997; Kessler and Benecke, 1997; Halpern and Neale, 1995; Arnon, 1997; Wheeler, 1997; Averbuch-Heller and Leigh, 1997; Carter and Seiff, 1997.
Vibrio cholerae	Salt water habitats	Consumption of sewage contaminated water and food.	Cholera Toxin	Cholera	Bacteria multiplies in intestinal epithelial cells and produces an enterotoxin that binds irreversibly to epithelial cells, thereby stimulating the production of cyclic AMP which changes cell permeability, leading to the secretion of water and electrolytes into the intestinal lumen.	Incorporated into human vaccines because of its adjuvant properties. Used for understanding mechanism of adenylate cyclase activation and the role of cyclic AMP as a second messenger.	Harnett, 1994; Bokoch, 1983; Neer, 1995; Snider, 1995; Holmgren, 1993
Castor Bean plant	Tropical forests of Africa	Oral	Ricin	Diarrhoea	Ricin binds specifically to cell surface galactosides of the intestinal wall. It then enters the cytosol and inhibits protein sythesis by specifically and irreversibly inactivating eukaryotic ribosomes.	Part of the Ricin protein is used in the production of RTA-immunotoxins. In bone marrow transplant procedures, RTA-	Frankel, 1993; Knight, 1979; Robertus, 1991; Vitetta and Thorpe,

					Digestive distress occurs as a result.	immunotoxins was used successfully to destroy T lymphocytes in bone marrow taken from histocompatible donors. This reduces rejection of the donor bone marrow, a problem called "graft-vs-host disease" (GVHD). In steroid-resistant, acute GVDH situations, RTA-immunotoxins helped alleviate the condition. Also, in autologous bone marrow transplantation, a sample of the patients own bone marrow is treated with anti-T cell immunotoxins to destroy malignant T-cells in T cell leukemias and lymphomas.	1991; Wiley, and Oeltmann, 1991.
Foxglove	Southern Europe and Asia	Oral	Digitoxin	Heart failure on overdose	Digitoxin inhibits Na^+/K^+-ATPase and results in an increase in intracellular Na^+ concentration. This increased Na^+ concentration inhibits the Na^+/Ca^{2+}-exchanger. Inhibiting this exchange system results in less Ca^{2+} being extruded from the cell and, therefore, results in an increased intracellular Ca^{2+} concentration. More Ca^{2+} ions available for the contraction mechanism enables an increased force of contraction	Congestive heart failure, atrial fibrillation, severe heart failure and sinus cardiac rhythm	Braunwaldy, 1985; Hoffman *et al*., 1990; Smith *et al*., 1984

1.2 SYNANCEJA HORRIDA

1.2.1 INTRODUCTION

The stonefish *S. horrida* belongs to the family Scorpaenidae which is comprised of a large array of fish characterized by their ability to envenomate with various types of specialized spines. This group of fish is responsible for the second most common piscine envenomation after stingrays. Included in the family are 3 genera characterized by their venom organ structure and toxicity – *Pterosis* (e.g. lionfish, zebrafish, and butterfly cod), *Scorpaena* (e.g. scorpionfish, bullrout, and sculpin) and *Synanceja* (e.g. stonefish) (Figure 2).

Within the genus *Synanceja*, there are 10 species as recorded in FishBase (http://www.fishbase.org/home.htm), a relational database developed at the WorldFish Center in collaboration with the Food and Agriculture Organization of the United Nations and other partners. These species include *S. horrida*, *S. verrucosa*, *S. platyrhyncha*, *S. alula*, *S. nana*, *S. asteroblepa*, *S. erosa*, *S. uranoscopa*, *Erosa daruma*, and *Pseudosynanceia melanostigma*. Of these species, only *S. horrida* and *S. verrucosa* have been studied. In addition, *S. trachynis* as described by Endean (1961) has an ambiguous identity and is thought by some to be actually *S. horrida*. Studies have also been carried out on *S. trachynis*.

Figure 2. Pictures showing the 3 genera of the Scorpinaedae family. (a) Lionfish (genus *Pterois volitans*) have long, slender spines with small venom glands, and they have the least potent sting of the Scorpaenidae family. (b) Scorpionfish (genus *Scorpaena*) has shorter, thicker spines with larger venom glands than lionfish do, and they have a more potent sting. (c) Stonefish (genus *Synanceia*) have short, stout spines with highly developed venom glands, and they have a potentially fatal sting. In spite of this, they are said to be edible, with tender and tasty flesh.

(a) 

(b) 

(c) 

1.2.2 NATURAL HABITAT

S. horrida is widely distributed in the waters around Singapore, Malaysia, Indonesia, and as far as India and South Africa (Khoo, 2002). It is often found well camouflaged in rock crevices and half buried in sand and mud with only its mouth and eyes fully exposed. The coloring and shape of the stonefish covered by algae make them excellent ambush predators.

1.2.3 STRUCTURAL FEATURES

1.2.3.1 GROSS ANATOMY

Two species of the stonefish *S. horrida* and *S. verrucosa* exist in Australian waters and McKay (1987) has devised a method to distinguish them based on facial features and eye position. A simple identification key is shown in Figure 3 (McKay, 1987; Gwee *et al*., 1994).

The venom apparatus of the *S. horrida* consists of enlarged venom glands that adhere closely to the short, stout and thick 13 dorsal spines, 2 pelvic and 3 anal spines (Gopalakrishnakone and Gwee, 1993; Gwee *et al*., 1994; Low, 1995) (Figure 4). A loose integumentary sheath that covers each dorsal spine is pushed down during envenomation to compress upon the venom glands such that venom is involuntarily

Figure 3. Identification key for *S. horrida* and *S. verrucosa* differentiation (adapted from Gwee *et al*., 1994).

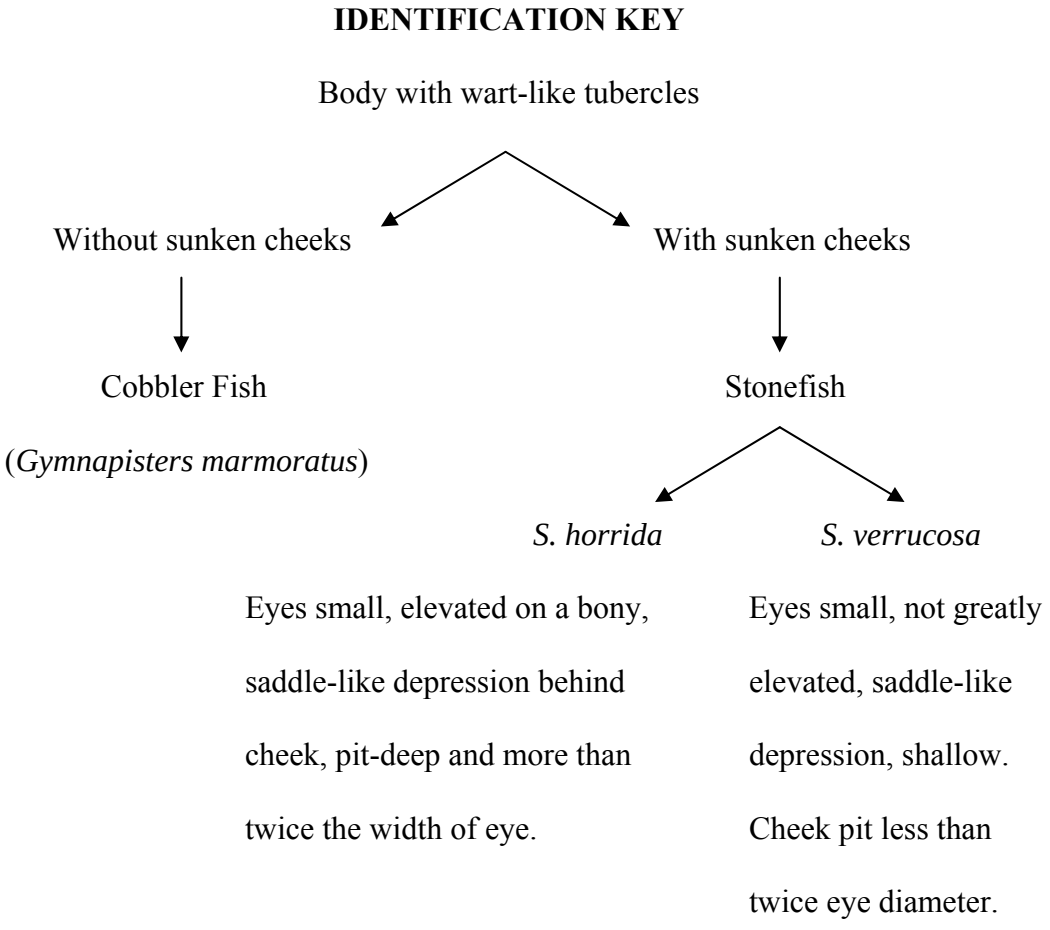

Figure 4. Pictures of *S. horrida* showing its hypothermic needle-like dorsal spines. (Pictures adapted from Australian Museum Archives).

(a)

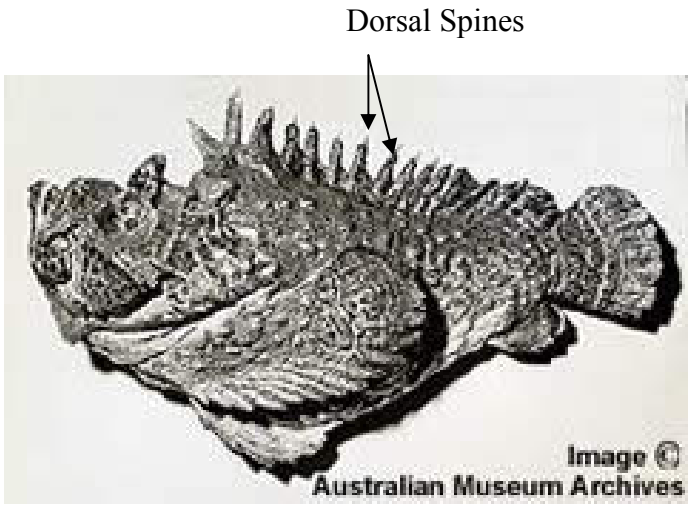

(b)

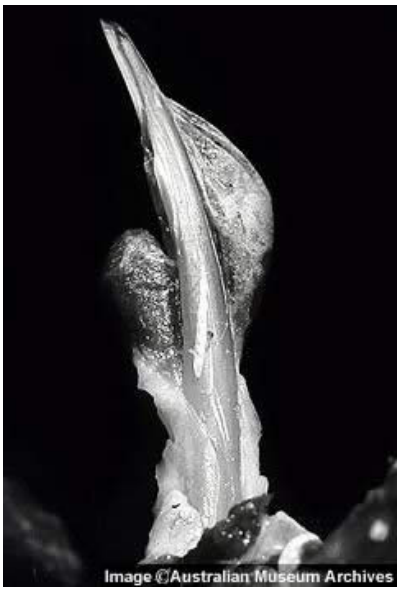

expelled through the spines. The anal and pelvic spines are completely enclosed by their integumentary sheath and appear as non-functional venom organs (Low, 1995).

1.2.3.2 MICROSCOPIC OBSERVATIONS

The structure of the venom gland of *S. horrida* has been studied using light microscopy, and transmission and scanning electron microscopy (Gopalakrishnakone and Gwee, 1993). The glands were covered with a fibrous capsule which divided the glandular tissue into many septa which carried numerous nerves and blood vessels. Two venom gland cells are apparent. In particular, the venom secreting cell (Type I) is unique and completely different from any other venom-secreting cells described so far in snakes (Gopalakrishnakone 1985a, 1986; Gopalakrishnakone and Kochva, 1990), scorpions (Gopalakrishnakone, 1985b) or spiders (Gopalakrishnakone, 1987).

The Type I cells do not have any features of a protein-secreting cell such as Golgi apparatus, or rough endoplasmic reticulum. The presence of vacuoles of varying size, accompanied by the presence of glandular material of different electron densities in varying amounts suggest that these are various stages in the maturation of the Type I glandular cell. The whole Type I cell completely transforms into granules, suggestive of a holocrine type of secretion. The type II cells, which are much fewer in number, showed a vacuolated appearance, and some vacuoles contained electron dense globular granules which are much larger than the granules seen in Type I cells. Even

the Type II cells did not show any characteristic features of secretory cells, as in the case of Type I cells.

Scanning electron microscope confirmed that the secretory mechanism is holocrine. The breakdown of cell membrane was clearly seen and the secreted granules were membrane bound. It is possible that the Type I cells contribute most of the venom components, with some contribution from the Type II cell. This glandular model appears to be very different from snakes, scorpions, and spiders. Further studies are needed to elucidate the exact secretory granules which are involved in venom production in *S. horrida*.

1.2.4 ENVENOMATIONS & TREATMENT

Several interesting names have been given to the stonefish and include Ikan Hantu (Devil fish), the Warty Ghoul and Nohu (the Waiting One). Generally, stonefish are only dangerous if accidentally stepped on. The venom apparatus is used for defense only and never to get food. Wounds produced by the hypodermic needle-like dorsal spines of the fish (Figure 4) may be small but are sometimes fatal because of the discharge of extremely potent venom into the victim. Severity of the symptoms of envenomation is related to the depth of penetration of the spines and the number of spines involved.

Envenomation by stonefish is typified by a wide array of responses including fever, sweating, nausea, excruciating pain at wound sites, tremendous swelling and death of tissues, respiratory difficulties due to pulmonary edema, hypotension, bradycardia, arrhythmia, paralysis, convulsions and death (Phoon & Alfred, 1965; Saunders *et al.*, 1962). In spite of these, stonefish is also known to be a delicacy (Khoo, 2002).

Some of the treatments for envenomation as recommended by eMedicine (http://www.emedicine.com/) include:

1. Prevent movement of the affected part.
2. Gentle removal of visible spines to prevent further penetration and breakage, meanwhile recognizing their potential for further envenomation.
3. Apply appropriate analgesia if needed and irrigate the wound copiously.
4. Apply direct pressure to control excessive bleeding.
5. Immerse the injured site in warm water water (upper limit of 114 °F or 45 °C) in order to inactivate the thermolabile components of the venom that might otherwise cause a severe systemic reaction (Be careful not to inflict thermal burns to insensate limb).
6. Look for broken spines. Apply adjunctive regional or local anesthesia for debridement of embedded spines when they are in proximity to joints, nerves, or vessels. Embedded structures should be pulled straight out with forceps to avoid breaking them.

7. Treatment for anaphylaxis. Tetanus prophylaxis using epinephrine and antihistamines is indicated in all patients who have experienced traumatic marine injury and who have insufficient or uncertain immunization histories.
8. Recognition of serious systemic symptoms and prompt institution of appropriate life-saving procedures, such as cardiopulmonary resuscitation (CPR) and advanced cardiac life support (ACLS) procedures are rarely indicated but always take absolute precedence
9. Antivenom administration. Stonefish antivenin from Australia's Commonwealth Serum Laboratories (CSL) is recommended only for predilution intramuscular usage. However, for serious envenomations, this route may not be ideal because of erratic absorption. Following dilution, a slow intravenous administration may be preferable: 1 ampule (2000 U) for every 1-2 punctures, up to 3 ampules for more than 4 punctures. Antivenin should be diluted in 50-100 ml isotonic sodium chloride solution and run through at least 20 minutes. As this is hyperimmunized equine antisera, there are risks of allergic reaction and serum sickness in the recipient. Skin testing and/or pretreatment should precede administration. Rather than skin testing, Australian sources tend to recommend pretreatment with subcutaneous epinephrine and an intramuscular antihistamine, adding an intramuscular corticosteroid for known hypersensitivity.
10. Ultrasound and plain radiographs to help locate retained fragments. Retained fragments should be removed as they act as foreign bodies, causing

inflammation and eventually becoming encapsulated into granulomata, which may lead to delayed healing and secondary infection.

1.2.5 S. HORRIDA VENOM & ITS BIOLOGICAL ACTIVITIES

As with the venoms of other organisms, *S. horrida* venom is a complex mixture. The fresh venom is opalescent and has a pH of 6.8 (Poh *et al*., 1991). The protein content accounts for 20% of the dry weight of the lypophilized venom (Poh *et al*., 1991). The LD_{50} (i.v.) of the venom was found to be 0.3μg/g in mice (Khoo *et al.*, 1992). Extrapolated to a 60kg human, this value suggests that 18mg venom would cause death. This dose could be relayed from six intact spines (Khoo *et al.*, 2002). A lethal dose of the venom caused convulsive movements, respiratory arrest, urination, hypersalivation and death within 3-30min of injection (Poh *et al*., 1991).

The venom of *S. horrida* was screened to check the biological activities it possesses (Khoo *et al*., 1992). It exhibited edema-inducing, species-specific hemolysis and high hyaluronidase activities. Weak thrombin-like, alkaline phosphomonoesterase, 5'-nucleotidase, acetylcholinesterase, phosphodiesterase, arginine esterase, and arginine amidase activities were also detectable. Recalcification clotting time, prothrombin, and kaolin-cephalin clotting ties were increased 1.7, 2.3 and 2.4-fold respectively. Its effects on uptake and stimulation of neurotransmitter synthesis and release in rat brain synaptosomes were also evaluated. In the presence of 100ug venom, uptake of [methyl-^{3}H]-choline in rat brain synaptosomes was inhibited 70%, while that of 4-

amino-n-[U-14-c] butyric acid was inhibited 20%. The toxin also stimulated the release of [^{3}H]-acetylcholine from the synaptosomes. Currently, two proteins have also been isolated from the venom, namely Stonustoxin (Poh *et al.*, 1991) and hyaluronidase (Poh *et al.*, 1992).

1.2.6 STO*NUS*TOXIN (SNTX) – A MULTIFUNCTIONAL LETHAL PROTEIN ISOLATED FROM S. HORRIDA VENOM

1.2.6.1 PURIFICATION

Sto*nus*toxin (***Sto***nefish ***N***ational ***U***niversity of ***S***ingapore, SNTX) was purified to homogeneity from *S. horrida* venom via a two-step procedure using Sephacyl S-200 High Resolution (HR) gel filtration chromatography and DEAE Bio-Gel A anion exchange chromatography (Poh *et al.*, 1991). The first process resolved the venom into three major fractions, of which only one exhibited lethal activity. This lethal fraction was then subjected to anion exchange chromatography which yielded four fractions of which one shows lethal activity. This lethality-inducing fraction gave only a single protein band in a 5% non-denaturing polyacrylamide gel. This protein was thus designated SNTX. High performance size exclusion liquid chromatography showed that SNTX has a native molecular weight of 148kDa. Reducing and non-reducing SDS-polyacrylamide gel electrophoresis revealed that SNTX is made up of two subunits, SNTX-α and SNTX-β with molecular weights of 71kDa and 79kDa respectively (Ghadessey *et al.*, 1996). The subunits are postulated to associate via

non-covalent intra-chain linkages not involving disulfide linkages. In addition, it was found that SNTX has an isoelectric point of 6.9 (Poh *et al*., 1991). The purified SNTX has an LD_{50} of 0.017μg/g which is 22-fold more potent than that of the crude venom.

1.2.6.2 cDNA CLONING & CHARACTERIZATION

cDNA clones encoding SNTX-α and SNTX-β had been isolated and sequenced from a *S. horrida* venom gland cDNA library (Ghadessey *et al*., 1996) (Figure 5 & 6). In addition, the genomic region which encodes SNTX-β was found to possess an intron (Ghadessey *et al*., 1994). The SNTX subunits lack typical N-terminal signal sequences commonly found in proteins that are secreted via the endoplasmic reticulum Golgi apparatus pathway, indicating the possibility of it being secreted by a non-classical pathway (Ghadessey *et al*., 1996). Previously, it has been found that the venom secreting cells of *S. horrida* lack features of a protein-secreting cell such as Golgi apparatus, or rough endoplasmic reticulum (Gopalakrishnakone amd Gwee, 1993) that are present in snakes (Gopalakrishnakone 1985a, 1986; Gopalakrishnakone and Kochva, 1990), scorpions (Gopalakrishnakone, 1985b) or spiders (Gopalakrishnakone, 1987).

Figure 5. *S. horrida* SNTX-α mRNA (2171 bp), complete cds (NCBI: U36237). Revised: October 24, 2001. The B30.2 domain ranges from 1638bp (Cys^{526}) to 2168bp (His^{696}).

```
1     gaagtcagga cgactctcac aactcagcag atctacacaa cttcatcagg gttgcaggca
61    tgtcttcaga tttggtaatg cctgctctgg gtcgaccttt cacccttggg atgctgtatg
121   atgctcgcag agagaaactg atcccaggtt tctcattatt tggtgatgaa actctacaaa
181   aatatcaatc aagtaacgct caacgcagca gtgaattcaa aatcgttgct tctgattcca
241   ctgagtccaa gtcctctgcg atggatattg aagcttctct tggagtcagt ttcctgggag
301   gactggttga agttggagga tctgccaagt atctcaacaa tacgaagaaa taccagaatc
361   agagcagagt tacactcaag tacaaagcta ccaccgtcta taaacagttc acagcacctc
421   ctgggactgt gacagtgcaa gaaacagcta ttactgagaa gggattggca acacatgtag
481   taacaagcat cctttatggg gcaaatgctt tctttgtgtc tgacagtgac aaggtagagg
541   ataccaacct tcaggacatc cagggcaaaa tggaagccgc aataaagaag attcctacga
601   ttagtattga ggggtctgca tctgtccaac tgactgatga agaaaagtct ctggccagca
661   atctctcctg caagtttcat ggagacttcc ttcttgaaag cctccctaca acgtttgaag
721   atgcagtgaa gacctaccag acacttccaa cacttattgg agaagacgga gccaattcag
781   ttccaatgaa ggtctggctg gcacccttga agagctataa ttctaaagcc caacagctga
841   tccaagagat caatgttagt aaagtgagaa ggattcacac taccttagaa gagttgcata
901   aactgaagag gagagccaat gaagccatgg atgtcaaact tgtgcaacga attccattga
961   ttcatgacaa gattagcaat ttccaacaga tatttcagga ttacatgctt accgtgcaaa
1021  agaaaattgc agagaaactt ccactggttc gagcaggtac agaaagtgag cagtcattgc
1081  agaagataat tgatgacaga gcccagtcac cattcagcaa tgaaaaagtg agcaagtggc
1141  tggatgccgt agagagagaa atcgctgtct taaagtcctg tgcaggcatg gttgagggaa
1201  cacaggcaaa atttgtctca aatcagacag agttggacag agaggttctt gttggaaagg
1261  taaagcatgc tgtgtgcttt attttcacct cagtggaacg caatgatcct taccttaaag
1321  tgttgtccga ctattgggaa tcacccccct caaataatgc aaaggatgtt gcgccatcta
1381  ctgaagacaa gtggtgtttc tccactgagg tggtactcaa aatgcaacaa agagcccaaa
1441  cattttgtga tcatgtcaac gattttgaga aaagcagaaa cgttggtttc tttatcacag
1501  ccttggaaaa tggaaaattc caaggagcaa gcatctacta ttacaaggag ggcagtctgg
1561  ccactcagga cttcacattc cctcgcatgc cttttgtgca gggttacaaa aagagaagtg
1621  atttactttg gtatgcctgt gacctcacct ttgaccgaaa caccataaac aactggatct
1681  ctctttctga caacgataca tttgcagcct ctgagcatgg aaaacggcag aactatccaa
1741  aacacccaga acgttttgtt agttttaatc aggtgttgtg caatgagggg ctgatgggga
1801  aacattactg ggaggtggag tggaacggat acattgatgt aggtattgct tacatttcca
1861  tccccaggaa agaaattgac tttgcgagtg ctttcgggta caatacctat tcctgggttt
1921  taagctataa tcccaaaatt ggatacatcg aaaggcataa aaaaagagaa tataatgtca
1981  gggcgcccaa tccaggcttt aaacgactag gactgtttct cgattggcgt tatggcagta
2041  tatctttcta tgctgtctcc tctgatgaag tgcaccatct tcacaccttc aaaaccaaat
2101  ttactgagcc tgtttatccg gccttcagta tcgggcctgc cggtaaccac ggaactctca
2161  gattacttta a
```

Figure 6. *S. horrida* SNTX-β mRNA (2740bp), complete cds (NCBI: U32516). Revised: October 24, 2001. The B30.2 domain ranges from 1630bp (Cys^{523}) to 2142bp (His^{693}).

```
1     gaagtcagga agactcctac tgaactcaac tgatctgcac aagttcatca ggttggagtc
61    atgccttcag atatcttggt ggtggctgct ctgggccgac cgttcacgct ggggatgctc
121   tatgacgctc gaaatgataa actgatccca gggttcacat tgtgggaaga tgaagttata
181   gaagagagca cacttgaaag cagtcagccc agcagtgcat ttgaaattat tgcatctgat
241   tctactgatg acaagtcttc tctgatggat attgaagcat ctctgaaagc cagtttcctg
301   ggtggactgg tagaagttgg aggatcagcc aagtatctga ataatcagaa gaaattcaag
361   aatcagagtc gagtgactct tcagtacaaa gctaccacta gcttcaaaca gctgatgact
421   aatcttggaa ccaaacatgt agaatattct gaattatttg agaacatcca ggcaactcat
481   gtagtgatag ggatccttta tggggccaat gccttctttg tctttgacag taacaaagtg
541   gattcaacca atgttcagga aatccagggc caaatggaag ctgtaataaa gaagattcct
601   tcagttgaaa tctcagggaa agcttctgtc cagctaaccg gtgaggaaac tgatataacc
661   aacagctttt cctgtgaatt ccatggggac ttctttctca ctaccaaccc tacaactttt
721   gaggatgcag ttaaaacata ccagcaactt ccacaaatga tggggaaaga caatgctgtc
781   ccaatgacgg tctggctcgt gccaatggta aatttttatt ctgaagcacc tcaactgatg
841   gctgatagca gcactccaat acttaggaag gttcgcaaca ctctggaagc catagtgcaa
901   gttcaaatga gatgcaacga tgcactggat gaccccacag tgaacctgtt cacagaggtt
961   caaaagaagt tgagcgattt ccaaaaaatt tgtgatgatc atatgtcaaa actccaggcg
1021  acgattgcga agaaactttt tgccatccgg agtggagatg aagatgaaag tgccttactg
1081  aacctttttg aagaaaacct tcaatcacca ttcaacatcg aaagcctaaa catgtggatg
1141  gagtttgaag aaagagagat caatgtcctc aggtcctgca tggatatttt aacgaaagca
1201  aaacctaagg ttatttttaa tcaaggtgta cttttaaag gactttatga ttcaaaagta
1261  aagcatgctt tgtgctatgt ctttaccaat gtgacaaaga atgatgtctt cctgaacgtg
1321  ttaaatgagt tcttggattc acctcaaagc agaccaaaga aactcagacc ttcaccaaaa
1381  gactactggt atagctatga tgacatacca gagacgatga gggaaaaagc ttacctttc
1441  cgcaaccttg ccaaagagat gaacaaccgc tgtgtccatt tctttgtaac ggctatacat
1501  aatccaaagc aagaaggagc aggcatccac tactacaggg agagcatcca gatcattgat
1561  gagtttacaa aaccttacat gcctggtgtg gagagcataa aagacagaag agagttacag
1621  tggtatgact gtgagctcac cctggaccca gaaacagcac accaggtcct gactctgtcc
1681  gagggcaaca aaaaggcagt ttcagggaat acgaagtcac ccaccgatca cctagagaag
1741  ttcagccact ttcagcaggt gatgtgcacc aaggggctga gtgggcgcca ttactgggag
1801  ttagagtggt ctggttacgt tggtgcaggt gtcacatata aaggaatcgg taggaaaaca
1861  tctacctcag attcctccct tggaaaaaat gagaagtcct ggctttttga atattctaca
1921  aaatcaggct accaacaaat tcataatagt aaaaagactc gtgtcactgt gtcctccact
1981  ggctttaaac ttttaggagt gtatctggac tggcctgctg gcactctgtc cttctacatg
2041  gtcaacaaag cctgggttac tcatctccac actttccaca ccaaatttaa tgaagctgtt
2101  tatccagcct tcttgattgg ggatgcacaa cagaaagtca atggtcaaat taaattattg
2161  taaaatgttt gtgcaccaaa tccagactct ttagcagtac atgtagttgg ttcctcagag
2221  ttagtggaat aattacacaa caataataat aataattata ataattacag gaagttgatg
2281  ccaatatatg cttaaaaaaa taaatggcat caatattgtc aagaatccat ttggaattgt
2341  gggggtttcc tattttgggt ggcagtagca gtaatagtag taatagtagt agtagtagta
2401  atcagagatc ctactacaag tgtgttttaa tataaattta tacgcaataa atgatacgtt
2461  aaaataagat aatgttggat acagtaaaaa gattcaaaat gcagagaaac attatgagtt
2521  actgtggaaa cagctttaaa tgttacatgg aagttacaaa ttgcaattaa aaaaaagcat
2581  gtaataggaa tataattaaa catttgggga acttgctatc ttgatttctt gcagtgttac
2641  tttaatgaca agtatcgtgt ttttacattg ctattattgt cctattagtt tttacatcag
2701  tgcacaataa gccgcaacaa tcaacaacag attctagtat
```

1.2.6.3 AMINO ACID SEQUENCE ALIGNMENT

Amino acid sequence alignment using BLAST indicates that the SNTX subunits exhibit 47% homology to each other. More sequence alignments with BLAST showed that SNTX-β exhibits 90% homology to both verrucotoxin-α and verrucotoxin-β subunits that make up Verrucotoxin. Verrucotoxin, a lethal hypotensive and cytolytic factor from stonefish *S. Verrucosa* is made up of 4 subunits, 2 α subunits (83kDa) and 2 β subunits (78kDa) (Garnier *et al.*, 1995).

SNTX-α in contrast, exhibited only 46% homology to the verrucotoxin alpha and beta subunits. SNTX like verrucotoxin, show no significant homology to other proteins except that they possess a small stretch of amino acids that make up a B30.2 domain.

1.2.6.4 THE B30.2 DOMAIN

1.2.6.4.1 INTRODUCTION

SNTX shows no significant homology to other proteins except that it possess a small stretch of amino acids that make up a B30.2 domain that is present in many proteins of diverse functions and cellular locations (Henry *et al.*, 1998). These proteins include the human 52 kDa Sjogren's syndrome nuclear antigen A/Ro (SSA/Ro), the ret finger protein (rfp), Xenopus nuclear factor 7 (xnf7), bovine butyrophilin (BTN), etc. This

huge family of B30.2 domain-containing proteins is classified by Henry *et al.* (1998) and Seto *et al.* (1999) according to the type of N-terminal domain found in each protein (Figure 7).

The first category of B30.2 domain-containing proteins comprises a subset of RING finger proteins with Bbox and coiled-coil domains, and includes rfp, SSA/Ro, acid fingerprotein (AFP), RING finger B30 protein (RFB30) and transcription regulator Staf-50 protein (Staf50). Two other members of this family contain an additional N-terminal region with an acidic character, xnf7 and Pleurodeles waltl (PwA33). Other

Figure 7. The B30.2-domain containing family of proteins. (Diagram adapted from Seto *et al*., 1999)

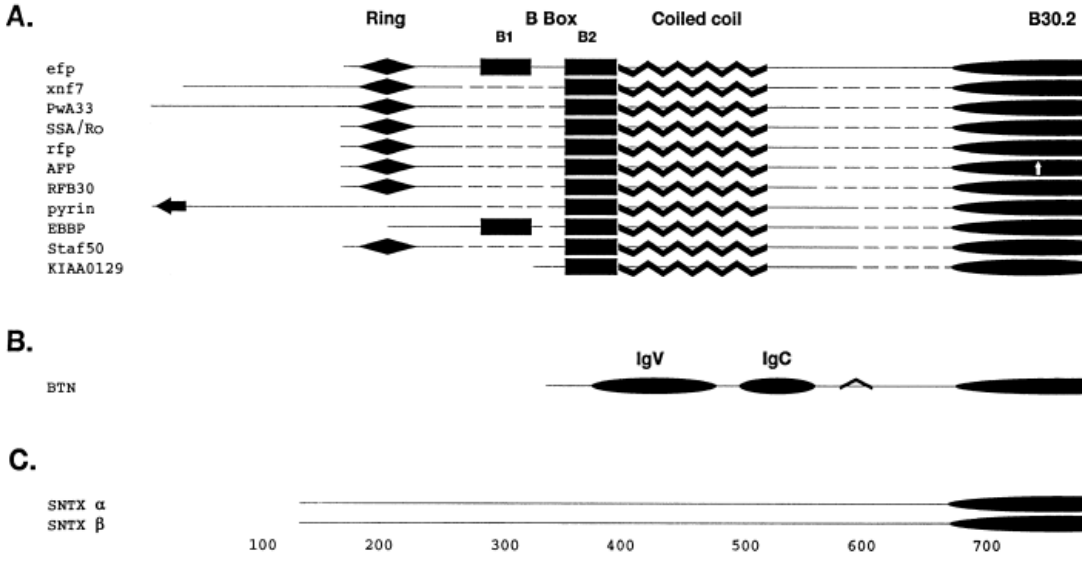

family members comprise variations of this canonical structure. In pyrin, the N-terminal domain is unique, and there is no RING motif, and the B30.2 domain is truncated, while the estrogen finger protein (efp) has two Bbox motifs. Currently, this category of B30.2 domain containing proteins are found to be involved in the regulation of cell growth and differentiation (Inoue *et al.,* 1993; Reddy *et al.,* 1991; Tissot *et al.,* 1995; Bellini *et al.,* 1993; Itoh *et al.,* 1991; Takahashi *et al.,* 1988). Their subcellular localization has also been shown to be both nuclear and cytoplasmic (Liu *et al.,* 1998; El-Hodiri *et al.,* 1997; Miyagawa *et al.,* 1998).

The second type of N-terminal region associated with B30.2-like domains comprises two extracellular immunoglobulin-like domains, IgV and IgC, and is present in a family of butyrophilin-related proteins (Henry *et al.,* 1997; Taylor *et al.,* 1996). The B30.2 domain of BTN, shown to be associated with xanthine dehydrogenase/oxidase, has been suggested to function in a complex with other proteins in the budding and release of milk-fat globules from the apical membrane during lactation (Ishii *et al.,* 1995; Banghart *et al.,* 1998). Although BTN is a transmembrane protein, the B30.2-like domain of BTN is cytoplasmic.

The third family of B30.2 domain-containing proteins consists of SNTX-α and SNTX-β, two subunits within SNTX that is secreted possibly via the non-classical pathway (Ghadessey *et al.,* 1994 & 1996). SNTX possess various biological activities that include potent species-specific hemolysis (Duhig & Jones, 1928; Poh *et al*., 1991), platelet aggragation (Khoo *et al*., 1995), oedema induction (Poh *et al*., 1991),

endothelium-dependent vasorelaxation (Low *et al*., 1993), hypotension (Low *et al*., 1993), inhibition of neuromuscular junction (Low *et al*., 1994) and lethality (Poh *et al*., 1991; Low *et al*., 1993).

1.2.6.4.2 CLONING AND EXPRESSION

The B30.2 domain in SNTX-α and SNTX-β have been amplified by PCR and cloned into various bacterial expression systems (Sung, 2001).

In the first instance, the B30.2 domains of SNTX-α and SNTX-β were expressed as fusion proteins with 6X His tag using the pQE QIAexpress System. pQE30 vector and *E. coli* M15 host cells were used. The cultures were induced in late logarithmic phase at 30°C by 0.1 to 1mM IPTG for four hours and SDS-PAGE showed that the His-αB30.2 and His-βB30.2 recombinant proteins were highly expressed within the inclusion bodies. In the presence of 0.1mM IPTG at 30°C, the expression of the major part of the recombinant proteins as inclusion bodies increased with time from 1-4 hours. Very little recombinant protein was expressed as soluble fractions in the supernatant. An attempt at purifying recombinant His-αB30.2 under native conditions from the soluble fraction resulted in no significant yield of pure protein. Under denaturing conditions, there was a significant yield of His-αB30.2. However according to the author, attempts made to refold His-αB30.2 using slow dialysis against decreasing concentration of urea or direct dilution with 1X PBS was not successful.

Sung (2001) also tried expressing the B30.2 domains of SNTX-α and SNTX-β as fusion proteins using the pET system. pET-22b(+) vector and *E. coli* BL21(DE3) host cells were used. pET-22b(+) has a signal sequence that directs expressed heterologous proteins to the periplasm, a common strategy employed when attempting to isolate active and folded proteins. However, both the expressed pET22b(+)-αB30.2 and pET22b(+)-βB30.2 fusion proteins were found as inclusion bodies in the cytoplasmic fraction instead, presumably due to the incompetent nature of the protein to localize to the periplasm. The recombinant proteins were expressed in majority as insoluble inclusion bodies at a temperature of 37°C with different IPTG concentration for 4hrs.

Lastly, the pGEX system was employed to try to increase the solubility of the cloned B30.2 domains of SNTX-α and SNTX-β by utilizing the hydrophilic nature of the GST affinity tag. pGEX-5X-1 vector and *E. coli* BL21(DE3) host cells were used (Sung, 2001). Bacterial cultures were grown at 30°C until OD_{600} = 0.5 before being induced with different concentrations of IPTG for 4hrs. GST-αB30.2 and GST-βB30.2 were found to be expressed both in the soluble fraction and as inclusion bodies, with no conclusive evidence showing the preferential distribution of the fusion proteins. Using the soluble fractions, purification attempts with glutathione-agarose columns resulted in the co-purification of GroEL with both GST-αB30.2 and GST-βB30.2. To remove co-purifying Gro-EL, an ATP washing step was applied while the GST fusion proteins remained attached to the affinity column. GST-βB30.2 but not GST-αB30.2 was efficiently removed from GroEL. As a further attempt to

remove GroEL from GST-αB30.2, an ATP-GroES washing step was used but pure GST-αB30.2 cannot be obtained. The amount of GST-αB30.2 (copurified with GroEL) and pure GST-βB30.2 obtained after purification inclusive of an ATP wash were approximately 340μg/l and 230μg/l respectively.

1.2.6.5 SPECIES-SPECIFIC HAEMOLYTIC ACTIVITY: PORE FORMATION AND THE ROLE OF CATIONIC AMINO ACID RESIDUES

SNTX causes species-specific haemolytic activity (Duhig & Jones, 1928; Poh *et al*., 1991). It lyses washed erythrocytes and diluted blood of rat, guinea-pig and rabbit, but not rabbit or human red blood cells. Haemolysis was postulated to be due to a pore-forming mechanism by SNTX and cationic residues in SNTX may play a crucial role (Chen *et al*., 1997).

SNTX-induced haemolysis was completely prevented by osmotic protectants of adequate size [poly(ethylene) glycol 3000: molecular diameter approx. 3.2nm]. Uncharged molecules of smaller size, such as raffinose and poly(ethylene) glycol 1000-2000, failed to protect against cell lysis. In addition, SNTX lost its haemolytic activity when the positively charged side chains of lysine residues were neutralized or converted into negatively charged side chains upon carbamylation or succinylation respectively. The haemolytic activity of SNTX was also inhibited by the modification of positively charged arginine residues using 2, 3-butanedione. The loss of haemolysis showed strong correlation with the number of Lys or Arg residues

modified. CD analysis, however, showed that the conformation of SNTX was not severely affected by these chemical modifications. Further, the haemolytic activity of SNTX was competitively inhibited by various negatively charged lipids, such as phosphatidylserine, cardiolipin and monosialogangliosides. Neutral or zwitterionic lipids such as phophatidylcholine, phosphatidylethanolamine, sphingomyelin and cholesterol did not affect the hemolytic activity of SNTX.

1.2.6.6 EFFECTS ON PLATELET AGGREGATION

SNTX induces platelet aggregation in whole blood which correlates with its effects on species-restricted haemolysis (Khoo *et al*., 1995). SNTX induced a concentration-dependent and irreversible platelet aggregation in rabbit or rat but not in human or mouse whole blood. Although SNTX itself could not induce platelet aggregation in rabbit or rat platelet-rich plasma (PRP), it had biphasic effects on collagen- or ADP-induced platelet aggregation in PRP. It inhibited collagen- or ADP-induced platelet aggregation at high concentrations (0.08-0.8μg/ml) but the response was potentiated by lower stonustoxin concentrations (0.008-0.016μg/ml).

The inhibition of collagen- or ADP-induced platelet aggregation might be due to the lytic activity of SNTX on the platelets. However, lysis of platelets caused by SNTX did not appear to affect platelet aggregation observed in whole blood. A possible reason postulated is that the ratio of the concentration of platelets to erythrocytes is about 1 to 28 in rabbit blood and so when added to whole blood, SNTX would have a

higher probability of lysing the RBCs instead of the platelets although the ED_{50} of SNTX is approximately 0.06μg/10^9 RBC for haemolysis and 0.038μg/10^7 platelets for platelet lysis. The number of lysed platelets would therefore be relatively low and therefore enough platelets would still be available for aggregation to proceed.

Low concentrations of SNTX potentiated collagen-induced platelet aggregation in rabbit PRP. At these concentrations, platelet lysis was undetectable. The potentiation was not inhibited by apyrase which is an ADP scavenger. Thus the potentiation did not appear to be mediated by ADP released from the platelets. Further work should be done to elucidate the underlying mechanism(s) by which SNTX potentiates platelet aggregation, such as activating the cyclooxygenase pathway, mobilizing Ca^{2+} from intracellular stores, decreasing cAMP levels or activating endogenous phospholipase A_2.

1.2.6.7 EDEMA-INDUCING ACTIVITY

SNTX exhibits potent edema-inducing activity (Poh *et al*., 1991). The minimum edema dose (MED) is 0.15 μg in mouse paw and maximum swelling occurs within 60 min of SNTX injection. The edema inducing effect was not inhibited by diphenhydramine, suggesting that histamine release did not mediate the increase in vascular permeability. Such venom-induced modifications of vascular permeability may account for the potent hypotension associated with *S. horrida* envenomation.

1.2.6.8 CARDIOVASCULAR EFFECTS

1.2.6.8.1 HYPOTENSION

SNTX (5-20μg/kg) produced dose-dependent falls in blood pressure in anaesthetized rats (Low *et al*., 1993). At the highest dose used, there was no recovery from the marked fall in blood pressure and cessation of respiration occurred. SNTX at these doses used, caused no significant effects on the twitch responses of the tibialis and diaphragm muscles to stimulation by the sciatic and phrenic nerve respectively.

1.2.6.8.2 VASORELAXATION OF PRECONTRACTED RAT AORTA

1.2.6.8.2.1 STUDIES BY LOW *et al.*, 1993 – ENDOTHELIUM-DEPENDENCE & INVOLVEMENT OF L-ARGININE-NITRIC OXIDE SYNTHASE PATHWAY, A DETAILED RELOOK

SNTX (20-160ng/ml) causes an endothelium-dependent vasorelaxant effect on rat's aortic strips pre-contracted with 25nM noradrenaline (NA). The relaxation was fairly well-sustained and lasted between 10-20min. The aortic strips used were shown before actual experimentation to possess an intact endothelium: when precontracted with 25nM NA, they further respond to 0.8mM acetylcholine (Ach) with nearly complete relaxation (82.2 ± 7.9%). Higher concentrations of SNTX (> 0.4μg/ml)

caused rapid, transient relaxations that were quickly followed by an increase in tone of these endothelium-intact, NA-precontracted aortic strips.

In NA-precontracted aortic strips with endothelium removed, no relaxation to 0.8mM Ach or to SNTX at concentrations up to 160ng/ml was observed. SNTX (> 0.4μg/ml) added to these precontracted strips denuded of endothelium caused a rapid increase in tone without producing any relaxant effect. It was also observed that SNTX at concentrations up to 400ng/ml did not affect the resting tension of intact or endothelium-denuded aortic strips.

Preincubation of endothelium-intact aortic strips with 25μM L-N^G-nitro arginine methyl ester (L-NAME), 10μM methylene blue or 5mM hemoglobin for 25min completely abolished the relaxations induced by 20-160ng/ml SNTX on 25nM NA-precontracted aortic strips. L-NAME is a specific and competitive nitric oxide synthase (NOS) inhibitor while methylene blue inhibits guanylate cyclase activation (Gruetter *et al*., 1981; Rapoport and Murad, 1983). On the other hand, hemoglobin binds nitric oxide (NO) (Martin *et al*., 1985; Ignarro *et al*., 1987). These inhibitions of SNTX's effects were not reversed by flushing L-NAME out of the organ bath with fresh Krebs but were reversed by flushing away methylene blue and hemoglobin. In addition, upon addition of 25nM NA to aortic strips preincubated with 25μM L-NAME or 10μM methylene blue, there was an approximately 2-fold and 1.3-fold increase in the contraction of the intact aortic strip in response to 25nM NA respectively. In addition, incubation of intact aortic strips with 75μM L-arginine led

to the reversal of the inhibitory effect of L-NAME on SNTX's effect. From these, it was concluded that SNTX possibly mediates its relaxant activity via the L-arginine-nitric oxide synthase pathway.

1.2.6.8.2.2 STUDIES BY SUNG *et al.*, 2002 – INVOLVEMENT OF SUBSTANCE P RECEPTORS, INDUCIBLE NITRIC OXIDE SYNTHASE AND POTASSIUM CHANNELS

Sung *et al*. (2002) further characterized the mechanisms that are responsible for SNTX-mediated vasorelaxation of 75.2μM L-phenylephrine (PE) precontracted, endothelium-intact rat's thoracic aortic rings that are 4mm in length. Endothelium-intact aortic rings in their work refer to 75μM PE-precontracted aortic rings that respond to 2μM Ach with greater or equal 70% vasorelaxation. PE used in these experiments like NA used by Low *et al*. (1993), produces vasoconstriction of vascular smooth muscle by binding to alpha adrenoceptors (Katzung, 1998). However, PE unlike NA is not a catechol derivative that is inactivated by Catechol-O-methyltransferase (COMT). Hence PE produces a more easily monitored stable contractile response of the aorta than NA. The vasorelaxant effect produced by SNTX on PE-precontracted aortic rings should theoretically show less variation than NA-precontracted aortic rings.

Sung *et al.* (2002) showed that progressive addition of SNTX to 75.2μM PE-precontracted endothelium intact aortic rings results in a cumulative dose-relaxant

effect. The SNTX cumulative dose-response curve has an IC_{50} of 132.7ng/ml and a maximum vasorelaxation of 72.7 ± 6%. She also showed that preincubation of the aortic rings for 30min with 0.5mM 2-amino-5,6-dihydro-6-methyl-4H-1,3-thiazine (AMT-HCl) or 0.5mM N-acetyl-L-tryptophan-3,5-bis(trifluromethyl)-benzyl ester (NATB) completely abolished the vasorelaxant effect of SNTX. AMT-HCl is a specific inducible nitric oxide synthase (iNOS) inhibitor (Nakane *et al.*, 1995), while NATB is a substance P (SP) receptor antagonist. In addition, preincubation of the aortic rings for 30 min with 3mM tetraethylammonium (TEA) led to the partial inhibition of SNTX's effect with maximum vasorelaxation decreased to 25.4 ± 8%. TEA is a non-selective K^+-channel inhibitor (Armstrong, 1971).

Combining the results by Low *et al*. (1993), Julia *et al*. (2002) postulated that a component of SNTX-mediated vasorelaxation in precontracted rat aortic rings is via binding of either SNTX or SP to the SP receptors that are located on the endothelial cells (Figure 8). Occupation of these SP receptors causes the subsequent activation of nitric oxide synthase (NOS) and the production of NO that diffuses into vascular smooth muscle to affect an increase in the levels of cyclic guanylyl monophosphate (cGMP) via the activation of guanylyl cyclase. cGMP then activates K^+-channels, thereby causing membrane hyperpolarization and vasorelaxation.

Figure 8. Postulated components of SNTX-mediated vasorelaxation in the endothelium-intact rat aortic ring.

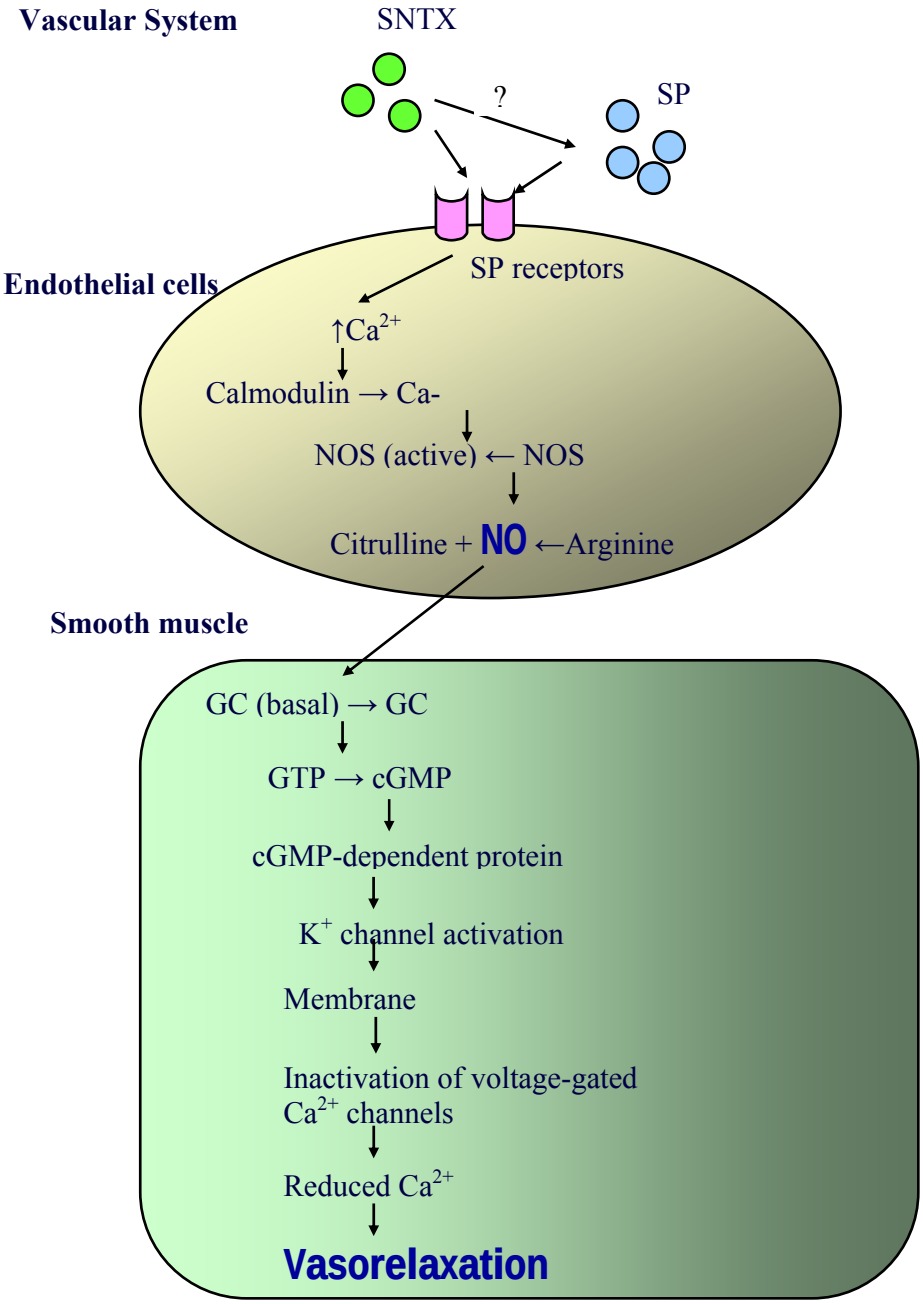

1.2.6.9 NEUROMUSCULAR EFFECTS

SNTX (8-50μg/ml) produced a rapid and concentration-dependent rise in tension (contracture) of electrically-stimulated mouse hemidiaphragm followed by a gradual waning of tension from the peak to the baseline; the nerve-evoked and the directly (muscle)-evoked twitches of the hemidiaphragm were also progressively and irreversibly blocked in a time- and concentration-dependent manner (Low *et al*., 1994). The muscle contracture produced by SNTX was blocked by dantrolene sodium (6μM) but not by tubocurarine (15μM). SNTX (22 and 44μg/ml) produced a similar rapid rise in tension of the chick biventer cervicis muscle (CBCM) as well as irreversible and concentration dependent blockade of nerve-evoked twitches and contractures produced by acetylcholine (200μM), carbochol (8μM) and KCl (40mM). In addition, SNTX (40μg/ml) did not inhibit any nerve conduction in the toad sciatic nerve and SNTX (60μg/ml) did not exhibit any anticholinesterase activity.

SNTX produced marked and concentration-dependent contractures of the mouse hemidiaphragm in the presence of 15μM tubocurarine which indicated that SNTX can act directly on the muscle to produce a contractile response and ruled out the involvement of a prejunctional mechanism in the mediation of the contractures which also could not be attributed to any anticholinesterase activity of SNTX since this was found to be absent in the toxin. The marked blockade by dantrolene sodium of the SNTX-induced contractures of the mouse hemidiaphragm indicates that SNTX could not have acted directly on the contractile muscle proteins to produce the contractures,

since dantrolene mediates its blocking action primarily by inhibiting the release of calcium from the sarcoplasmic reticulum, i.e. prior to activation of the contractile proteins (Hainut and Desmedt, 1984). SNTX-induced contracture may be the result of SNTX causing direct muscular depolarization, since the crude venom of *S. trachynis* has been shown to produce extensive depolarization of skeletal muscle fibres of the rat (Kreger *et al*., 1993).

Blockade of indirectly evoked twitches by SNTX is not likely to be due to nerve conduction block since, at the concentrations used, SNTX did not affect action potentials in the toad sciatic nerve. The ability of SNTX to block directly evoked twitches indicates that SNTX acts directly on the muscle to inhibit neuromuscular function. The complete blockade of the contractile responses of the CBCM to Ach and CCh, as well as to KCl, also provides strong evidence that the inhibitory action of SNTX on neuromuscular function may be attributed to some direct effects of SNTX on the muscle. Since SNTX produced irreversible blockade of directly and indirectly evoked twitches of the skeletal muscle preparations used, it is likely that SNTX induced some permanent damage to the neuromuscular apparatus in skeletal muscle. It has recently been reported that large concentrations (100-300μg/ml) of the crude venom of *S. trachynis* produced muscle and nerve damage visible under the electron microscope; it was reported also that the crude venom of *S. trachynis* can cause depletion of neurotransmitter as a consequence of massive transmitter release as well as block of synaptic vesicle recycling (Kreger *et al*., 1993), prejunctional actions which also contribute to the neuromuscular function in skeletal muscle.

1.2.6.10 DEVELOPMENT OF MONOCLONAL ANTIBODIES

Eight monoclonal antibodies have been developed by Yuen *et al.* (1995) using the Balb/C mouse, and purified by Protein G affinity membrane disc chromatography. These MAbs are designated as MAbs 8A, 31A, 32B, 38A, 43B, 43D, 44G, 46A respectively. Four of the Mabs were found to have similar epitope specificity while the rest were directed at different epitopes on the SNTX molecule. Although six of these monospecific antibodies were able to protect mice from a challenge of a lethal dose of SNTX, not all the protective MAbs were able to neutralize the hemolytic effect of SNTX in vitro; which suggests the domain(s) responsible for both biological activity may be different.

1.2.6.11 CRYSTALLIZATION AND PRELIMINARY CRYSTALLOGRAPHIC STUDY

Crystals of SNTX have been obtained and diffract to a 3.4 Å resolution (Yew *et al*., 1999). The crystals belong to the tetragonal space group P422, with unit cell constants a = b = 109.0 Å, c = 245.7 Å. A native SNTX has two subunits, designated α and β, respectively, and there is one SNTX molecule per asymmetric unit.

1.2.6.12 CHEMICAL MODIFICATIONS

Chemical modifications of proteins in solution can provide important structural and functional information. In many ways, chemical modification is complementary to site-directed mutagenesis as a methodology for the study of protein variants. Although the latter method is favorable because the importance of specific amino acid residues can be determined, chemical modification is still useful when biologically active recombinant proteins of interest is not available for site-directed mutagenesis studies. SNTX have been characterized by chemical modification and several amino acids such as cationic lysine and arginine residues, free thiol and tryptophan have been found to play important roles in its various biological activities including lethality and haemolysis (Yew *et al*., 2000; Khoo *et al*., 1998a; Khoo *et al*., 1998b; Chen *et al*., 1997).

1.2.7 HYALURONIDASE – A SECOND PROTEIN ISOLATED FROM S. HORRIDA VENOM

Hyaluronidase was purified from *S. horrida* venom via a Sephacryl S-200 High Resolution (HR) gel filtration chromatography, followed by a Heparin Agarose affinity chromatography (Poh *et al.*, 1992). The first process involved resolving the venom into five fractions, of which fraction 2 exhibited hyaluronidase activity. This fraction was then subjected to affinity chromatography which yielded four fractions of which fraction 4 contained hyaluronidase. This fraction gave only a single band in

a 10% SDS-PAGE gel. The purified hyaluronidase has a molecular weight of 62 kDa, as obtained by SDS-PAGE and Sephadex G-100. It has a pI of 9.2, is heat sensitive and is inhibited by Cu^{2+}, Hg^{2+} and heparin. It does not contain hemorrhagic or lethal activity. Its N-terminal sequence has also been determined to be A-P-S-X-D-E-G-N-K-K-A-D-N-L-L-V-K-K-I-N.

The reaction products of the hyaluronidase purified from stonefish venom consists of tetra-, hexa-, octa- and deca-saccharides as major end products, but not disaccharides (Sugahara *et al*., 1992). The structure of the tetrasaccharide product was determined by enzymic analysis, in conjuction with HPLC and H-NMR, as GlcAβ1-3GlcNAcβ1-4GlcAβ1-3GlcNAc. Chemical shifts of the structural-reporter-group protons of the constituent monosaccharides for the tetrasaccharide have been assigned. The enzyme did not act on chondroitin sulphate or dermatan sulphate. The results indicate that stonefish hyaluronidase is an endo-β-N-acetylglucosaminidase specific for hyaluronate.

1.2.8 OTHER SYNANCEJA SPECIES

1.2.8.1 SYNANCEJA TRACHYNIS

Trachynilysin (TLY), a dimeric protein purified from *S. trachynis* venom has a molecular weight of 158kDa and a pI of 5.7 (Kreger, 1991). It contains the venom's haemolytic, as well as the lethal and vascular permeability increasing activity

(Kreger, 1991). TLY forms pores in planar lipid bilayers (Mattei *et al*., 2000) and mediates soluble N-ethylmaleimide-sensitive fusion protein attachment protein receptor (SNARE)-dependent release of catecholamines from chromaffin cells via external and stored Ca^{2+} (Meunier *et al*., 2000) It increases spontaneous quantal acetylcholine release from neuromuscular junctions (Ouanounou *et al*., 2000). It also enhanced the release of Ach from atrial cholinergic nerve terminals and indirectly activated muscarinic receptors (Sauviat *et al*., 2000). It was also shown that TLY selectively stimulated the release of small, clear synaptic vesicles and impaired the recycling of small, clear synaptic vesicles but did not affect the release of large dense-core vesicles (Colasante *et al*., 1996).

1.2.8.2 SYNANCEJA VERRUCOSA

Unlike SNTX and TLY, verrucotoxin (VTX) purified from *S. verrucosa* venom was found to be a glycoprotein with a high molecular weight of 322kDa, comprising four subunits, 2 α- (83 000) and 2 β- (78 000) (Garnier *et al*., 1995). Just like the crude venom, VTX was lethal in mice, lysed washed rabbit erythrocytes and induced a fall in blood pressure (Garnier *et al*., 1995). VTX was found to inhibit calcium channels and may activate ATP-sensitive K^+ channels in frog atrial heart muscle (Garnier *et al*., 1997). In addition to TLY, *S. verrucosa* venom also contained noradrenaline and other biogenic amines, such as dopamine and tryptophan, but not 5-hydroxytryptamine (Garnier *et al*., 1996). Numerous enzymatic activities, i.e.

hyaluronidase, esterase and aminopeptidase are also present in the crude venom (Garnier *et al*., 1995).

1.3 HYDROGEN SULFIDE (H_2S)

1.3.1 INTRODUCTION

Hydrogen sulfide (H_2S) is commonly known as "Sewer Gas". It is a colorless, flammable gas with a strong odor of rotten eggs. It occurs naturally in crude petroleum, natural gas, volcanic gases, hot springs and is produced from the bacterial breakdown of organic matter, human and animal wastes (US Environmental Protection Agency - Public health statement for H_2S, 1999). It is produced from industrial activities such as food processing, coke ovens, kraft paper mills, tanneries and petroleum refineries. Throughout the years, hydrogen sulfide has been associated with many industrial fatalities (Burnett *et al.*, 1977; Guidotti, 1994; Synder *et al.*, 1995). The detectable level of this gas by the human nose is at a concentration 400-fold lower than the toxic level and desensitization of the olfactory system can occur within minutes. Symptoms associated with H_2S exposure include eye irritation, sore throat, cough, shortness of breath and fluid in the lungs upon low levels of exposure to the gas. Upon long-term exposure, H_2S causes fatigue, loss of appetite, headaches, irritability, poor memory and dizziness. At high levels of exposure to the gas, there can be loss of consciousness and death can occur.

Despite the toxicity associated with H_2S, it has been found to be produced endogenously in mammalian cells during L-cyst(e)ine metabolism (Stipanuk & Beck, 1982). In rat serum, circulating H_2S concentration is ~ 46μM (Zhao *et al.*, 2001). Relatively high levels of H_2S (50-160μM) have also been measured in brains of rats, humans and bovine (Goodwin *et al*., 1989; Warenycia *et al*., 1989; Savage and Gould, 1990). Rat ileum as well as different vascular tissues such as rat thoracic aorta and portal vein also generate measurable amounts of H_2S (Zhao *et al.*, 2001; Hosoki *et al.*, 1997). In addition, H_2S-generating enzymes have also been detected in liver, kidney and heart (Stipanuk and Beck, 1982; De La Rosa *et al*., 1987; Nagahara *et al*., 1998). Currently, the physiological roles of this novel H_2S biological gas are being explored.

1.3.2 ENDOGENOUS GENERATION OF H_2S: DESULFHYDRATION OF L-CYST(E)INE

The synthesis of H_2S occurs during the desulfhydration of L-cyst(e)ine. L-cysteine is a semi-essential amino acid that can be synthesized from methionine and serine via a unidirectional transulfuration pathway. Methionine is an essential amino acid and like L-cysteine, is normally consumed as components of dietary proteins. The biochemical pathways leading to H_2S production in mammalian mitochondria and cytosol involves several enzymes (Stipanuk & Beck, 1982; Stipanuk, 2004; Kamoun, 2004). Some of these enzymes are produced both in mitochondria and in the cytosol i.e. cysteine aminotransferase and 3-mercaptosulfurtransferase (MSPT; 2.8.1.2) whereas others i.e.

cystathionine-γ-lyase (CSE; EC 4.4.1.1) and cystathionine-β-synthase (CBS; EC 4.2.1.22) are only produced in the cytosol. Cytosolic and mitochondrial cysteine aminotransferase are identical to cytosolic (Akagi, 1982) and mitochondrial (Ubuka *et al*., 1978) aspartate aminotransferase, respectively (EC 2.6.1.1 and EC 2.6.1.3, respectively). The expression of H_2S-generating enzymes depends on the species and organ involved. Generally, the pathways leading to H_2S production in mammalian tissues elucidated to-date using liver and kidney tissues are depicted in Figures 9 and 10.

One pathway of L-cysteine metabolism involves its oxidation to cysteinesulfinate. Cysteinesulfinate is then either decarboxylated in cytosol to yield hypotaurine which is further oxidized to taurine (Figure 9) or transaminated in mitochondria to yield pyruvate and sulfite (Stipanuk, 1986) (Figure 10). The sulfite produced is readily oxidized to sulfate. L-cyst(e)ine is also metaboilized via cysteinesulfinate-independent pathways (Coloso & Stipanuk, 1989). Cystathionine-γ-lyase, a pyridoxal 5'-phosphate-dependent enzyme, catalyzes a β-disulfide elimination reaction that cleaves the sulfur from L-cyst(e)ine, resulting in the production of pyruvate, NH_4^+ and thiocysteine (Figure 9). Thiocysteine may react with L-cysteine or other thiols to form H_2S (Stipanuk and Beck, 1982; Yamanashi and Tuboi, 1981). Cystathionine-β-synthase, another pyridoxal 5'-phosphate-dependent heme protein can synthesize H_2S from L-cysteine (Stipanuk and Beck, 1982; Griffith, 1987; Swaroop *et al*., 1992) (Figure 9). H_2S is formed by the substitution of the thiol group of L-cysteine with a variety of thiol compounds to form the corresponding thioether. Another pathway

leading to H_2S generation involves transamination of L-cysteine by aminotransferases to yield 3-mercaptopyruvate which is further catabolised by 3-mercaptopyruvate sulfurtransferase (Stipanuk and Beck, 1982; Stipanuk, 1986) (Figure 9 and 10).

Figure 9. Hydrogen sulfide production in the cytosol (Adapted from Kamoun, 2004).

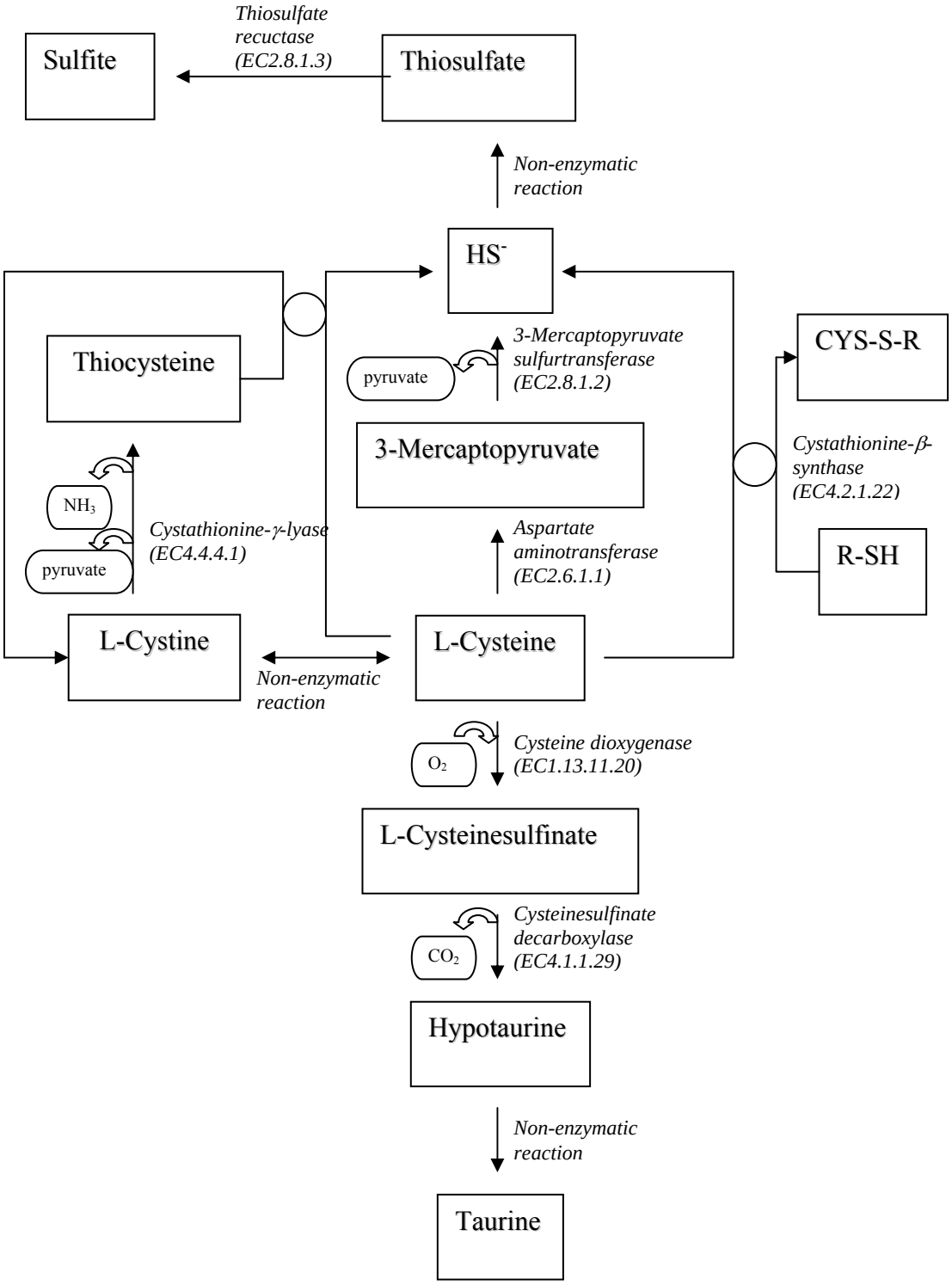

Figure 10. Hydrogen sulfide and other sulfur compounds production in mitochondria (Adapted from Kamoun, 2004).

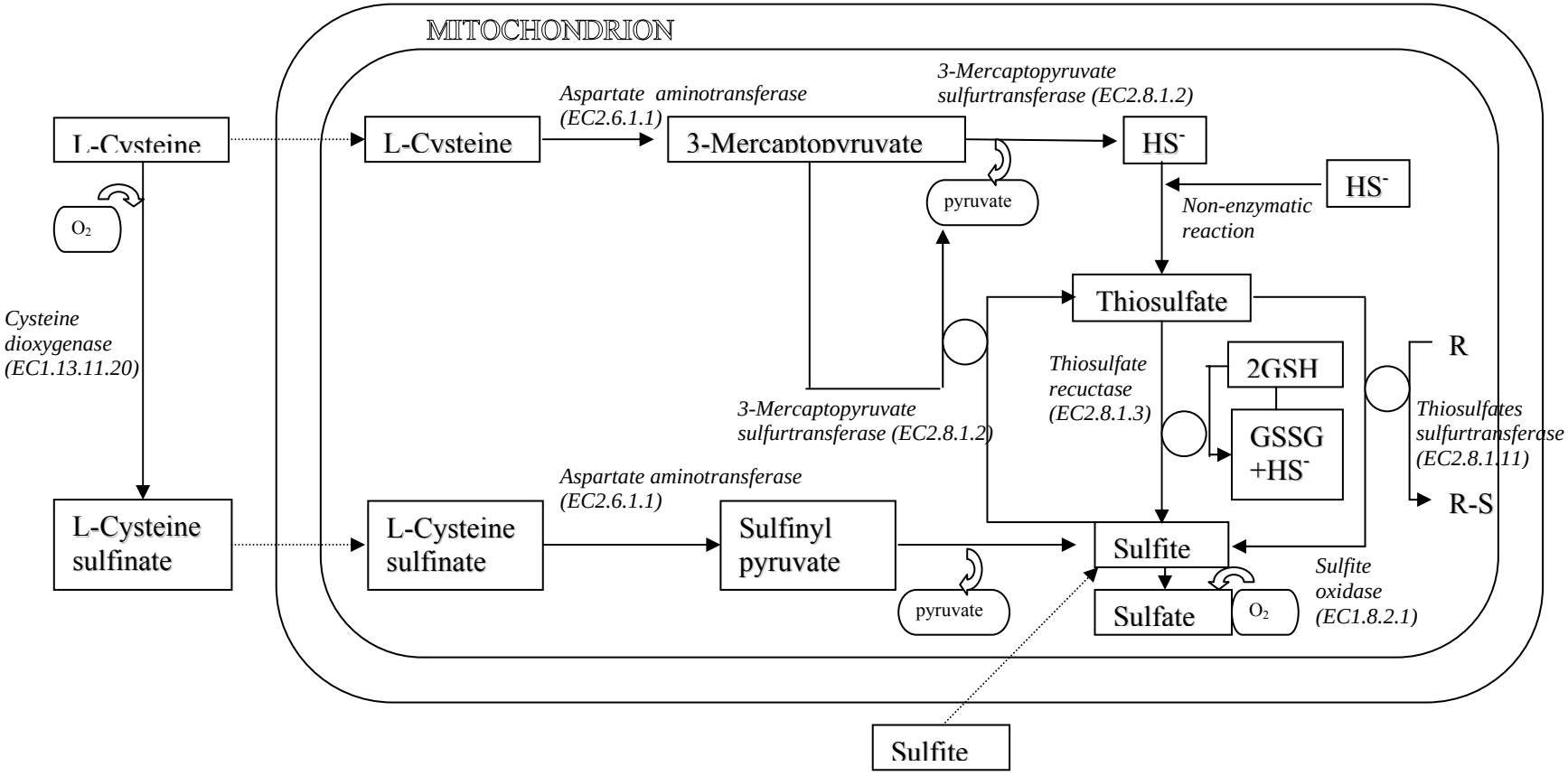

1.3.3 CATABOLISM OF H_2S

The pathways by which hydrogen sulfide is converted to sulfate in mammalian tissues (Figures 9 and 10) have been explored mainly using liver and kidney tissues (Bartholomew *et al*., 1980; Ubuka *et al*., 1990, 1992; Huang *et al*., 1998). The oxidation of hydrogen sulfide to thiosulfate is catalyzed by heme compounds (Sorbo, 1958), metal-protein complexes and ferritin (Ubuka *et al*., 1992). One molecule of thiosulfate is formed from two molecules of hydrogen sulfide. Two enzymes thiosulfate sulfurtransferase and thiosulfate reductase then act on thiosulfate (Westley, 1980). Thiosulfate reductase catalyzes the reaction of thiosulfate with reduced glutathione. Oxidized glutathione is reduced by mitochondrial glutathione reductase. Thiosulfate sulfurtransferase, in comparison, was found to be poorly efficient in the catabolism of thiosulfate (Huang *et al*., 1998). Sulfite oxidase (EC 1.8.2.1) a soluble protein found in the intermembrane space of mitochondria (Cohen *et al*., 1972) has ready access to its reducing substrate, sulfite, which can diffuse across mitochondrial membranes, and to its physiological acceptor, cytochrome c. Sulfite oxidase, a molybdenum containing enzyme, forms sulfate from sulfite. In mammals, H_2S is excreted mainly by the kidney as free or conjugated sulfate (Beauchamp *et al.*, 1984).

1.3.4 H_2S & THE CARDIOVASCULAR SYSTEM

1.3.4.1 EXPRESSION OF H_2S-GENERATING ENZYMES

In vascular tissues, CSE is the only H_2S-generating enzyme that has been identified to-date (Hosoki *et al.*, 1997; Zhao *et al*., 2001). CSE in rat mesenteric artery (Pubmed ID: AB052882) and other vascular tissues (Pubmed ID: AY032872) has been cloned and sequenced (Zhao *et al*., 2001). mRNA of this enzyme was expressed solely in vascular smooth muscle cells as detected by RT-PCR and in situ hybridization (Zhao *et al*., 2001). No transcript of CSE was found in the endothelium layers of intact vascular tissues or cultured endothelial cells (Zhao *et al*., 2001). Expression levels of CSE mRNA varied in different types of vascular tissues, with an intensity rank of pulmonary artery > aorta > tail artery > mesenteric artery (Zhao *et al*., 2001). The expression of CSE (43kDa) at protein level has also been demonstrated in rat aorta, mesenteric artery smooth muscle, tail artery smooth muscle and pulmonary artery smooth muscle (Cheng *et al*., 2004). The expression level of CSE protein was similar in the different vascular tissues.

In contrast, no/little expression of cystathionine-β-synthase (CBS) has been found in human atrium, ventricle tissues, internal mammary arteries, saphenous veins, coronary arteries, or aortic arteries (Chen *et al*., 1999; Bao *et al*., 1998). As such, CBS does not appear to play a major role in generating H_2S in cardiovascular tissues under physiological conditions.

1.3.4.2 PHYSIOLOGICAL EFFECTS OF H_2S

1.3.4.2.1 IN VIVO: DECREASE IN BLOOD PRESSURE

An intravenous bolus injection of H_2S at 2.8 and 14μmol/kg body weight transiently decreased blood pressure of rats by ~ 12 and 30 mmHg respectively, an effect mimicked by pinacidil (a K_{ATP} channel opener) and antagonized by glibenclamide (a K_{ATP} channel blocker) (Zhao *et al*., 2001).

1.3.4.2.2 IN VITRO: VASORELAXATION

1.3.4.2.2.1 ROLE OF ENDOTHELIUM & ENDOTHELIUM-DERIVED RELAXING FACTOR (EDRF)

H_2S induced in vitro dose-dependent relaxation of rat precontracted aorta, portal vein and mesenteric artery beds (MAB), as well as electrically stimulated vas deferens (Hosoki *et al*., 1997; Zhao and Wang, 2002; Wang, 2002; Teague *et al*., 2002; Cheng *et al*., 2004). The H_2S-induced vasorelaxation of precontracted rat aorta was not affected significantly by vascular denervation, suggesting that the vasorelaxant effect of H_2S is not due to the altered neurotransmitter release from the autonomous or NANC nerve endings (Zhao and Wang, 2002). H_2S-induced relaxation of precontracted aorta and MAB was assessed after endothelium-removal, application of L-NAME or coapplication of apamin and charybdotoxin, and the H_2S concentration-response curve was shifted to the right in all cases ($P<0.05$) (Zhao *et al*., 2001; Cheng

et al., 2004). In the presence of NO-donors such as Na-nitroprusside (SNP) and morpholinosydnonimine, H_2S-induced vasorelaxation of precontracted thoracic aorta was greatly enhanced (Hosoki *et al*., 1997). These results suggest that H_2S-induced vasorelaxation may be partially facilitated by an enodothelium-dependent mechanism involving the release of EDRF such as NO from the vascular endothelium. However, the NO-/endothelium-dependence of H_2S-induced vasorelaxation is controversial as studies by Zhao and Wang (2002) showed that preincubation of aortic tissues with 60 μM H_2S for 15mins significantly inhibited SNP-induced vasorelaxation.

1.3.4.2.2.2 INVOLVEMENT OF K_{ATP} CHANNELS

It was postulated that H_2S targets K_{ATP} channels in vascular SMCs to bring about vasorelaxation (Zhao *et al*., 2001; Cheng *et al*., 2004). H_2S-induced relaxation of rat aortic tissues or mesenteric artery beds (MAB) precontracted with phenylephrine was mimicked by a K_{ATP} channel opener pinacidil but concentration-dependently inhibited by glibenclamide (Zhao *et al*., 2001; Cheng *et al*., 2004). In isolated single SMCs, K_{ATP} channel currents in rat aortic or MAB SMCs were significantly and reversibly increased by either H_2S or pinacidil (Zhao *et al*., 2001; Cheng *et al*., 2004). Increased potassium conductance led to membrane hyperpolarization of SMCs that was reversible by gibenclamide (Zhao *et al*., 2001). A direct action of H_2S on K_{ATP} channel proteins, rather than the interfered ATP metabolism by H_2S, was proposed based on three lines of evidence (Zhao *et al*., 2001). First, intracellular ATP concentration in these studies was clamped at a fixed level by dialyzing cells with the

pipette solution. Second, the effect of H_2S on K_{ATP} channels was quickly reversed on washing out H_2S from the bath solution. Third, intentionally varying ATP concentrations inside the cell (from 0.2 to 3 mM) did not change the excitatory effect of H_2S on K_{ATP} channels. The results by Zhao *et al*., 2001 identified H_2S as the first gaseous opener of K_{ATP} channels in vascular SMCs.

1.3.4.2.2.3 INDEPENDENCE OF cGMP PATHWAY

Unlike NO or CO, H_2S relaxation of vascular tissues was found to be independent of the activation of cGMP pathway (Zhao and Wang, 2002). Whereas the vasorelaxation induced by NO was virtually abolished by 1*H*-[1,2,4]oxadiazolo-[4,3-a]quinoxalin-1-one (ODQ) or NS-2028, inhibitors of soluble guanylyl cyclase (sGC), the H_2S-induced vasorelaxation was potentiated by the inhibitors. The potentiated vasorelaxant effect of H_2S by QDQ was suppressed by superoxide dismutase, suggesting that free radicals such as superoxides may be generated during QDQ-potentiated H_2S-induced vasorelaxation.

1.3.4.3 ROLE OF H_2S IN VASCULAR DISEASES

Reduced expression and activity of CSE in lung tissues of hypoxic pulmonary hypertensive rats (Zhang *et al*., 2003) and in thoracic aorta of spontaneously hypertensive rats (Yan *et al*., 2003) was coupled with a decrease in plasma H_2S concentration. In contrast, in septic and endotoxin shock rats, arterial H_2S was

significantly increased (Yan *et al*., 2003). Exogenous supply of H_2S could increase the plasma level of H_2S, enhance CSE activity, oppose the rise in pulmonary arterial pressure as well as blood pressure, and lessen the pulmonary vascular and aorta structural remodeling that occurs during hypoxic pulmonary hypertension (HPH) and spontaneous hypertension respectively (Zhang *et al*., 2003; Yan *et al*., 2003). H_2S may play a regulatory role in the pathogenesis of HPH through up-regulating the carbon monoxide/heme oxygenase pathway (Zhang *et al*., 2004). In addition, endogenous H_2S/CSE pathway may be involved in the pathogenesis of isoproterenol-induced myocardial injury (Geng *et al*., 2004). Administration of exogenous H_2S effectively protects myocytes and contractile activity, at least by its direct scavenging of oxygen-free radicals and reducing the accumulation of lipid peroxidations (Geng *et al*., 2004).

1.4 AIMS OF STUDY

Sto*nus*toxin (***Sto***nefish ***N***ational ***U***niversity of ***S***ingapore, SNTX) is a 148kDa, 2-subunit, multifunctional lethal factor isolated from Stonefish, *Synanceja horrida* venom (Poh *et al*., 1991). The myriad number of biological activities it cause include species-specific haemolysis and platelet aggregation, edema-induction, hypotension, endothelium-dependent vasorelaxation, and inhibition of neuromuscular function in the mouse hemidiaphragm and chick biventer cervicis muscle (Low *et al*., 1993; Khoo *et al*., 1995; Chen *et al*., 1997; Sung *et al*., 2002). In this thesis, the focus will be on delineating the biochemical pathways and the possible structural elements involved in the potent vasorelaxation caused by SNTX. Of interest is the potential involvement of hydrogen sulfide (H_2S) acting in synergy with nitric oxide (NO) in SNTX-induced vasorelaxation. In addition, the role played by the SNTX B30.2 domains in SNTX-induced vasorelaxation will also be investigated.

CHAPTER TWO

MATERIALS AND METHODS

2.1 GENERAL MOLECULAR METHODS

2.1.1 RNA AGAROSE/FORMALDEHYDE GEL ELECTROPHORESIS

2.1.1.1 GEL PREPARATION

Dissolve 1.0g agarose in 87ml H_2O in microwave and cool to 60°C. Add 10ml 10X MOPS running buffer (0.4M MOPS, pH 7.0, 0.1M sodium acetate, 0.01m EDTA), 3ml 12.3M (37%) formaldehyde, and 2µl ethidium bromide (10mg/ml). Pour the gel inside the fume hood and allow it to set.

2.1.1.2 RNA SAMPLE PREPARATION AND ELECTROPHORESIS

1. Prepare the total RNA sample as follow:

RNA (0.5 – 10µg)	4.5µl
10x MOPS running buffer	2.0µl
12.3M formaldehyde	3.5µl
Dionized formamide	10.0µl

2. Incubate the sample at 65°C for 10mins and spin-down the sample.
3. Add 2µl sterile RNA loading buffer (1mM EDTA, pH 8.0, 0.25% (w/v) bromophenol blue, 50% (v/v) glycerol) to the sample.
4. Electrophoresis at 80V was carried out using 1x MOPS running buffer.
5. After electrophoresis, wash the gel twice in deionized water.

2.1.1.3 QUANTITATION AND QUALITATIVE ANALYSIS OF TOTAL RNA

Samples were diluted appropriately and OD_{260} and OD_{280} were measured using a quartz cuvette. 1 OD_{260} = 40 µg/ml RNA. OD_{260}/OD_{280} should be between 1.5 and 2.

2.1.2 DNA AGAROSE GEL ELECTROPHORESIS

0.8% agarose gel in 1X TAE was prepared. After the molten agarose has cooled to ~55°C, add ethidium bromide to a final concentration of 0.5µg/ml. Mix DNA with 6X DNA gel loading buffer before gel loading.

Composition of 6X DNA gel loading buffer: 0.09% bomophenol blue, 0.09% xylene cyanol FF, 60% glycerol and 60mM EDTA.

2.1.2.1 PURIFICATION OF DNA CYCLE SEQUENCING PRODUCTS

Ethanol Precipitation Protocol:

1. For each reaction, prepare a 1.5ml microcentrifuge tube by adding 2µl of 3M sodium acetate, pH 4.6 and 50µl of 95% ethanol.
2. Transfer the entire 20µl of cycle sequencing reaction product to the microcentrifuge tubes. Vortex and place on ice for 10mins.
3. Centrifuge at 12,000X g for 20mins.

4. Remove the ethanol solution completely and rinse the pellet with 70% ethanol. Remove the ethanol and dry the pellet.

2.1.3 POLYACRYLAMIDE GEL ELECTROPHORESIS (PAGE)

Methods for denaturing (SDS) PAGE were adapted from Current Protocols in Molecular Biology (1999). Bio-Rad Mini-PROTEAN II gel set was used.

2.1.3.1 SAMPLE PREPARATION

For reducing SDS-PAGE, dissolve samples 1:5 with 6X PAGE loading buffer: 3.5M Tris-HCl, pH 6.8, 10.28% (w/v) SDS, 36% (v/v) glycerol, 5% mercaptoethanol, 0.012% (w/v) bromophenol blue. Then, immediately heat the sample at 100°C for 5 mins.

For non-reducing SDS-PAGE, omit mercaptoethanol in the preparation of 6X PAGE loading buffer.

2.1.3.2 GEL PREPARATION

Table 2. Receipe for denaturing polyacrylamide separating gels.

Stock Solution	**Final acrylamide concentration in separating gel (%)**									
	5	**6**	**7**	**7.5**	**8**	**9**	**10**	**12**	**13**	**15**
30% acrylamide / 0.8% bisacrylamide	1.67	2.00	2.33	2.50	2.67	3.00	3.33	4.00	4.33	5.00
1.5M Tris-C / 0.4% SDS; pH 8.8	2.50	2.50	2.50	2.50	2.50	2.50	2.50	2.50	2.50	2.50
MilliQ water	5.83	5.50	5.17	5.00	4.83	4.50	4.17	3.50	3.17	2.50
10% (w/v) ammonium persulfate	0.03	0.03	0.03	0.03	0.03	0.03	0.03	0.03	0.03	0.03
TEMED	0.01	0.01	0.01	0.01	0.01	0.01	0.01	0.01	0.01	0.01

Table 3. Receipe for denaturing polyacrylamide stacking gels.

Stock Solution	**Final acrylamide concentration (3.9%)**
30% acrylamide / 0.8% bisacrylamide	0.65
0.5M Tris-Cl / 0.4% SDS; Ph 6.8	1.25
MilliQ water	3.05
10% (w/v) ammonium persulfate	0.025
TEMED	0.005

2.1.3.3 PROTEIN MARKERS

For SDS-PAGE, Bio-Rad's broad range molecular weight standard was used.

2.1.3.4 RUNNING BUFFER

The electrode buffer for SDS-PAGE is 0.025M Tris-HCl, pH 8.3 containing 0.192M glycine and 0.1% SDS.

2.1.3.5 PAGE RUNNING CONDITION

For one minigel, run at 15mA of constant current until the dye front reached the end of the gel. For two gels, the current was doubled.

2.1.3.6 STAINING AND DESTAINING PAGE GELS

Gels were stained for 30mins in solution containing 0.25g Coomassie Blue R-250 in 45ml methanol, 45ml water and 10ml glacial acetic acid. Then destain gels in solution I (500ml methanol, 70ml glacial acetic acid and 880ml water) for repaid destaining, or in solution II (50ml methanol, 70ml glacial acetic acid ad 880ml water) for normal destaining.

For proteins not detectable by Coomassie Blue staining, Bio-Rad Silver Staining kit was used.

2.1.3.7 PERMANENT RECORD OF PAGE GELS

Gels were photographed with Kodak Science digital camera DC120, and dried in between two pieces of cellophane paper.

2.1.4 DETERMINATION OF PROTEIN CONCENTRATION

The Bio-Rad protein assay kit based on the principle of Bradford (1976) was used for the determination of protein concentration. Bovine serum albumin (BSA) was used in the construction of the standard curve.

2.1.5 BIOINFORMATICS ANALYSIS

Bioinformatics analysis of recombinant fusion proteins were carried out using bioinformatics tools available on the NUS website: www.bic.nus.edu.sg. In particular, the programs PRETTYSEQ and PEPSTATS were used.

2.2 EXPRESSION STUDIES OF H_2S-GENERATING ENZYMES IN RAT THORACIC AORTA

2.2.1 TOTAL RNA EXTRACTION

Male Sprague-Dawley rats (280-300g) were killed by cervical dislocation and thoracic aorta weighing ~100mg/rat was dissected out, rinsed of blood in ice-cold saline and transferred to 1ml TRIzol reagent. The tissue was homogenized in ice and incubated for 5mins at room temperature. 0.2ml chloroform was added and reaction tubes were shaken vigorously for 15 sec and incubated for 2-3mins at room temperature. Centrifuge the samples at 12,000Xg, 15mins at 4°C. Transfer the upper aqueous phase to a fresh tube. Precipitate RNA from the aqueous phase by mixing it with 0.5ml isopropanol. Incubate samples at room temperature for 10mins and centrifuge at 12,000Xg, 10mins at 4°C. Remove supernatant and wash RNA pellet with 1ml 75% ethanol. Mix the sample by vortexing and centrifuge at 7,500Xg, 5mins at 4°C. Remove the ethanol and air dry RNA pellet. Then dissolve RNA in 20μl RNase-free water and incubate the solution at 55°C for 10mins.

2.2.2 PRIMER DESIGN FOR CYSTATHIONINE-γ-LYASE (CSE) AND CYSTATHIONINE-β-SYNTHASE (CBS)

Primers for detection of the H_2S-generating enzymes CSE and CBS were designed using Primer Premier 4 from PREMIER Biosoft International. AY032875, rattus

norvegicus CSE mRNA, complete cds from Pubmed was used for the design of primers for CSE. For the design of CBS primers, the rattus norvegicus CBS sequences NM_012522, M88344, M88345, M88346 and M88347 from Pubmed were used. The primers were purchased from Research BioLabs and the sequences are as follow:

CSE:

Forward 5'-CAT GGA TGA AGT GTA TGG AGG C-3'

Reverse 5'-CGG CAG CAG AGG TAA CAA TCG-3'

CBS:

Forward 5'-GAG CGA GCC GGA ACC TTG AAG C-3'

Reverse 5'-CAC CTA TCC ACC ACC GCC CTG TC-3'

2.2.3 ONE-STEP RT-PCR

Qiagen One-step RT-PCR kit was used to check for mRNA expression of CSE and CBS in the thoracic aorta.

Table 4. The reaction components for one-step RT-PCR of CSE and CBS were as follow:

Component	**Volume / reaction**	**Final Concentration**
Master Mix		
RNase-free water	11.5μl	-
5x QIAGEN OneStep RT-PCR buffer	4.0μ1	1x
dNTP Mix(containing 10mM of each dNTP)	0.8μ1	400μM of each dNTP
Primer A	1.2μl	400μM
Primer B	1.2μl	400μM
QIAGEN OneStep RT-PCR Enzyme Mix	0.8μ1	-
Template RNA	0.5μ1	0.5μg/reaction
Total Volume	**20.0μ1**	**-**

Table 5. The thermal cycler conditions for the one-step RT-PCR of CSE and CBS.

Reverse transcription:	30min	50°C
Initial PCR activation steps:	15min	95°C
3-step-cycling		
Denaturation:	30sec	94°C
Annealing:	30sec	60°C (CSE); 58°C (CBS)
Extension:	30sec	72°C
Number of cycles:	28 (CSE); 35 (CBS)	
Final extension:	10min	72°C

2.3 CONFIRMATION OF BACTERIAL CLONES

(E. COLI BL21- pGEX-5X-1-αB30.2 & E. COLI BL21- pGEX-5X-1-βB30.2)

2.3.1 EXTRACTION OF PLASMID DNA

E. coli-BL21-pGEX-5X-1-αB30.2 or *E. coli-BL21*-pGEX-5X-1-βB30.2 (refer to Appendix) was innoculated into Luria broth containing 100μg/ml ampilcillin and grown overnight at 37°C. Plasmid was then extracted from the clones using Bio-Rad's Quantum Prep Plasmid Miniprep.

2.3.2 POLYMERASE CHAIN REACTION AMPLIFICATION OF B30.2 DOMAINS

PCR was carried out using Qiagen's Taq polymerase kit. Finnzymes dNTP mix and 5'- and 3'- pGEX sequencing primers from Amersham Biosciences were used.

5'-pGEX sequencing primer

5'-GGG CTG GCA AGC CAC GTT TGG TG-3'

3'-pGEX sequencing primer

5'-CCG GGA GCT GCA TGT GTC AGA GG-3'

Table 6. The reaction components for B30.2 PCR were as follow:

Component	**Volume / reaction**	**Final Concentration**
Master Mix		
10X Qiagen PCR buffer	10.0µl	1X
dNTP mix (10mM each)	2.0µ1	200µM of each dNTP
5'-pGEX sequencing primer	4.0µ1	0.2µM
3'-pGEX sequencing primer	4.0µl	0.2µM
Taq DNA polymerase	0.5µl	2.5 units/reaction
Distilled water	59.5µ1	-
Template DNA	20.0µ1	≤1µg/reaction
Total Volume	**100.0µ1**	**-**

Table 7. The thermal cycler conditions for B30.2 PCR.

Initial Denaturation:	3min	94°C
3-step-cycling		
Denaturation:	1min	94°C
Annealing:	1min	50°C
Extension:	1min	72°C
Number of cycles:	25	
Final extension:	10min	72°C

2.3.3 DNA CYCLE SEQUENCING OF PCR PRODUCTS

DNA cycle sequencing was carried out using ABI Prism dRhodamine Terminator Cycle Sequencing Ready Reaction Kit with AmpliTaq DNA Polymarease, FS from Applied Biosystems. PCR products were purified for DNA sequencing using Microcon YM-100 Centrifugal unit.

Table 8. The reaction components for B30.2 cycle sequencing were as follow:

Reagent	**Quantity**
Terminator Ready Reaction Mix	8.0µl
Template purified PCR product, 10-30ng/µl	6.0µ1
5'-pGEX sequencing primer (3.2pmol)	1.3µ1
MilliQ water	4.7µ1
Total Volume	**20.0µ1**

Table 9. The thermal cycler conditions for B30.2 cycle sequencing.

Repeat for 25 cycles:
Rapid thermal ramp to 96°C
96°C for 30secs
Rapid thermal ramp to 50°C

50°C for 15secs
Rapid thermal ramp to 60°C
60°C for 4 mins
Rapid ramp to 4°C and hold

The cycle sequencing products were purified by ethanol precipitation and sent to National University Medical Institute Sequencing Laboratory for electrophoresis on ABI Prism 377.

2.4 PROTEIN PURIFICATION

2.4.1 PURIFICATION OF STONUSTOXIN FROM SYNANCEJA HORRIDA

The method of Poh *et al.*, 1991 was used with some modifications.

2.4.1.1 EXTRACTION OF S. HORRIDA VENOM

Live stonefish (*Synanceja horrida*) was kept at 4 °C overnight and their dorsal fin excised (Figure 11). The 13 dorsal spines in the fin were pulled out and the venom was extracted from the venom sac using a 1ml syringe fitted with a G-21 gauge needle. The venom was lyophilized and stored at -80 °C until protein purification.

2.4.1.2 SEPHACRYL S-200 HR GEL FILTRATION OF S. HORRIDA VENOM

All operations were carried out at 4°C. 253.6mg lyophilized *S. horrida* venom was reconstituted in 1.0ml of 0.05M sodium phosphate buffer, pH 7.4 and centrifuged at 12,000 g for 15mins to remove insoluble material. The supernatant was applied to a Sephacryl S-200 HR gel filtration column (1.6 X 100cm) previously equilibrated with the same buffer. Elution was carried out at a constant flow rate of 1ml/min and 3ml fractions were collected. The absorbance of the fractions was monitored at OD_{280}.

2.4.1.3 DEAE BIO-GEL A (100-200 MESH) ANION EXCHANGE CHROMATOGRAPHY

Peak 1 fractions from Sephacryl S-200 HR gel filtration was pooled together and loaded onto a DEAE Bio-Gel A (100-200 mesh) gel column (1.2 X 8.8 cm) that was pre-equilibrated with 0.05M sodium phosphate buffer, pH 7.4. The column was washed with 60ml of the same buffer before a linear sodium chloride gradient (0 to 0.15M sodium chloride in 0.05M sodium phosphate buffer pH 7.4, 150ml) was initiated. 2.5ml fractions were collected and their absorbance monitored at OD_{280}.

2.4.1.4 STORAGE OF PURIFIED STONUSTOXIN

Protein concentration of purified Stonustoxin was determined and stored at appropriate aliquots at -80°C after purification prior to usage.

Figure 11. Extraction of *Synanceja horrida* venom.

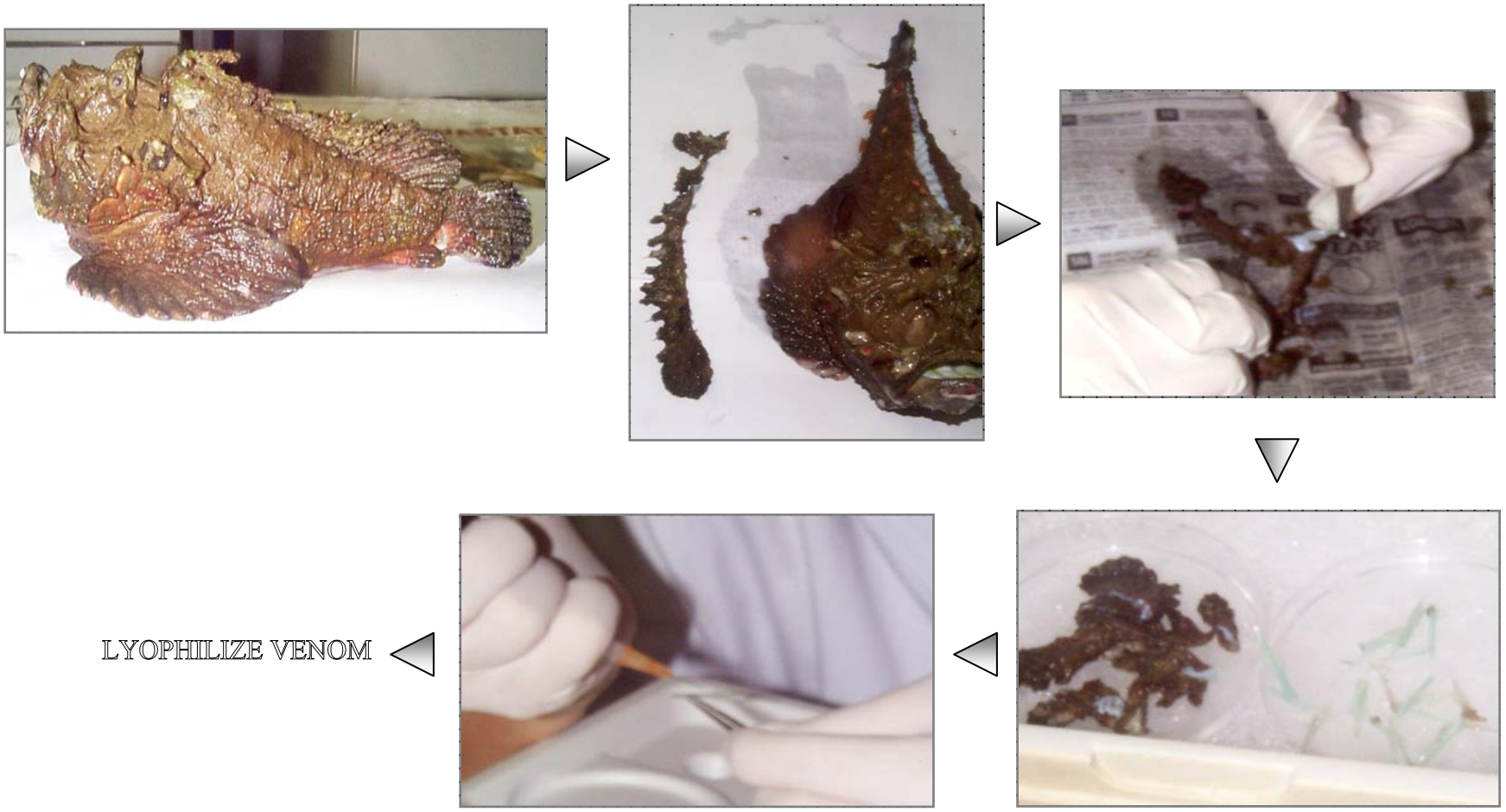

2.4.2 PURIFICATION OF GST, GST-αB30.2 AND GST-βB30.2 PROTEINS

For references, refer to GST Gene Fusion System, 3rd edition, Revision 2, Amersham Pharmacia Biotech, 1997; GSTrap FF, 1ml and 5ml Instruction Manual, Amersham Biosciences, 1996.

2.4.2.1 INDUCTION OF PROTEIN EXPRESSION IN BACTERIAL CELLS

E. coli BL21-pGEX-5X-1, *E. coli BL21*-pGEX-5X-1-αB30.2 or *E. coli BL21*-pGEX-5X-1-βB30.2 (refer to Appendix) was inoculated in 10ml Luria Broth (LB) broth containing 100μg/ml of ampicillin and incubated for 12-15 hours overnight at 37°C with vigorous shaking. The overnight culture was diluted 1:100 into 1*l* fresh pre-warmed LB broth containing 100μg/ml ampicillin and grown at 30°C with shaking until OD_{600} reaches 0.7. IPTG was added to a final concentration of 0.1mM and the culture was incubated with shaking at 30°C for 4 hours. The culture was then centrifuged at 7,700X g for 10 min at 4°C. The supernatent was discarded and the pellet was stored at -20°C.

Note: To ensure adequate aeration of the bacterial cultures, culture flasks were filled only to 20-25% of maximum capacity.

2.4.2.2 CELL LYSIS

Suspend frozen cell pellet (from 1*l* bacterial culture; 2.4.2.1) in 50ml ice-cold 1X phosphate buffered saline (PBS). Disrupt suspended cells in ice using a sonicator at strength 3, 10s pulse, 10s stop for a total of 8 min. Centrifuge sonicate at 12,000X g for 10 min at 4°C. Transfer the supernatent to a fresh container for purification of soluble GST, GST-αB30.2 or GST-βB30.2. Store the cell debris at -20 °C for possible purification of GST, GST-αB30.2 or GST-βB30.2 from inclusion bodies.

2.4.2.3 AFFINITY PURIFICATION OF SOLUBLE GST, GST-αB30.2 OR GST-βB30.2

Bacterial supernatent containing soluble GST, GST-αB30.2 or GST-βB30.2 proteins obtained from 2.4.2.2 was filtered through a 0.45μm Millipore filter. Fast Performance Liquid Chromatography (FPLC) was then employed for the purification of GST, GST-αB30.2 or GST-βB30.2. The filtered bacterial supernatant was applied to a 5ml GSTrapFF column previously equilibrated with 1X PBS. Binding of proteins to the GSTrappFF column occurs at a rate of 5ml/min. The column was washed thoroughly with 1X PBS (15 column volumes; 10ml/min) before being eluted with 50mM Tris-HCl, 10mM reduced glutathione (2ml/min; 1ml fractions collected).

2.4.2.4 ATTEMPTED REMOVAL OF GRO-EL FROM SOLUBLE GST-αB30.2 AND GST-βB30.2 USING AN ATP WASH BUFFER

Re: Trends in Genetics (1996) vol. 12, no. 6, pg 209-210. A method for separation of GST fusion proteins from co-purifying GroEL.

GST-αB30.2 or GST-βB30.2 was bound to 5ml GSTrapFF column as normal (section 2.4.2.3), and equilibrated with buffer 1 (50mM TEA pH 7.5, 50mM KCl, 20mM $MgCl_2$). After equilibration, the column was washed with 20 column volumes of 5mM adenosine 5' triphosphate (ATP) in buffer 1 (10ml/min). The column was then equilibrated in buffer 2 (50mM TEA, pH 8), and eluted with 50mM reduced glutathione in buffer 2 (2ml/min; 1ml fractions collected).

2.4.2.5 ATTEMPTED REMOVAL OF GRO-EL FROM SOLUBLE GST-αB30.2 USING AN ATP WASH BUFFER AND GRO-ES

Re: Trends in Genetics (1996) vol. 12, no. 6, pg 209-210. A method for separation of GST fusion proteins from co-purifying GroEL.

GST-αB30.2 was bound to 5ml GSTrapFF column as normal (section 2.4.2.3), and equilibrated with buffer 1 (50mM TEA pH 7.5, 50mM KCl, 20mM $MgCl_2$). After equilibration, the column was washed with 50 column volumes of 5mM adenosine 5' triphosphate (ATP) and 2.5μM GroES in buffer 1 (10ml/min). The column was then

equilibrated in buffer 2 (50mM TEA, pH 8), and eluted with 50mM reduced glutathione in buffer 2 (2ml/min; 1ml fractions collected).

2.4.2.6 PURIFICATION OF GST-αB30.2 AND GST-βB30.2 FROM INCLUSION BODIES

2.4.2.6.1 METHOD 1

Re: BioTechniques (1992) vol. 13, no. 6, pg 856-857. An improved procedure for purification of protein fused to glutathione-S-transferase.

Cell debris from the clarification of sonicated bacterial cells (from section 2.4.2.2) was suspended in 25ml 1.5% N-lauroylsarcosine, 25mM triethanolamine, 1mM EDTA, pH 8.0 and mixed for 10mins at 4°C. Centrifuge the suspension at 7,750X g; 4°C. Collect the supernatant and add Triton X-100 and $CaCl_2$ at final concentrations of 2% and 1mM respectively. Then add 25ml 1X PBS to the supernatant. Proceed with FPLC purification after filtering the supernatant through a 0.45µm Millipore filter. Binding of the proteins to the GSTrappFF 5ml column occurs at a rate of 5 ml/min. The column was washed thoroughly with 1X PBS (50 column volumes; 10ml/min) before elution with 50mM Tris-HCl, 10mM reduced glutathione at pH 8.0 (2ml/min; 1ml fractions collected).

2.4.2.6.2 METHOD 2

Re: Protein Expression and Purification (1999) vol. 16, pg331-339. Penicillin-binding protein 2a of *Streptococcus pneumoniae*: Expression in *Escherichia coli* and purification and refolding of inclusion bodies into a soluble and enzymatically active enzyme.

Cell debris collected from section 2.4.2.2 was resuspended in 70 ml of 50 mM Tris-HCl, pH 7.5, 1 mM EDTA, and 100 mM KCl (buffer A), and centrifuged at 12,000*g* for 10 min. This process was repeated five to six times. The pellet was collected, resuspended in 70 ml buffer A, and centrifuged at 760*g* for 10 min. The supernatent fraction was collected and designated as inclusion bodies preparation. The inclusion bodies preparation was centrifuged at 12,000*g* for 10 min. The resulting pellet was resuspended in 40 ml of 8M urea and then diluted gradually with 70 ml of buffer A until a small amount of white precipitate appeared. This preparation was centrifuged at 12,000*g* for 10 min, and the pellet was discarded. The supernatent fraction was dialyzed (10 kDa cutoff dialysis tubing) in 4 liters of buffer A at 4 °C overnight and then another 4 liters of buffer A for 10 hours. After dialysis, the protein preparation was centrifuged at 12,000*g* for 10 min to remove any remaining insoluble material. The supernatent fraction was desalted using Microcon (10 kDa cutoff membrane) and the protein retentate was redissolved in 1X PBS.

2.4.2.7 BUFFER EXCHANGE & STORAGE OF PURIFIED PROTEINS

Purified proteins were resuspended in 1X PBS using Centricon YM-10. The proteins were then quantitated and stored at appropriate aliquots at -80°C.

2.5 WESTERN BLOTTING: IMMUNORECOGNITION OF GST-αB30.2 AND GST-βB30.2 BY POLYCLONAL ANTIBODIES DIRECTED AGAINST SNTX

Electrophoresce proteins using SDS-PAGE. Prewet a sheet of polyvinylidene difluoride (PVDF) membrane in 100% methanol (10sec). Then wash the membrane in distilled water for 5 min before equilibrating it in protein transfer buffer (25 mM Tris, 190 mM glycine, 20% MeOH) for at least 10 min. Rinse the gel obtained from SDS-PAGE) with protein transfer buffer. Assemble the electroblotting casette and transfer the proteins from the gel to the membrane at 400mV, 50mA for 1 hr. Following transfer, mark the orientation of the gel. Rinse the PVDF membrane with 1X PBS, and block non-specific binding sites on the membrane by incubating it with 0.1%(v/v) Tween 20, 5%(w/v) dried skim milk in 1X PBS for 1 hr. After that, rinse the membrane twice with PBS-T (0.1%(v/v) Tween 20 in 1X PBS) followed by subsequent washing with excess PBS-T for 2 X 10 mins. Incubate the membrane for 1 hr with polyclonal anti-SNTX antibody obtained from rabbits by the subcutaneous injection of native SNTX (120μg) emulsified in complete Freund's adjuvant. Rinse the membrane again with PBS-T followed by more thorough washing with an excess of PBS-T for 2 X 10 mins. Then, incubate the membrane with anti-rabbit antibodies for 1 hr, followed by a similar washing step as above. Apply ECL detection reagents that have been pre-mixed in equal volumes to the membrane. Expose the membrane to an x-ray film.

2.6 ORGAN BATH STUDIES

As reference, refer to Current Protocols in Pharmacology, 2001.

2.6.1 KREBS PHYSIOLOGICAL SOLUTION

Krebs physiological solution (in mM): NaCl 118; KCl 4.8; KH_2PO_4 1.2; $CaCl_2$ 2.5; $NaHCO_3$ 25; $MgSO_4$ 2.4; D-(+)-glucose 11.0. The solution was aerated vigorously with 5% CO_2; 95% O_2 for ten minutes prior usage. Throughout the entire experiment, Krebs solution containing tissue was bubbled with 5% CO_2; 95% O_2.

Table 10. Preparation of Krebs' physiological solution.

Salt	**NaCl**	**KCl**	**$CaCl_2$**	**$MgSO_4$**	**KH_2PO_4**	**$NaHCO_3$**	**Glucose**
Stock Concentration	25%	10%	10%	10%	5%	-	-
Volume	(ml)	(ml)	(ml)	(ml)	(ml)	(g)	(g)
2 litre	55.2	7.2	5.6	5.8	6.4	4.2	4.0
3 litre	82.8	10.8	8.4	8.7	9.6	6.3	6.0
4 litre	110.4	14.4	11.2	11.6	12.8	8.4	8.0
5 litre	138.0	18.0	14.0	14.5	16.0	10.5	10.0

2.6.2 TISSUE PREPARATION

Male Sprague-Dawley (SD) rats (250-300g) were killed by cervical dislocation. The thoracic wall was cut open and thoracic aorta (immediately anterior to the spine) was extracted, washed of blood, cleaned of surrounding connective tissue and cut into rings of approximately 2 mm in length Figure 12. Care was taken not to pull on the aorta and not to damage the endothelium during the entire process. Aortic rings were gently hooked to a string and a metal hook, and transferred to a 2.5 ml organ bath filled with Krebs solution aerated with 5% CO_2; 95% O_2. The aortic ring was mounted such that its tension was measured with a force transducer (ADInstruments model: MLT0201) that can measure isometric forces in the range of 5mg to 25g weight. The basal tone of the aortic ring was set to a tension of 1.0 - 1.5g and the aortic rings were allowed to stabilize for 1 hr. The organ bath was maintained at $37 \pm 1°C$ throughout the entire experiment. Figure 13 shows a typical organ bath set-up.

Figure 12. Pictorial representation of the isolation and processing of Sprague Dawley (SD) rat's aorta for organ bath studies.

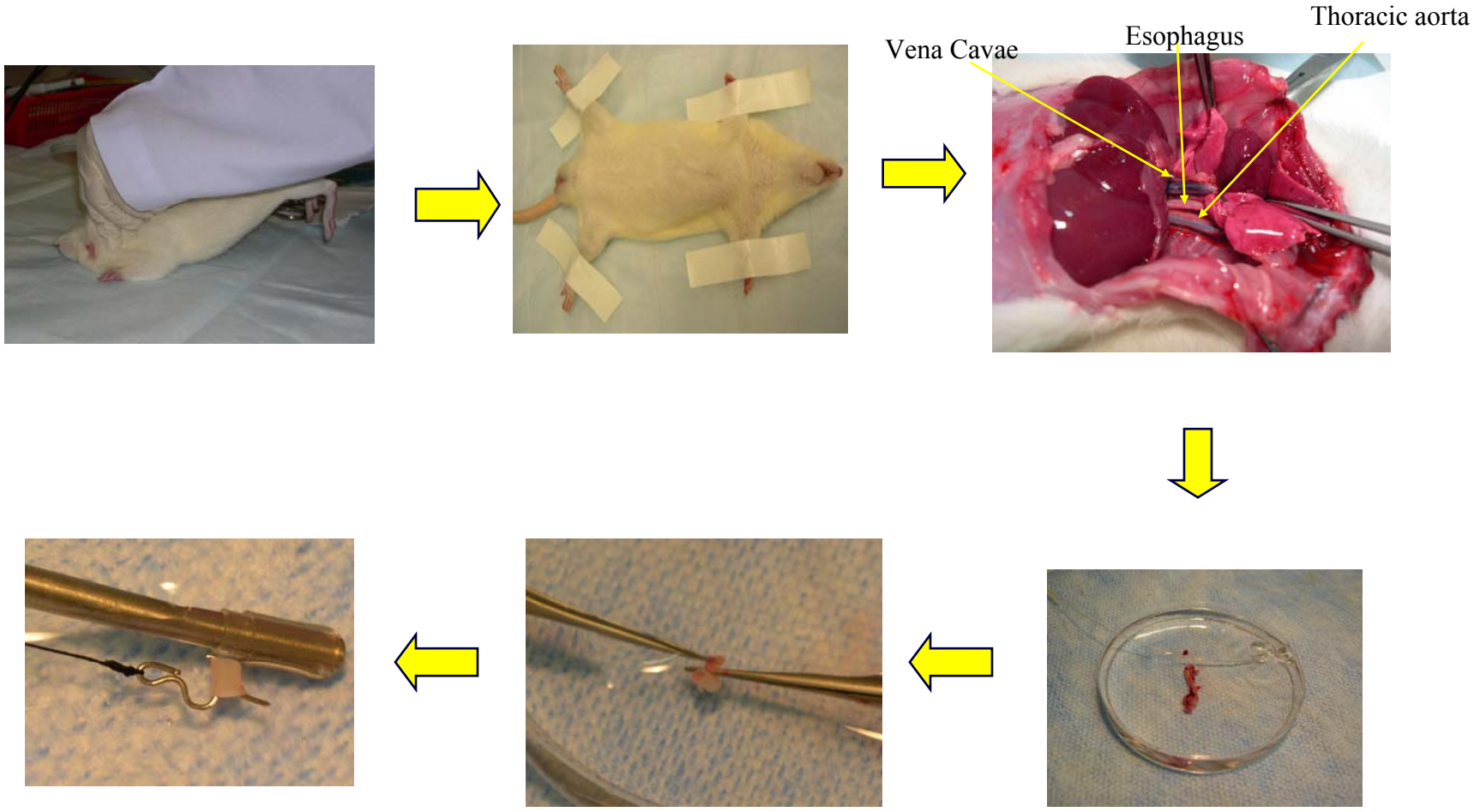

Figure 13. A typical organ bath set-up. The aortic ring was mounted in an organ bath filled with pre-warmed 37°C Krebs solution bubbled with 5% CO_2; 95% O_2. The tension of the aortic ring was monitored by an isometric force transducer connected to an ADInstrument PowerLab that is connected to a computer. The tension of the ring was monitored in real-time by the ADInstrument Chart 5 software.

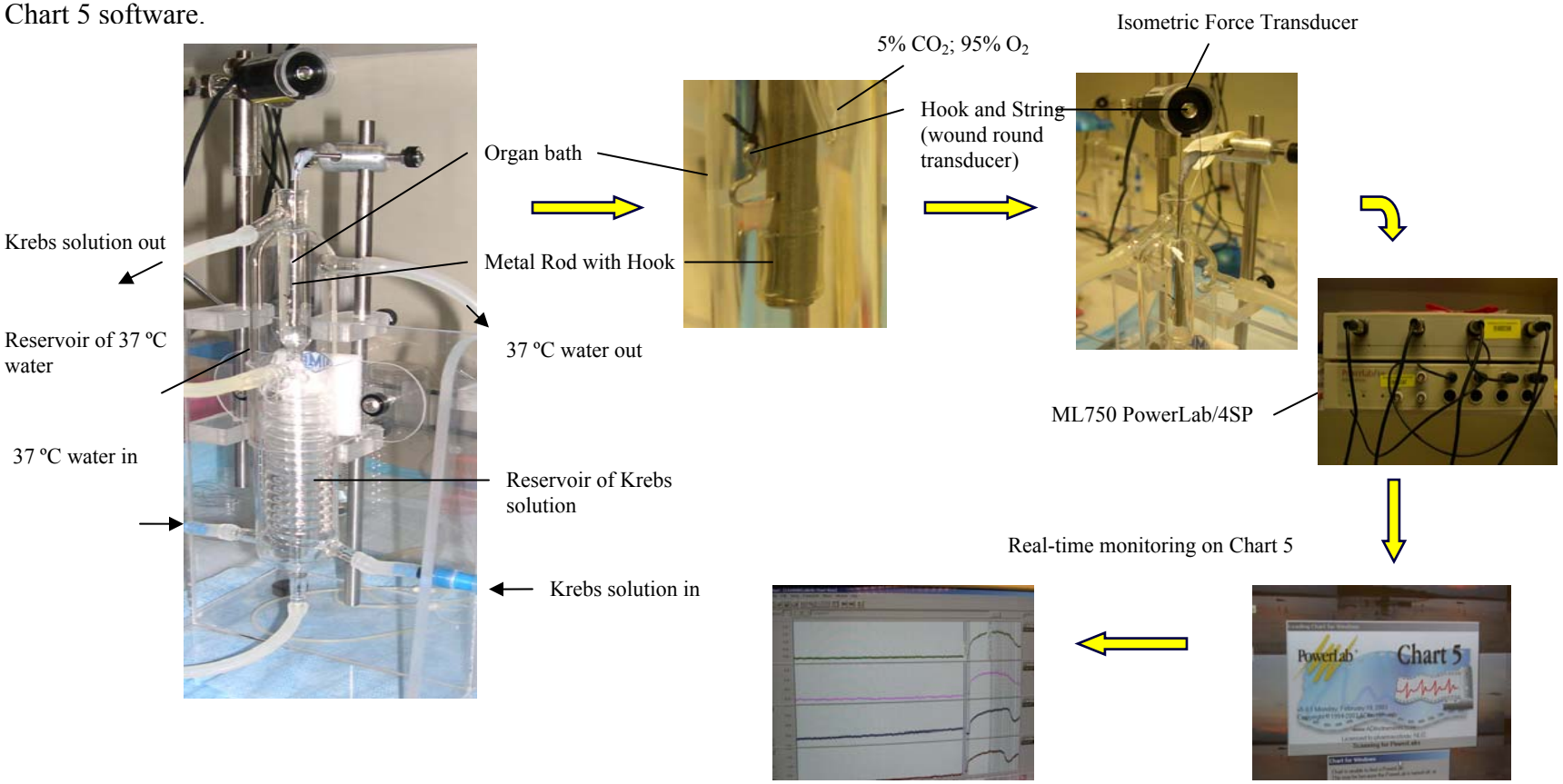

2.6.3 PRELIMINARY EXPERIMENTS

2.6.3.1 Testing the Response of 2mm Thoracic Aortic Rings to Cumulative Concentrations of L-phenylephrine hydrochloride (PE)

Table 11. Table showing the cumulative concentration of PE used in 2.5ml organ baths to contract 2mm thoracic aortic rings. The amount of drug to add each time to achieve the cumulative concentration was shown. The total volume of drug added to an organ bath should not exceed 10% of the organ bath's volume.

Conc (uM)	Cumulative Conc (uM)	Vol of 0.01M Stock (ul)	Vol of 0.0001M Stock (ul)
0.015	0.015	-	0.375
0.02	0.035	-	0.5
0.04	0.075	-	1
0.08	0.155	-	2
0.16	0.315	-	4
0.32	0.635	-	8
0.64	1.275	-	16
1.28	2.555	0.32	-
2.56	5.115	0.64	-
5.12	10.235	1.28	-
10.24	20.475	2.56	-
Total Volume		36.675 μl (i.e. 1.467% of organ bath's volume)	

2.6.3.2 Testing the Response of 0.32μM PE- precontracted 2mm Thoracic Aortic Rings to Cumulative Concentrations of Acetylcholine Chloride (Ach)

Table 12. Table showing the cumulative concentration of Ach used in 2.5ml organ baths to relax the 0.32μM PE-precontracted 2mm thoracic aortic rings. The amount of

drug to add each time to achieve the cumulative concentration was shown. The total volume of drug added to an organ bath should not exceed 10% of the organ bath's volume.

Conc (uM)	Cumulative Conc (uM)	Vol of 0.01M Stock (ul)	Vol of 0.0001M Stock (ul)
0.015	0.015	-	0.375
0.02	0.035	-	0.5
0.04	0.075	-	1
0.08	0.155	-	2
0.16	0.315	-	4
0.32	0.635	-	8
0.64	1.275	-	16
1.28	2.555	0.32	-
2.56	5.115	0.64	-
5.12	10.235	1.28	-
10.24	20.475	2.56	-
Total Volume		36.675 μl (i.e. 1.467% of organ bath's volume)	

2.6.4 EXPERIMENTS

Before actual experimentation, 2mm thoracic aortic rings were checked for their responsiveness and endothelial integrity. 0.32μM PE-precontracted aortic rings that exhibit greater or equal to 70% vasorelaxation with 2.56μM Ach were used for further experimentation (Figure 14).

Figure 14. Test of 2mm thoracic aortic rings with 0.32μM L-phenylephrine and 2.56μM acetylcholine before actual experimentation. 0.32μM L-phenylephrine precontracted aortic rings exhibiting greater or equal to 70% vasorelaxation with 2.56μM acetylcholine were used for further experimentation after a washing (with fresh Krebs) and stabilization period. Otherwise, they were disposed.

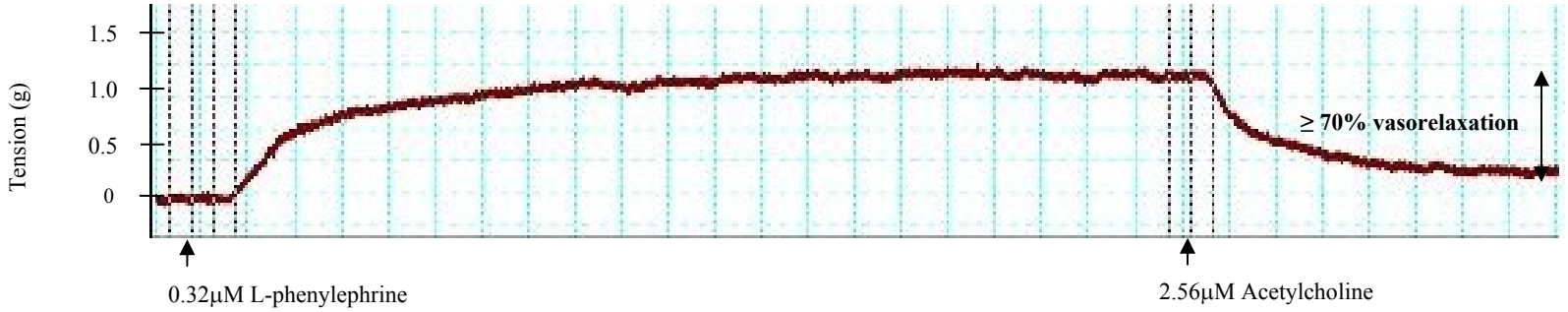

2.6.4.1 Response of 0.32μM PE- precontracted 2mm Rat Thoracic Aortic Rings to Cumulative Concentrations of Stonustoxin (P-C protein)

Table 13. Table showing the cumulative concentration of Stonustoxin (F68 of P-C protein) used in 2.5ml organ baths to relax 0.32μM PE-precontracted aortic rings. The amount of drug to add each time to achieve the cumulative concentration was shown. The total volume of drug added to an organ bath should not exceed 10% of the organ bath's volume.

Conc (ng/ml)	Conc (ng/2.5ml bath)	Cumulative Concentration (ng/ml)	Vol of 151.131 ng/μl Stock (ul)	Vol of 1:1 diluted Stock i.e. 75.566 ng/μl Stock (ul)
10	25	10	-	0.33
10	25	20	-	0.33
20	50	40	0.33	-
40	100	80	0.66	-
80	200	160	1.32	-
160	400	320	2.65	-
320	800	640	5.29	-
Total Volume		36.675 μl (i.e. 1.467% of organ bath's volume)		

2.6.4.2 Response of 0.32μM PE- precontracted 2mm Thoracic Aortic Rings to Cumulative Concentrations of Recombinant Proteins

Table 14. Table showing the cumulative concentration of recombinant proteins used in 2.5ml organ baths to relax 0.32μM PE-precontracted aortic rings.(Note: The total volume of drug added to an organ bath should not exceed 10% of the organ bath's volume.)

Conc added (nM)	Cumulative Concentration (nM)
0.0629	0.0629
0.0629	0.126
0.1258	0.252
0.2517	0.503
0.503	1.01
1.01	2.01
2.01	4.03

2.6.4.3 Inhibitor studies

To elucidate the mechanisms leading to vasorelaxation of thoracic aorta by stonustoxin, experiments were conducted with various inhibitors (PAG, BCA, L-NAME, etc) as shown in Figure 15.

2.6.5 DATA ANALYSIS

The results were expressed as mean ± SE. All concentration-response curves were fitted with a Hill equation, from which IC_{50} was calculated. Student's t-test for unpaired samples was used to compare the mean difference between control and tested groups. For comparison of differences between control and experimental groups, ANOVA followed by a post-hoc analysis Dunnett's t-test was used.

Figure 15. Experimental Protocol to see the effect of various inhibitors on vasorelaxation of 0.32µM L-phenylephrine precontracted aortic rings by Stonustoxin.

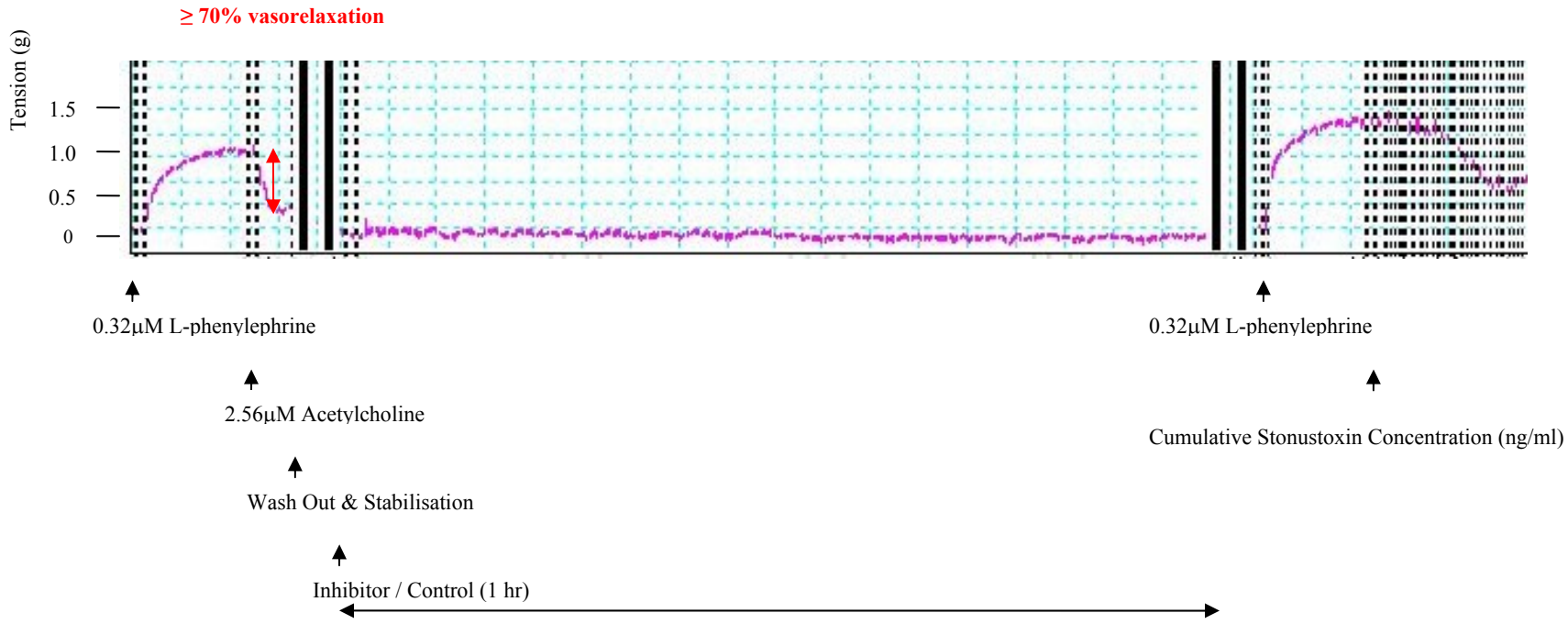

CHAPTER THREE

RESULTS

3.1 PURIFICATION OF STONUSTOXIN FROM *SYNANCEJA HORRIDA*

3.1.1 SEPHACRYL S-200 HR GEL FILTRATION OF *S. HORRIDA* VENOM

Gel filtration of crude *S. horrida* venom yielded three major protein peaks (P1, P2 and P3; Figure 16) as was obtained previously by Poh *et al.*, 1991. Fractions constituting P1 were pooled together for the next chromatographic step. P1 (containing 8.7mg protein) accounted for 38.7% of the total venom protein loaded onto the gel filtration column.

3.1.2 DEAE BIO-GEL A (100-200 MESH) ANION EXCHANGE CHROMATOGRAPHY OF P1

Anion-exchange chromatography of P1 yielded 3 protein peaks (P-A, P-B and P-C; Figure 17) instead of 4 protein peaks that were obtained by *Poh et al.*, 1991. Instead of using 4 days as was used by *Poh et al.*, 1991 for this purification step, one day is sufficient using the method described in Section 2.4.1.3.

Figure 16. Sephacryl S-200 HR (1.6 X 100 cm) gel filtration of 253.6mg lyophilized crude *S. horrida* venom suspended in 1ml of 0.05M sodium phosphate buffer, pH 7.4 (flow rate: 1ml/min). Elution buffer was 0.05M sodium phosphate buffer, pH 7.4. 3 ml fractions were collected.

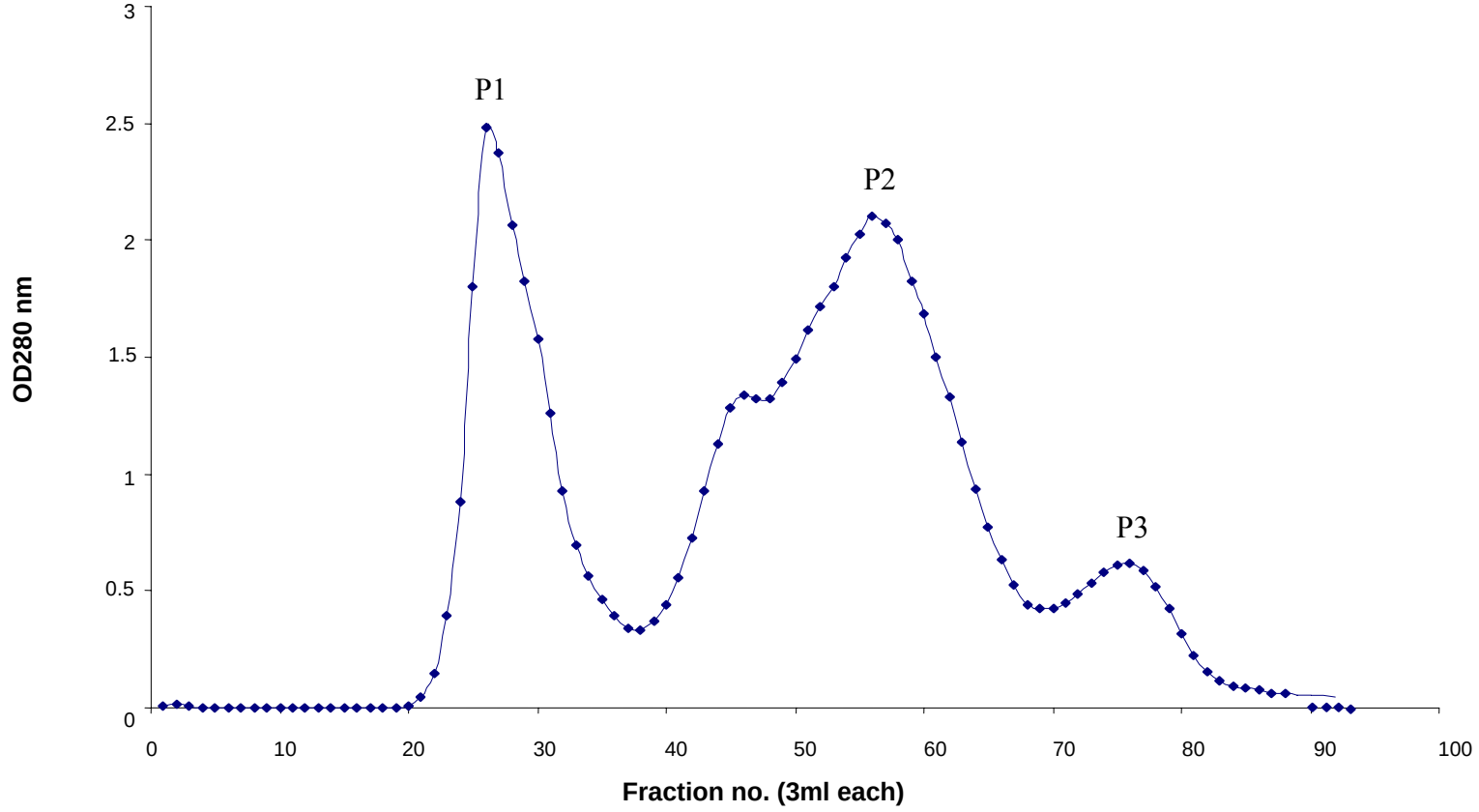

Figure 17. DEAE Bio-gel A (100-200mesh) anion-exchange chromatography of P1 (column dimension: 1.2 X 8.8 cm). 8.7mg protein was loaded onto the column and washed with 60ml of 0.05M sodium phosphate buffer before a linear sodium chloride gradient (0.15M NaCl in 0.05M sodium phosphate buffer, 150ml) was initiated. 2.5 ml fractions were collected.

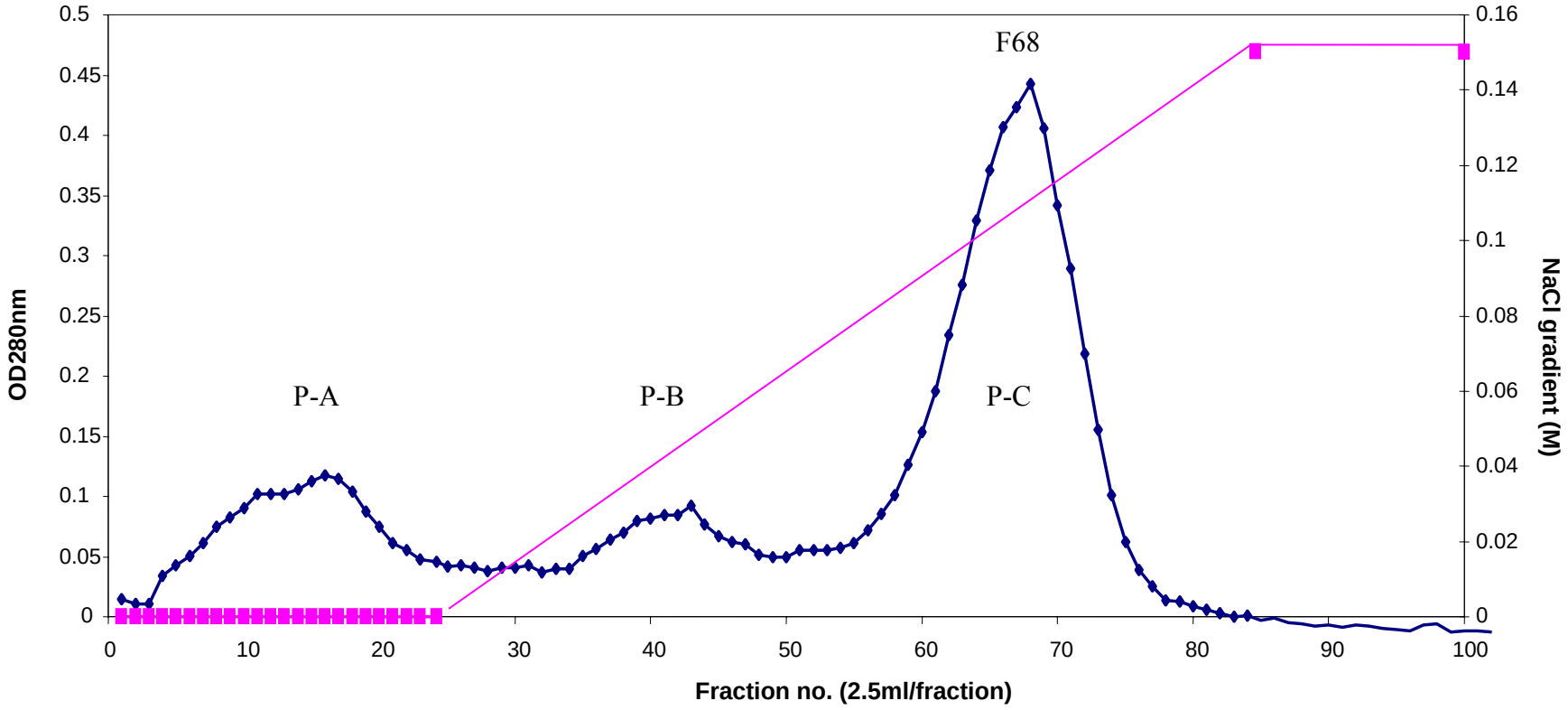

3.1.3 POLYACRYLAMIDE GEL ELECTROPHORESIS (PAGE) OF P-C

SDS-PAGE of F68 under both reducing (Figure 18) and non-reducing (results not shown) conditions shows 2 protein bands of ~71 and 79kDa. The protein in F68 that is made up of 2 subunits linked via non-sulfide bonds is probably Stonustoxin (SNTX). SNTX has a molecular weight of 148kDa made up of two subunits SNTX-α and SNTX-β with molecular weights of 71 and 79kDa respectively (Poh *et al.*, 1991). The subunits have been shown to be linked via non-disulfide linkages (Ghadessey *et al*., 1996). To confirm that the protein in F68 was indeed SNTX, it was tested for its vasorelaxing property (see Section 3.3).

Figure 18. Polyacrylamide gel electrophoresis of fraction 68 of P-C in 10% SDS-PAGE gel under reducing conditions. M stands for molecular weight marker.

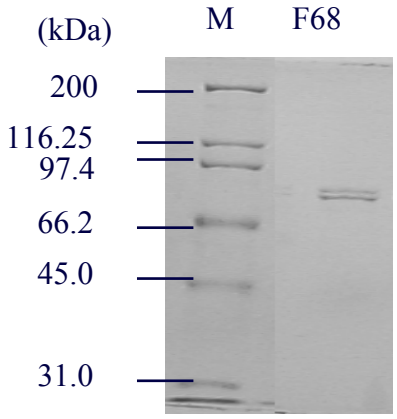

3.1.4 YIELD OF STONUSTOXIN FROM PURIFICATION

Approximately 3mg of SNTX was obtained from the purification process, i.e. 13.3% of total venom protein used for purification. The purification method by Poh *et al*., 1991 resulted in purification of SNTX which is 9 % of the total venom protein that was used for purification.

3.2 PRELIMINARY ORGAN BATH STUDIES

3.2.1 Response of 2mm Rat Thoracic Aortic Rings to Cumulative Concentrations of L-phenylephrine hydrochloride (PE)

Cumulative addition of PE to 2mm rat thoracic aortic rings led to progressive vasoconstriction (Figure 19). The cumulative dose-vasoconstriction curve produced by PE has an IC_{50} of 0.0390μM and an EC_{85} of 0.32μM. 0.32μM of PE was used to precontract 2mm rat thoracic aortic rings prior to any vasorelaxation experiments.

3.2.2 Response of 0.32μM PE- precontracted 2mm Rat Thoracic Aortic Rings to Cumulative Concentrations of Acetylcholine Chloride (Ach)

When the vasoconstriction response of 2mm rat thoracic aortic rings to 0.32μM PE has reached a stable plateau, Ach was added cumulatively. Cumulative addition of Ach to the 0.32μM PE-precontracted aortic rings led to progressive vasorelaxation (Figure 20). The cumulative dose-vasorelaxation curve produced by Ach has an IC_{50} of 0.0824uM, and an EC_{85} of 2.56μM.

3.2.3 Conclusive Remarks

Before any 2mm rat thoracic aortic rings was used for experimentation, it was tested with 0.32μM PE and 2.56μM Ach. 0.32μM PE-precontracted aortic rings that exhibit

at least 70% vasorelaxation with Ach were defined to be endothelium-intact and were used for further experimentation (Figure 14).

Figure 19. Vasoconstriction of 2mm rat thoracic aortic rings by cumulative concentrations of L-phenylephrine. (a) Experimental profile obtained. (b) Dose-Response Curve.

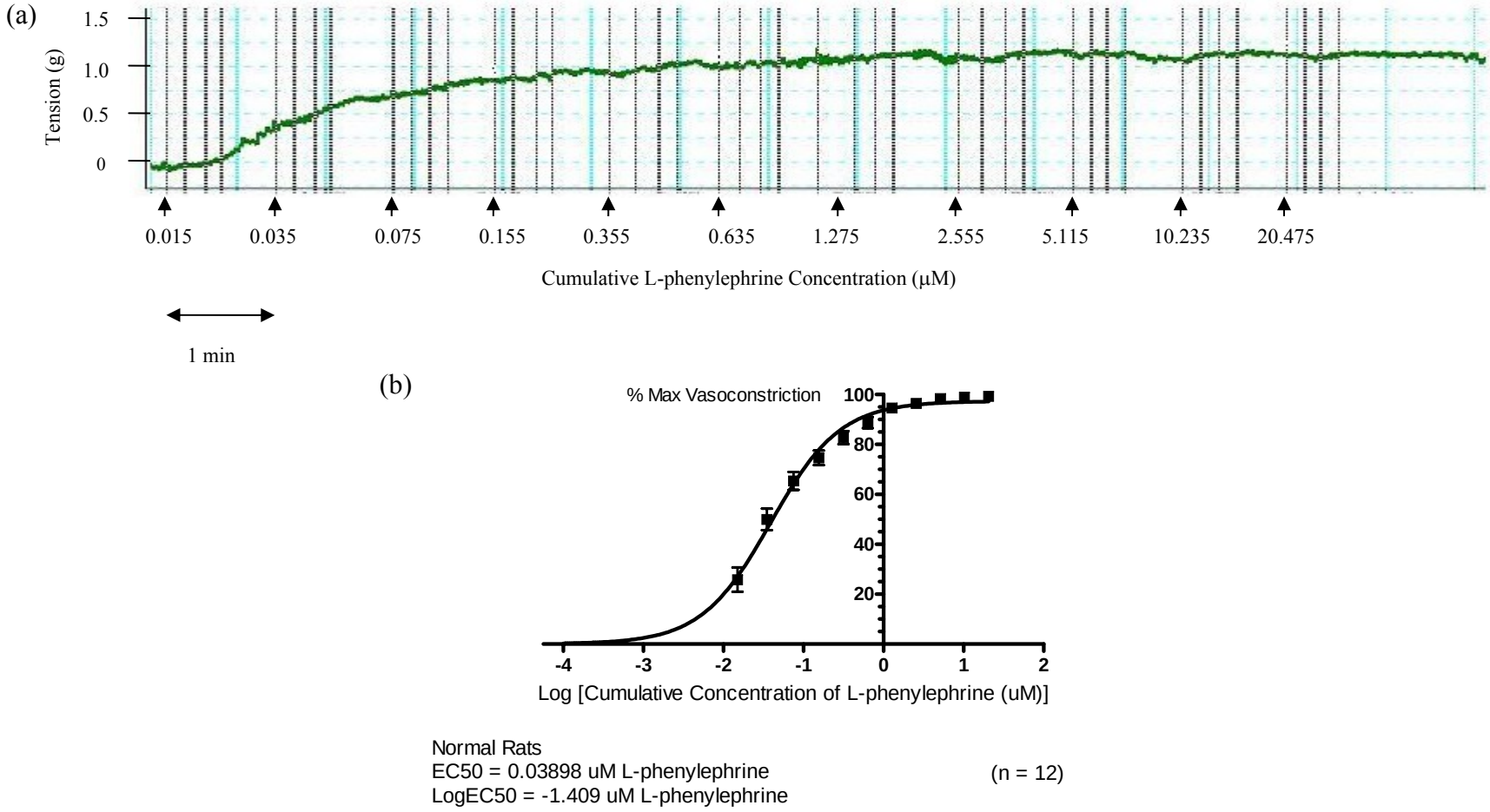

Figure 20. Response of 0.32μM L-phenylephrine precontracted 2mm thoracic aortic rings to cumulative concentration of acetylcholine. (a) Experimental profile obtained. (b) Dose-response curve.

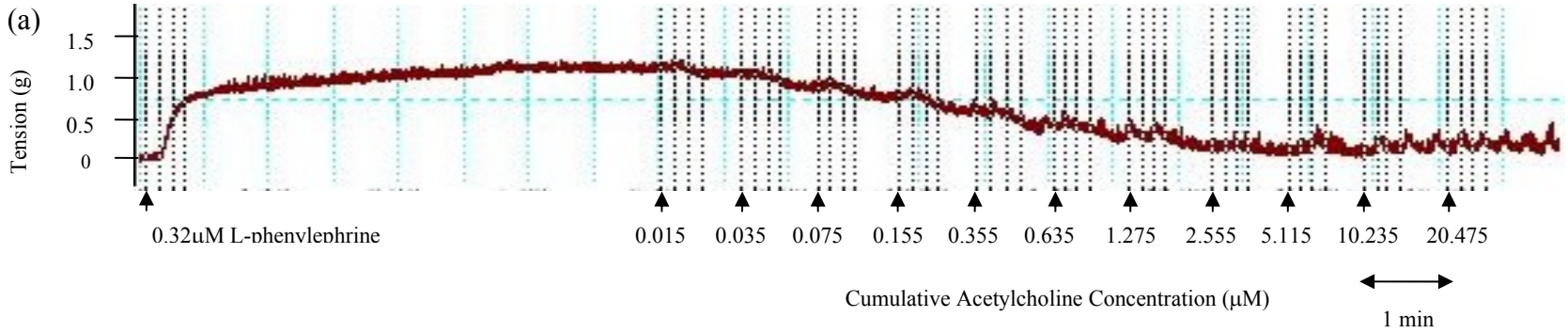

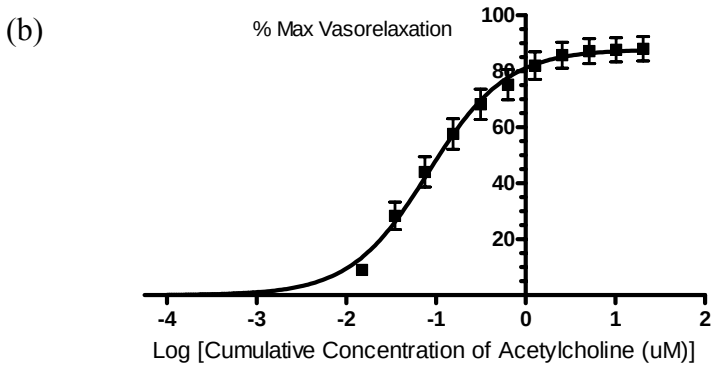

Normal Rats
EC50 = 0.08238 uM Acetylcholine
LogEC50 = -1.084 uM Acetylcholine

(n = 12)

*0.32uM L-phenyleprine ~ EC83
EC85 ~ 2.56uM Acetylcholine

3.3 VASORELAXATION BY STONUSTOXIN

3.3.1 Concentration-dependent vasorelaxation of 2mm, endothelium-intact, 0.32μM PE-precontracted thoracic aortic rings

To confirm that the purified protein in F68 of P-C (Section 3.1.3) was indeed stonustoxin, the protein was added cumulatively to endothelium-intact, 2mm, 0.32μM PE-precontracted rat thoracic aortic rings in organ bath studies to check whether if it causes vasorelaxation. Endothelium-intact aortic rings were defined as 0.32μM PE-precontracted 2mm thoracic aortic rings that exhibit at least 70% vasorelaxation with Ach (Figure 14). At concentrations ranging between 10 – 320ng/ml, the purified protein caused concentration-dependent vasorelaxation of the precontracted aortic rings, with $\log IC_{50}$ of 2.02 ± 0.00434ng/ml and maximum vasorelaxation of 49.1 ± 0.256 % (Figure 21).

3.3.2 Nitric oxide Involvement in SNTX-induced vasorelaxation

Earlier observations by Low *et al*., 1993 and Sung *et al*., 2002 showed that SNTX-induced vasorelaxation of precontracted aorta involve nitric oxide. To further confirm the identity of the purified protein (See Section 3.1.3), the protein was added to 2mm, endothelium-intact, 0.32μM PE-precontracted thoracic aortic rings that has been pre-incubated with 10μM L-NAME for 1hr. Preincubation of the aortic rings with 10 μM

L-NAME completely abolished the vasorelaxant effect of Stonustoxin on the PE-precontracted aortic rings (Figure 22).

3.3.3 Conclusive remarks

Together with the PAGE studies in Section 3.1.3, the experiments in this section confirmed that the protein in F68 was indeed SNTX.

Figure 21. Response of 0.32μM L-phenylephrine precontracted 2mm thoracic aortic rings to cumulative concentration of Stonustoxin (protein in F68 of P-C; refer to Section 3.1.3). (a) Experimental profile obtained. (b) Dose-response curve.

(a)

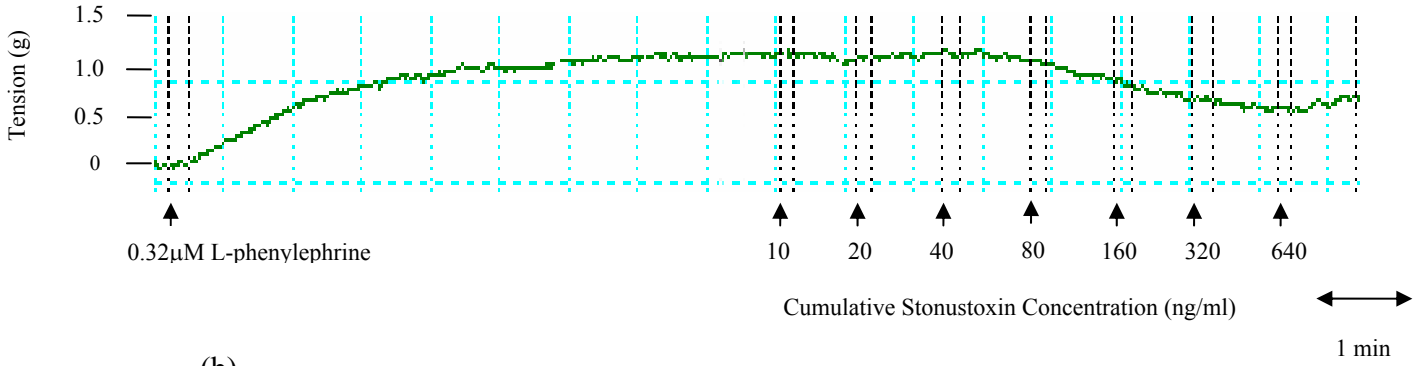

(b)

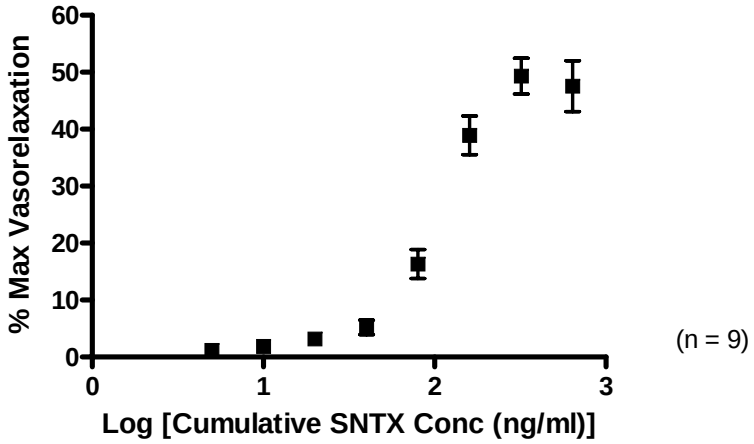

Figure 22. Nitric oxide involvement in SNTX-mediated vasorelaxation of 0.32µM PE-precontracted, endothelium-intact, 2mm thoracic aortic rings. The experimental profiles obtained in the presence of saline control or the nitric oxide-synthase inhibitor, L-NAME are shown.

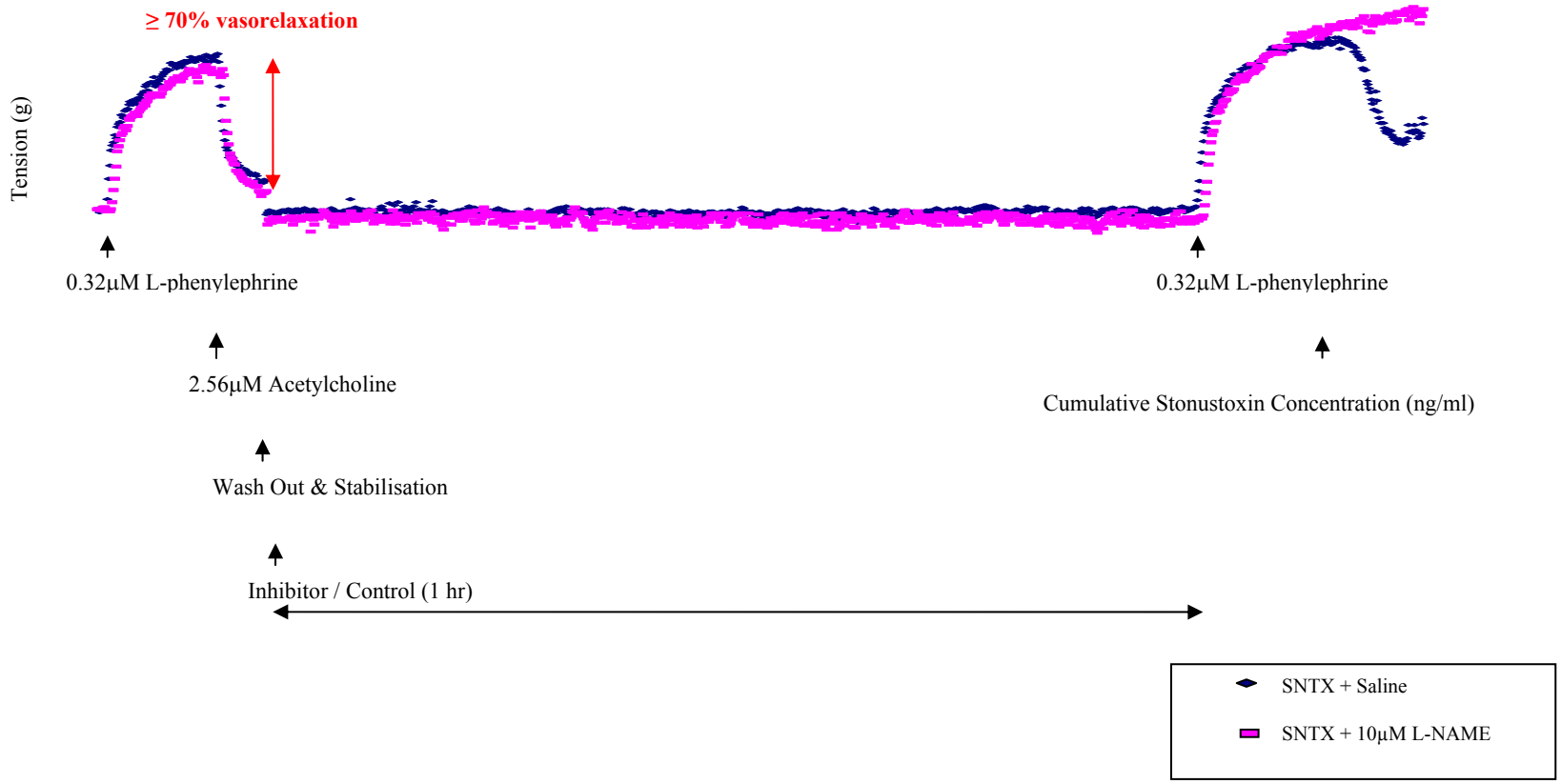

3.4 EXPRESSION STUDIES OF H_2S-GENERATING ENZYMES IN RAT THORACIC AORTA

Thoracic aorta weighing ~100mg was obtained from each rat weighing ~280-300g. For all RNA extractions, ~0.2μg of total RNA was obtained for 100mg of thoracic aorta. One-step RT-PCR using primers for the H_2S-generating enzymes cystathionine-γ-lyase (CSE) and cystathionine-β-synthase (CBS) showed that CSE but not CBS is expressed in rat thoracic aorta (Figure 23).

Figure 23. Expression of CSE but not CBS in rat thoracic aorta. Agarose gel electrophoresis of one-step RT-PCR products amplified using CSE and CBS primers and total RNA extracted from rat thoracic aorta. M is Promega's 100bp DNA ladder.

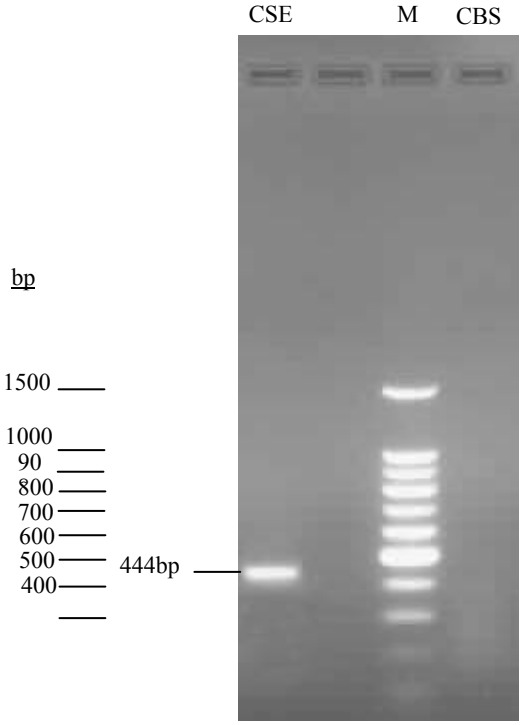

3.5 INVOLVEMENT OF HYDROGEN SULFIDE (H_2S) IN SNTX-INDUCED VASORELAXATION

Stonustoxin induced a concentration-dependent vasorelaxation of endothelium-intact, 2mm, 0.32μM PE-precontracted thoracic aortic rings ($logIC_{50}$ = 2.02 ± 0.00434 ng/ml). Using D, L-proparglyglycine (PAG) and β-cyano-L-alanine (BCA), irreversible and competitive inhibitors respectively of the H_2S-generating enzyme cystathionine-γ-lyase (CSE) in organ bath studies showed that H_2S is involved in SNTX-induced vasorelaxation of the PE-precontracted thoracic aortic rings (Figure 24; Table 16).

Pretreatment of the aortic rings with 1mM PAG for 1h prior to subsequent vasorelaxation of the endothelium-intact, PE-contracted aortic rings with Stonustoxin, shifted the $logIC_{50}$ of Stonustoxin to the right i.e. $logIC_{50}$ = 2.04 ± 0.00313 ng/ml ($P < 0.05$) (Figure 24a). Similar results were obtained with 1mM BCA, with $logIC_{50}$ of Stonustoxin shifted to the right, i.e. 2.14 ± 0.00310 ng/ml ($P < 0.05$) (Figure 24b). In addition, the maximum vasorelaxation induced by Stonustoxin was decreased from 49.1 ± 0.256 % to 39.0 ± 0.131 % in the presence of 1mM PAG ($P < 0.05$) (Table 16). In the presence of 1mM BCA, the maximum vasorelaxation induced by Stonustoxin is decreased to 38.8 ± 0.133% ($P < 0.05$). The maximum tension of the aortic rings induced by 0.32μM L-phenylephrine after pretreatment with inhibitors is not significantly different from the control ($P > 0.05$).

Figure 24. The effect of (a) D, L-proparglyglycine (PAG) and (b) β-cyano-L-alanine (BCA) on SNTX-induced vasorelaxation of 2mm, endothelium-intact, 0.32μM PE-precontracted thoracic aortic rings. The original records from experiments (inhibitor & control) conducted with segments of one aortae (top) and data represented as mean ± SEM (bottom) are shown. (c) Combination of (a) and (b). * $p < 0.05$ vs. saline control.

(a)

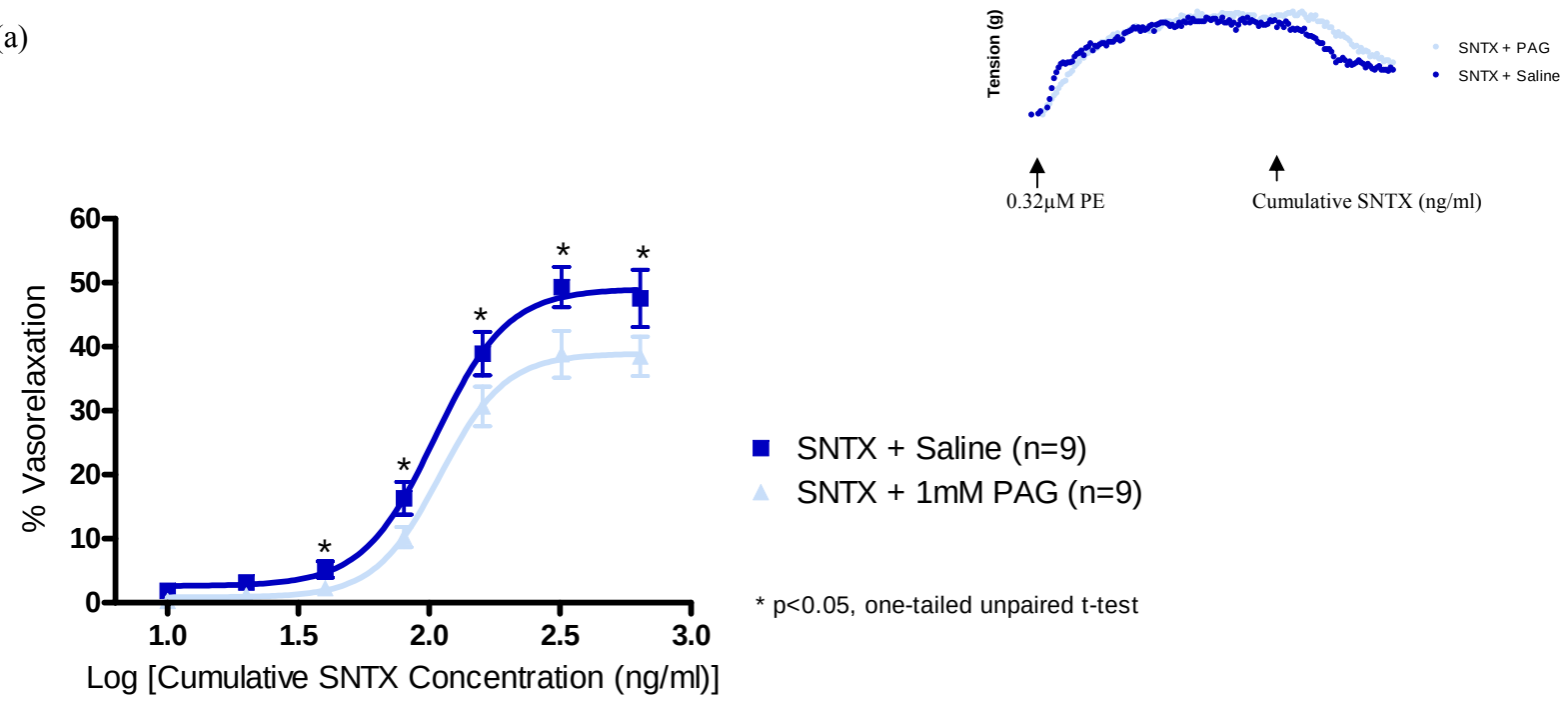

(b)

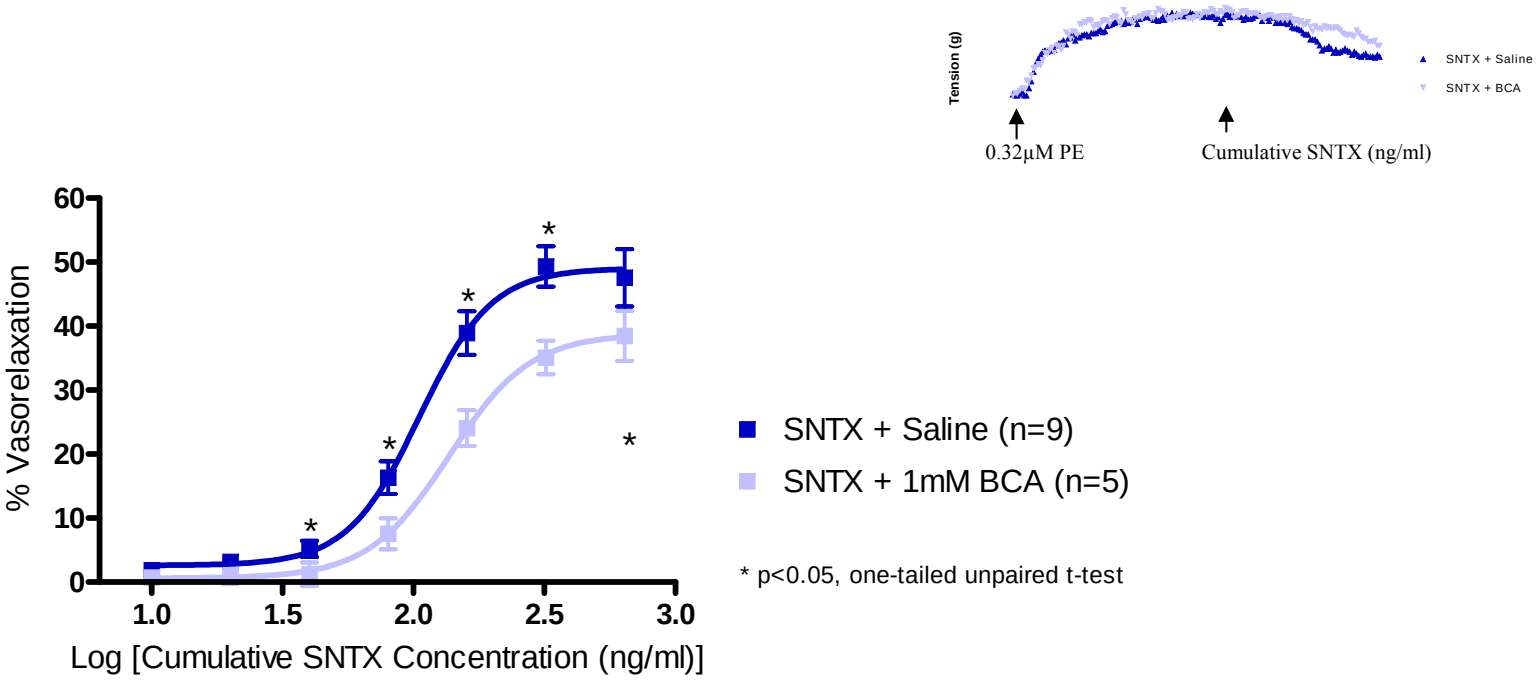
Tension (g)
SNTX + Saline
SNTX + BCA
0.32µM PE
Cumulative SNTX (ng/ml)
% Vasorelaxation
60
50
40
30
20
10
0
1.0
1.5
2.0
2.5
3.0
Log [Cumulative SNTX Concentration (ng/ml)]
*
SNTX + Saline (n=9)
SNTX + 1mM BCA (n=5)
* p<0.05, one-tailed unpaired t-test

(c)

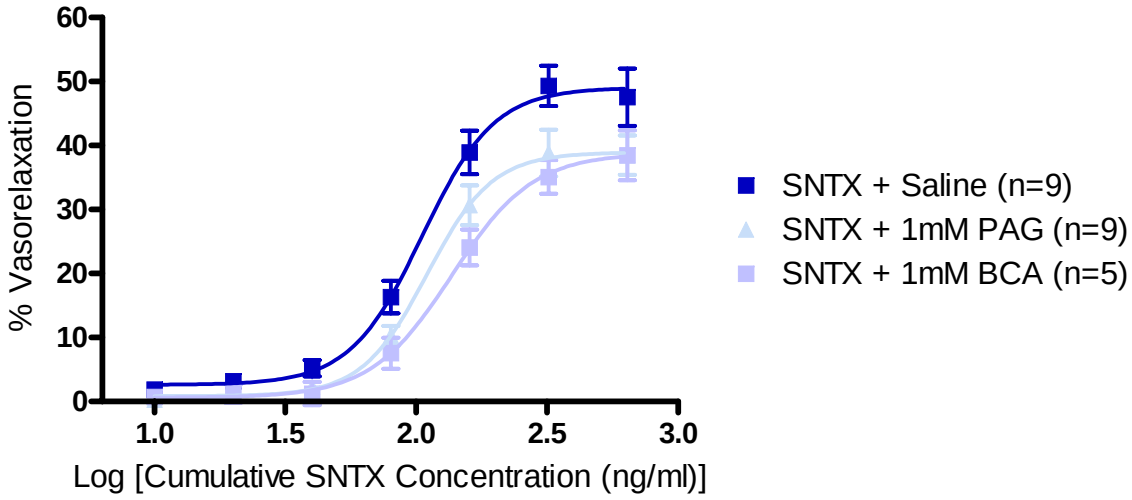
60
50
40
30
20
10
0
% Vasorelaxation
1.0
1.5
2.0
2.5
3.0
Log [Cumulative SNTX Concentration (ng/ml)]
SNTX + Saline (n=9)
SNTX + 1mM PAG (n=9)
SNTX + 1mM BCA (n=5)

Table 15. Table showing the effect of PAG and BCA on the $logIC_{50}$ and maximum vasorelaxation induced by Stonustoxin on endothelium-intact, 2mm, 0.32μM PE-precontracted thoracic aortic rings.

Experimental Group	**$LogIC_{50}$ (ng/ml)**	**Maximum Vasorelaxation (%)**
SNTX + Ctl	2.022 ± 0.004342	49.05 ± 0.2564
SNTX + 1mM PAG	2.041 ± 0.003128	38.93 ± 0.1312
SNTX + 1mM BCA	2.136 ± 0.003100	38.81 ± 0.1333

3.6 SYNERGY BETWEEN HYDROGEN SULFIDE (H_2S) & NITRIC OXIDE (NO) IN SNTX-INDUCED VASORELAXATION

The use of L-NAME and CSE inhibitors in organ bath studies showed that H_2S and NO work in synergy to cause SNTX-mediated vasorelaxation of endothelium-intact, 2mm, 0.32 μM PE-precontracted thoracic aortic rings (Figure 25; Table 17).

Since the preincubation of the aortic rings with 10μM L-NAME for 1hr completely abolished the vasorelaxant effect of SNTX on the PE-precontracted aortic rings (see Section 3.3.2), aortic rings were pre-incubated with 1μM L-NAME instead. In the presence of 1 μM L-NAME, the $logIC_{50}$ of Stonustoxin ($logIC_{50}$ = 2.02 ± 0.00434 ng/ml) is shifted to the right to $logIC_{50}$ = 2.26 ± 0.0107 ng/ml ($P < 0.05$) (Figure 25) and the maximum vasorelaxation is decreased from 49.1 ± 0.256% to 31.4 ± 0.559% ($P < 0.05$) (Table 17). 1μM L-NAME is thus used together PAG or BCA to check for synergism between NO and H_2S in SNTX-induced vasorelaxation of precontracted thoracic aortic rings.

In the presence of 1mM PAG and 1 μM L-NAME, the vasorelaxation of PE-precontracted aortic strips is completely abolished (Figure 25a). In the presence of 1mM BCA and 1μM L-NAME, the $logIC_{50}$ of Stonustoxin is decreased to 2.38 ± 0.00652ng/ml and the maximum vasorelaxation by Stonustoxin decreased to 25.6 ± 0.301% (Figure 25b; Table 17). Note that the maximum tension of the aortic rings induced by 0.32μM L-phenylephrine after pretreatment with inhibitors is not

significantly different from the control ($P > 0.05$). Since the use of 1μM L-NAME with 1mM PAG or 1mM BCA exhibits a greater inhibition of SNTX-relaxation of PE-precontracted aortic rings than when the inhibitors are used individually, this indicated synergism between H_2S and NO in mediating the vasorelaxing effect of SNTX.

Figure 25. Synergism between H_2S and NO in SNTX-induced vasorelaxation. (a) Synergistic inhibition by (a) PAG and L-NAME and (b) BCA and L-NAME on SNTX-induced vasorelaxation of endothelium-intact, 2mm, 0.32μM PE-precontracted thoracic aortic rings. * $p < 0.05$ vs. saline control.

(a)

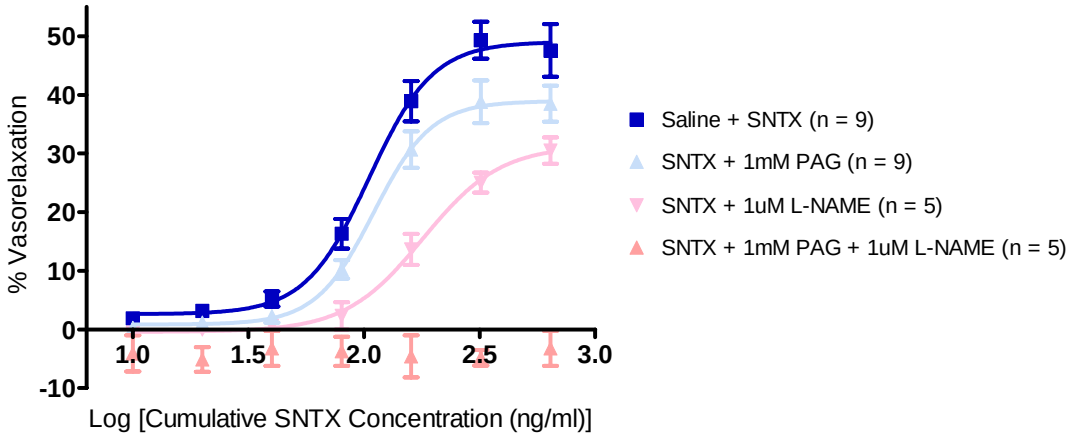

(b)

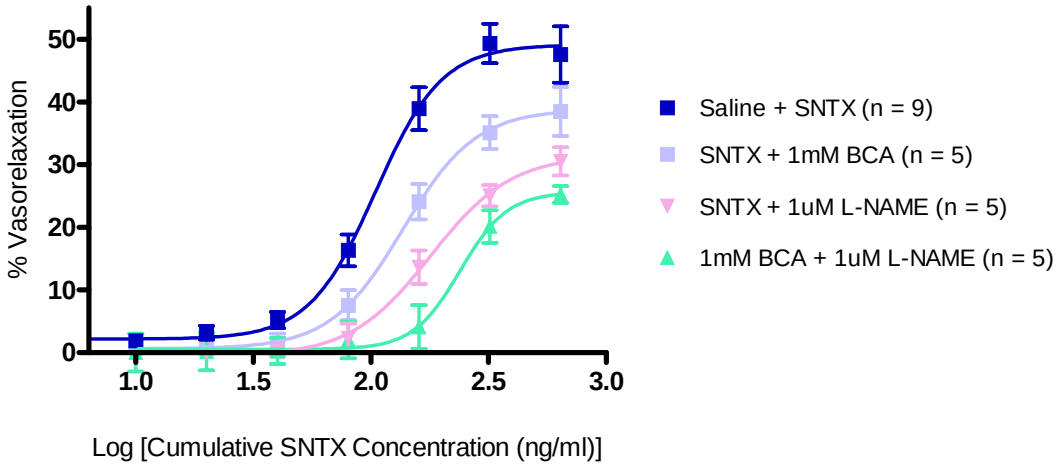

Table 16. Table showing the synergistic effect of PAG + L-NAME and BCA + L-NAME on the $logIC_{50}$ and maximum vasorelaxation induced by Stonustoxin on endothelium-intact, 2mm, 0.32μM PE-precontracted thoracic aortic rings.

Experimental Group	**$LogIC_{50}$ (ng/ml)**	**Maximum Vasorelaxation (%)**
SNTX + Ctl	2.022 ± 0.004342	49.05 ± 0.2564
SNTX + 1μM L-NAME	2.255 ± 0.01073	31.38 ± 0.5588
SNTX + 1mM PAG	2.041 ± 0.003128	38.93 ± 0.1312
SNTX + 1mM PAG + 1μM L-NAME	NA	NA
SNTX + 1mM BCA	2.136 ± 0.003100	38.81 ± 0.1333
SNTX + 1mM BCA + 1μM L-NAME	2.379 ± 0.006519	25.62 ± 0.3006

NA: not applicable

3.7 EFFECT OF L-CYSTEINE ON THORACIC AORTIC RINGS

Teague *et al.* (2001) showed that 1mM L-Cysteine was able to cause a slowly developing decline in the size of BCA-augmented twitch response of guinea pig ileum. Cheng *et al*. (2004) also showed that 1mM L-Cysteine increased endogenous H_2S production by 6-fold in rat mesenteric artery tissues and decreased contractility of mesenteric artery beds. As a result, 1mM L-cysteine (Sigma catalog no. C7352) was used to see whether it could reverse the inhibition by BCA on SNTX-induced vasorelaxation of 2mm, endothelium-intact, 0.32μM PE-precontracted thoracic aortic rings. However, when 1mM L-Cysteine was added to endothelium-intact, resting thoracic aortic rings preincubated for 30mins with BCA or control saline, an immediate transient increase in tone of the thoracic aortic rings was observed in all cases ($n \geq 3$) (Figure 26).

Figure 26. Effect of 1mM L-cysteine (free base) on endothelium-intact, resting thoracic aortic rings that was preincubated with Saline or 1mM BCA.

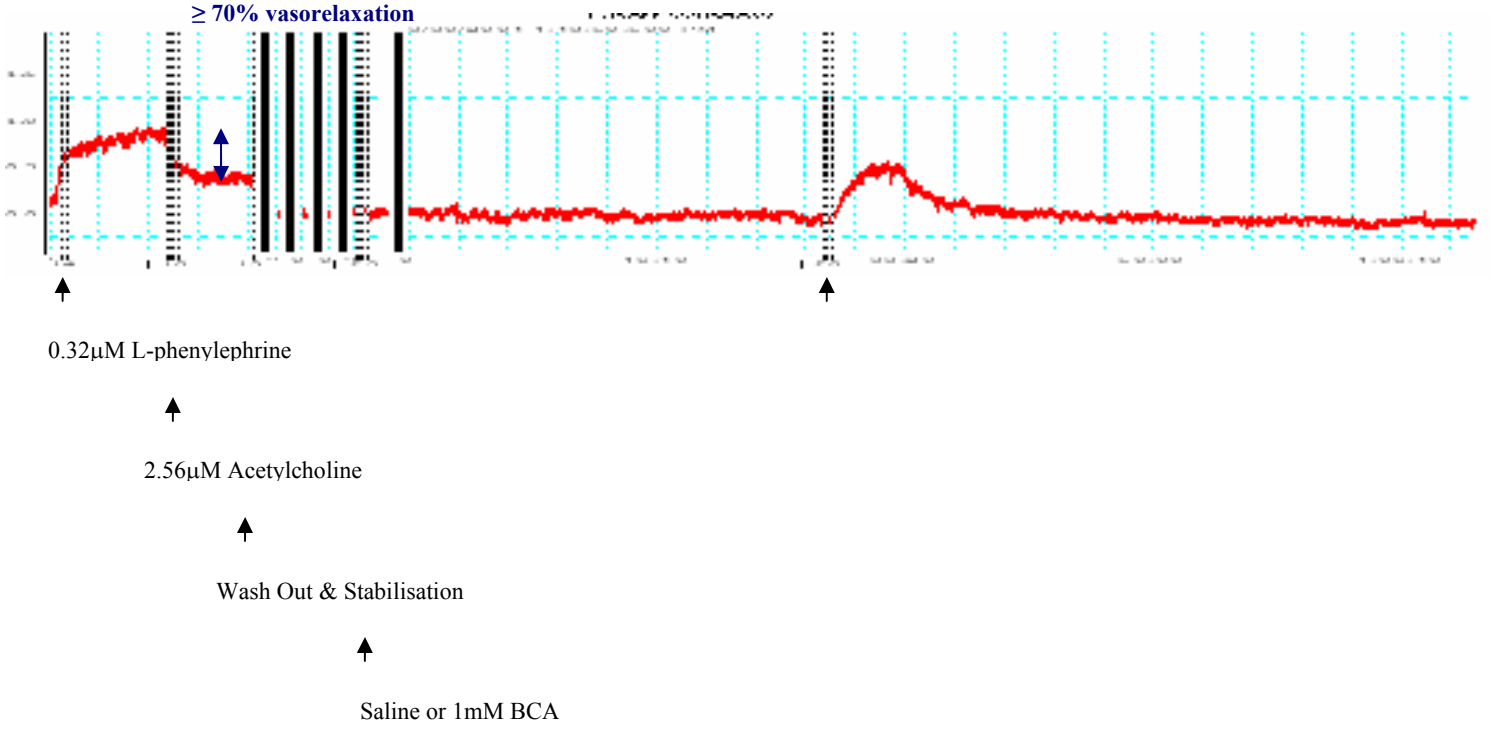

3.8 CONFIRMATION OF BACTERIAL CLONES

(E. COLI BL21- pGEX-5X-1-αB30.2 & E. COLI BL21- pGEX-5X-1-βB30.2)

The B30.2 domain of both SNTX-α and SNTX-β have been amplified by PCR and cloned into pGEX-5X-1 producing pGEX-5X-1-αB30.2 and pGEX-5X-1-βB30.2 respectively (refer to Appendix). The recombinant plasmids were transformed into *E. coli* BL21(DE3) thus producing *E. Coli* BL21-pGEX-5X-1-αB30.2 and *E. Coli* BL21-pGEX-5X-1-βB30.2. The bacterial clones were checked before being induced to synthesize recombinant B30.2 domain-containing proteins for pharmacological experiments (Sections 3.10 & 3.11).

3.8.1 POLYMERASE CHAIN REACTION AMPLIFICATION OF B30.2 DOMAINS

PCR amplification of the B30.2 domain in pGEX-5X-1-αB30.2 and pGEX-5X-1-βB30.2 using 5'-pGEX sequencing primer and 3'-pGEX sequencing primer produced expected PCR products that are 700bp in size (Figure 27).

3.8.2 DNA CYCLE SEQUENCING OF PCR PRODUCTS

To confirm that the B30.2 domains have been cloned in the correct frame into pGEX-5X-1, and to check that no mutations have occurred to the B30.2 domains during storage of *E. Coli* BL21-pGEX-5X-1-αB30.2 and *E. Coli* BL21-pGEX-5X-1-βB30.2,

DNA cycle sequencing was done. DNA sequencing of the amplified αB30.2 PCR product (Figure 28) and βB30.2 PCR product (Figure 29) shows that the B30.2 domains has been cloned in frame with the start codon of GST in pGEX-5X-1. No DNA mutations have occurred to the B30.2 domain in pGEX-5X-1-αB30.2. On the other hand, the B30.2 domain in pGEX-5X-1-βB30.2 has got 4 point mutations. One out of the 4 point mutations is not conserved. In 2 cases, UCA (Ser) has replaced UCC (Ser). In another case, UUG (Leu) has replaced CUG (Leu). For the non-conserved point mutation, UAU (Tyr) has replaced CAU (His). Tyr is a hydrophobic amino acid while his is a basic amino acid. Despite one non-conserved point mutation in the B30.2 domain of pGEX-5X-1-βB30.2, *E. Coli* BL21-pGEX-5X-1-βB30.2 was still used for protein purification (Section 3.10).

Figure 27. PCR amplification of the B30.2 domains in *E. coli* BL21- pGEX-5X-1-αB30.2 & *E. Coli* BL21- pGEX-5X-1-βB30.2. M refers to Promega's 1Kb DNA ladder.

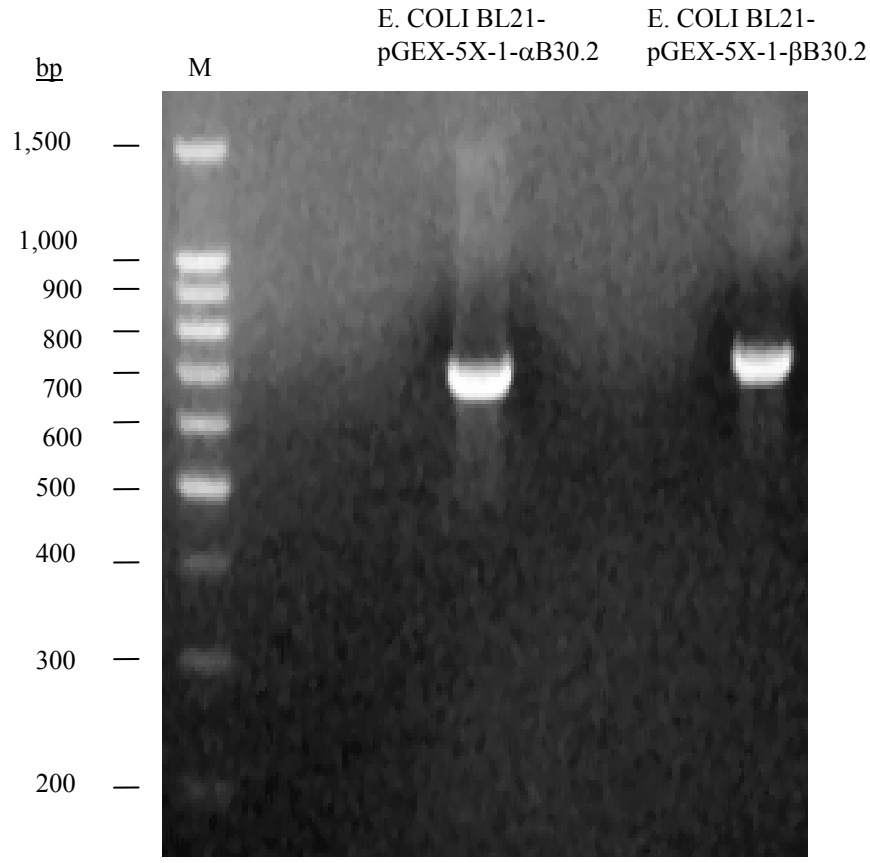

Figure 28. DNA sequencing of PCR-amplified αB30.2 PCR product (see Section 3.8.1). The αB30.2 domain has been cloned in frame with the start codon of GST in pGEX-5X-1. No DNA mutations have occurred to the B30.2 domain.

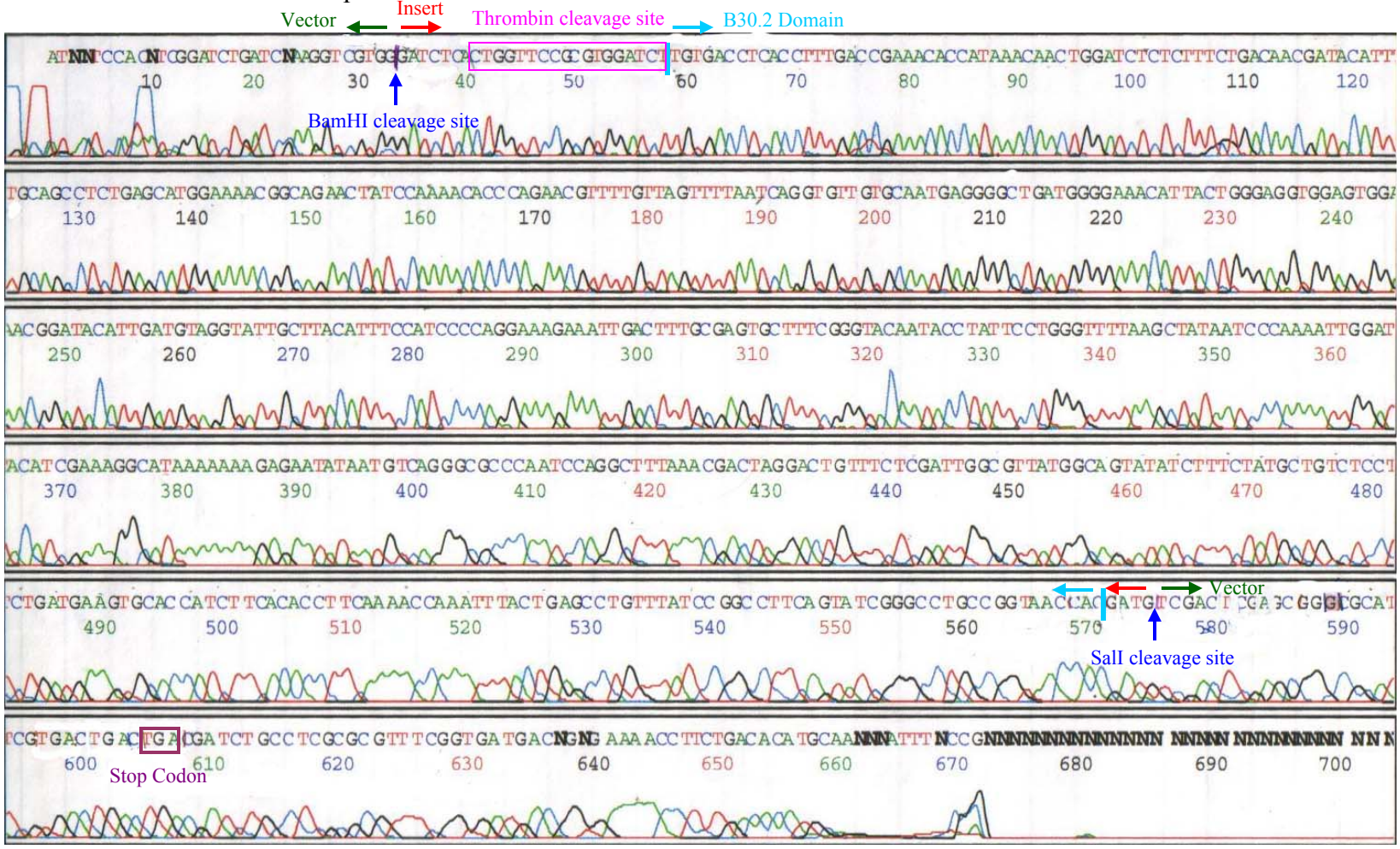

Figure 29. DNA sequencing of the amplified βB30.2 PCR product (see Section 3.8.1). The βB30.2 domain has been cloned in frame with the start codon of GST in pGEX-5X-1 and exhibits 4 point mutations. One out of the 4 point mutations is not conserved. In 2 cases, UCA (Ser) has replaced UCC (Ser). In another case, UUG (Leu) has replaced CUG (Leu). For the non-conserved point mutation, *UAU (Tyr) has replaced CAU (His). Tyr is a hydrophobic amino acid while his is a basic amino acid. Despite one non-conserved point mutation in the B30.2 domain of pGEX-5X-1-βB30.2, *E. Coli* BL21-pGEX-5X-1-βB30.2 was still used for protein purification (Section 3.10).

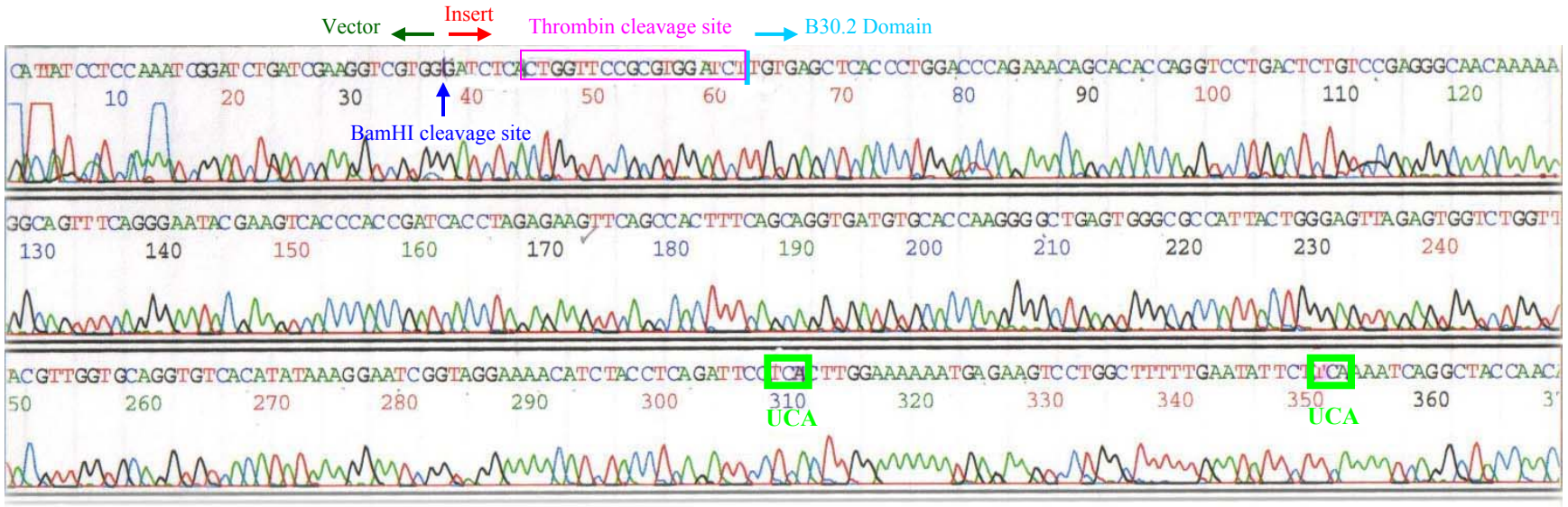

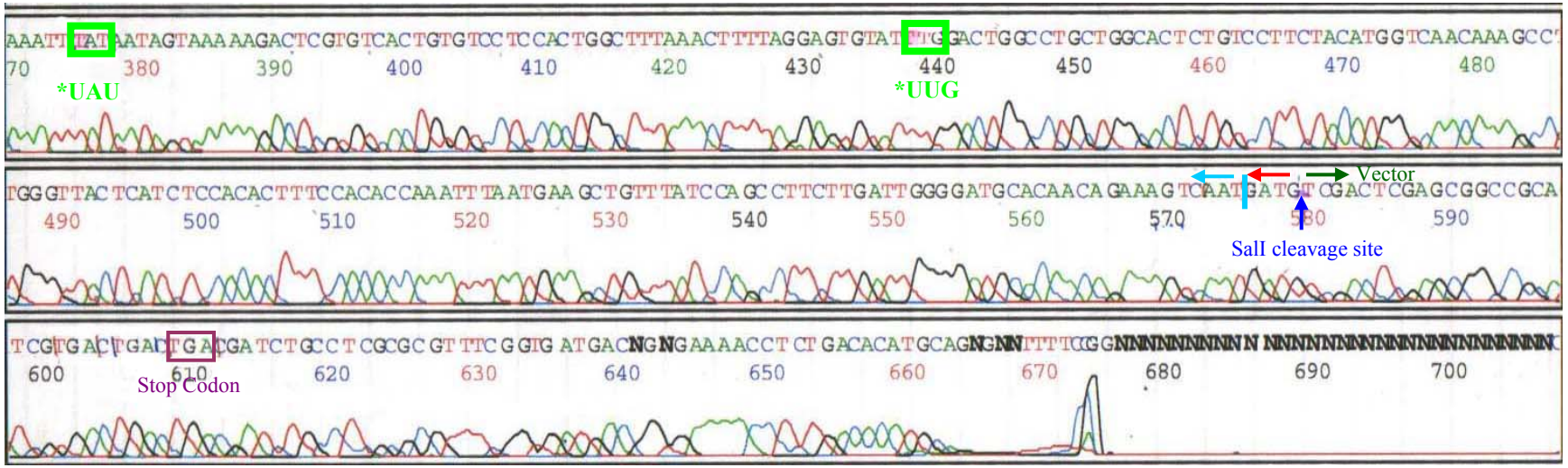
*UAU
*UUG
Vector
SalI cleavage site
Stop Codon

3.9 BIOINFORMATICS ANALYSIS OF GST, GST-αB30.2 AND GST-βB30.2 PROTEINS

Bioinformatics analysis were carried out to predict the properties of GST, GST-αB30.2 and GST-βB30.2 proteins that will be produced upon IPTG induction of the bacterial clones *E. coli* BL21-pGEX-5X-1, *E. Coli* BL21-pGEX-5X-1-αB30.2 and *E. Coli* BL21-pGEX-5X-1-βB30.2 respectively. The predicted properties of the fusion proteins such as isoelectric point and molecular weight are shown in the respective figures and may be employed in purification purposes.

Figure 30. PRETTYSEQ results showing nucleotide and amino acid sequence of GST.

```
    ---------|---------|---------|---------|---------|---------|
  1 atgtcccctatactaggttattggaaaattaagggccttgtgcaacccactcgacttctt 60
  1 M  S  P  I  L  G  Y  W  K  I  K  G  L  V  Q  P  T  R  L  L   20
    ---------|---------|---------|---------|---------|---------|
 61 ttggaatatcttgaagaaaaatatgaagagcatttgtatgagcgcgatgaaggtgataaa 120
 21 L  E  Y  L  E  E  K  Y  E  E  H  L  Y  E  R  D  E  G  D  K   40
    ---------|---------|---------|---------|---------|---------|
121 tggcgaaacaaaaagtttgaattgggtttggagtttcccaatcttccttattatattgat 180
 41 W  R  N  K  K  F  E  L  G  L  E  F  P  N  L  P  Y  Y  I  D   60
    ---------|---------|---------|---------|---------|---------|
181 ggtgatgttaaattaacacagtctatggccatcatacgttatatagctgacaagcacaac 240
 61 G  D  V  K  L  T  Q  S  M  A  I  I  R  Y  I  A  D  K  H  N   80
    ---------|---------|---------|---------|---------|---------|
241 atgttgggtggttgtccaaaagagcgtgcagagatttcaatgcttgaaggagcggttttg 300
 81 M  L  G  G  C  P  K  E  R  A  E  I  S  M  L  E  G  A  V  L   100
    ---------|---------|---------|---------|---------|---------|
301 gatattagatacggtgtttcgagaattgcatatagtaaagactttgaaactctcaaagtt 360
101 D  I  R  Y  G  V  S  R  I  A  Y  S  K  D  F  E  T  L  K  V   120
    ---------|---------|---------|---------|---------|---------|
361 gattttcttagcaagctacctgaaatgctgaaaatgttcgaagatcgtttatgtcataaa 420
121 D  F  L  S  K  L  P  E  M  L  K  M  F  E  D  R  L  C  H  K   140
    ---------|---------|---------|---------|---------|---------|
421 acatatttaaatggtgatcatgtaacccatcctgacttcatgttgtatgacgctcttgat 480
141 T  Y  L  N  G  D  H  V  T  H  P  D  F  M  L  Y  D  A  L  D   160
    ---------|---------|---------|---------|---------|---------|
```

```
 481 gttgttttatacatggacccaatgtgcctggatgcgttcccaaaattagtttgttttaaa 540
161 V  V  L  Y  M  D  P  M  C  L  D  A  F  P  K  L  V  C  F  K   180
    ---------|---------|---------|---------|---------|---------|
541 aaacgtattgaagctatcccacaaattgataagtacttgaaatccagcaagtatatagca 600
181 K  R  I  E  A  I  P  Q  I  D  K  Y  L  K  S  S  K  Y  I  A   200
    ---------|---------|---------|---------|---------|---------|
601 tggcctttgcagggctggcaagccacgtttggtggtggcgaccatcctccaaaatcggat 660
201 W  P  L  Q  G  W  Q  A  T  F  G  G  G  D  H  P  P  K  S  D   220
    ---------|---------|---------|---------|---------|---------|
661 ctgatcgaaggtcgtgggatccccgaattcccgggtcgactcgagcggccgcatcgtgac 720
221 L  I  E  G  R  G  I  P  E  F  P  G  R  L  E  R  P  H  R  D   240
    --------
721 tgactgac 728
241 *  L     242
```

Figure 31. PEPSTAT analysis of GST showing the predicted molecular weight, isoelectric point and other properties of the protein.

```
PEPSTATS of GST from 1 to 240

Molecular weight              = 28027.41            Residues = 240
Average Residue Weight        = 116.781             Charge   = -0.5
Isoelectric Point             = 6.4035
Probability of expression in inclusion bodies = 0.529

Residue        Number         Mole%          DayhoffStat
A = Ala        10             4.167          0.484
B = Asx        0              0.000          0.000
C = Cys        4              1.667          0.575
D = Asp        19             7.917          1.439
E = Glu        19             7.917          1.319
F = Phe        10             4.167          1.157
G = Gly        17             7.083          0.843
H = His        7              2.917          1.458
I = Ile        15             6.250          1.389
K = Lys        21             8.750          1.326
L = Leu        29             12.083         1.633
M = Met        9              3.750          2.206
N = Asn        4              1.667          0.388
P = Pro        16             6.667          1.282
Q = Gln        5              2.083          0.534
R = Arg        13             5.417          1.105
S = Ser        9              3.750          0.536
T = Thr        6              2.500          0.410
V = Val        9              3.750          0.568
W = Trp        4              1.667          1.282
X = Xaa        0              0.000          0.000
Y = Tyr        14             5.833          1.716
Z = Glx        0              0.000          0.000

Property       Residues                      Number         Mole%
Tiny           (A+C+G+S+T)                   46             19.167
Small          (A+B+C+D+G+N+P+S+T+V)         94             39.167
Aliphatic      (I+L+V)                       53             22.083
Aromatic       (F+H+W+Y)                     35             14.583
Non-polar      (A+C+F+G+I+L+M+P+V+W+Y)       137            57.083
Polar          (D+E+H+K+N+Q+R+S+T+Z)         103            42.917
Charged        (B+D+E+H+K+R+Z)               79             32.917
Basic          (H+K+R)                       41             17.083
Acidic         (B+D+E+Z)                     38             15.833
```

Figure 32. PRETTYSEQ results showing nucleotide and amino acid sequence of GST-αB30.2. The thrombin cleavage site that separates that GST domain and the αB30.2 domain is underlined and the 5'-pGEX sequencing primer binding site is highlighted in blue.

```
    ---------|---------|---------|---------|---------|---------|
  1 atgtcccctatactaggttattggaaaattaagggccttgtgcaacccactcgacttctt 60
  1 M  S  P  I  L  G  Y  W  K  I  K  G  L  V  Q  P  T  R  L  L   20

    ---------|---------|---------|---------|---------|---------|
 61 ttggaatatcttgaagaaaaatatgaagagcatttgtatgagcgcgatgaaggtgataaa 120
 21 L  E  Y  L  E  E  K  Y  E  E  H  L  Y  E  R  D  E  G  D  K   40

    ---------|---------|---------|---------|---------|---------|
121 tggcgaaacaaaaagtttgaattgggtttggagtttcccaatcttccttattatattgat 180
 41 W  R  N  K  K  F  E  L  G  L  E  F  P  N  L  P  Y  Y  I  D   60

    ---------|---------|---------|---------|---------|---------|
181 ggtgatgttaaattaacacagtctatggccatcatacgttatatagctgacaagcacaac 240
 61 G  D  V  K  L  T  Q  S  M  A  I  I  R  Y  I  A  D  K  H  N   80

    ---------|---------|---------|---------|---------|---------|
241 atgttgggtggttgtccaaaagagcgtgcagagatttcaatgcttgaaggagcggttttg 300
 81 M  L  G  G  C  P  K  E  R  A  E  I  S  M  L  E  G  A  V  L   100

    ---------|---------|---------|---------|---------|---------|
301 gatattagatacggtgtttcgagaattgcatatagtaaagactttgaaactctcaaagtt 360
101 D  I  R  Y  G  V  S  R  I  A  Y  S  K  D  F  E  T  L  K  V   120

    ---------|---------|---------|---------|---------|---------|
361 gattttcttagcaagctacctgaaatgctgaaaatgttcgaagatcgtttatgtcataaa 420
121 D  F  L  S  K  L  P  E  M  L  K  M  F  E  D  R  L  C  H  K   140

    ---------|---------|---------|---------|---------|---------|
421 acatatttaaatggtgatcatgtaacccatcctgacttcatgttgtatgacgctcttgat 480
141 T  Y  L  N  G  D  H  V  T  H  P  D  F  M  L  Y  D  A  L  D   160

    ---------|---------|---------|---------|---------|---------|
481 gttgttttatacatggacccaatgtgcctggatgcgttcccaaaattagtttgttttaaa 540
161 V  V  L  Y  M  D  P  M  C  L  D  A  F  P  K  L  V  C  F  K   180

    ---------|---------|---------|---------|---------|---------|
541 aaacgtattgaagctatcccacaaattgataagtacttgaaatccagcaagtatatagca 600
181 K  R  I  E  A  I  P  Q  I  D  K  Y  L  K  S  S  K  Y  I  A   200

    ---------|---------|---------|---------|---------|---------|
601 tggcctttgcagggctggcaagccacgtttggtggtggcgaccatcctccaaaatcggat 660
201 W  P  L  Q  G  W  Q  A  T  F  G  G  G  D  H  P  P  K  S  D   220

    ---------|---------|---------|---------|---------|---------|
661 ctgatcgaaggtcgtgggatctcactggttccgcgtggatcttgtgacctcacctttgac 720
221 L  I  E  G  R  G  I  S  L  V  P  R  G  S  C  D  L  T  F  D   240

    ---------|---------|---------|---------|---------|---------|
721 cgaaacaccataaacaactggatctctctttctgacaacgatacatttgcagcctctgag 780
241 R  N  T  I  N  N  W  I  S  L  S  D  N  D  T  F  A  A  S  E   260

    ---------|---------|---------|---------|---------|---------|
781 catggaaaacggcagaactatccaaaacacccagaacgttttgttagttttaatcaggtg 840
261 H  G  K  R  Q  N  Y  P  K  H  P  E  R  F  V  S  F  N  Q  V   280
```

```
    ---------|---------|---------|---------|---------|---------|
 841 ttgtgcaatgaggggctgatggggaaacattactgggaggtggagtggaacggatacatt 900
 281 L  C  N  E  G  L  M  G  K  H  Y  W  E  V  E  W  N  G  Y  I   300

    ---------|---------|---------|---------|---------|---------|
 901 gatgtaggtattgcttacatttccatccccaggaaagaaattgactttgcgagtgctttc 960
 301 D  V  G  I  A  Y  I  S  I  P  R  K  E  I  D  F  A  S  A  F   320

    ---------|---------|---------|---------|---------|---------|
 961 gggtacaatacctattcctgggttttaagctataatcccaaaattggatacatcgaaagg 1020
 321 G  Y  N  T  Y  S  W  V  L  S  Y  N  P  K  I  G  Y  I  E  R   340

    ---------|---------|---------|---------|---------|---------|
1021 cataaaaaaagagaatataatgtcagggcgcccaatccaggctttaaacgactaggactg 1080
 341 H  K  K  R  E  Y  N  V  R  A  P  N  P  G  F  K  R  L  G  L   360

    ---------|---------|---------|---------|---------|---------|
1081 tttctcgattggcgttatggcagtatatctttctatgctgtctcctctgatgaagtgcac 1140
 361 F  L  D  W  R  Y  G  S  I  S  F  Y  A  V  S  S  D  E  V  H   380

    ---------|---------|---------|---------|---------|---------|
1141 catcttcacaccttcaaaaccaaatttactgagcctgtttatccggccttcagtatcggg 1200
 381 H  L  H  T  F  K  T  K  F  T  E  P  V  Y  P  A  F  S  I  G   400

    ---------|---------|---------|---------|---------|-
1201 cctgccggtaaccacgatgtcgactcgagcggccgcatcgtgactgactga 1251
 401 P  A  G  N  H  D  V  D  S  S  G  R  I  V  T  D  *   416
```

Figure 33. Pepstat analysis of GST-αB30.2 showing the predicted molecular weight, isoelectric point and other properties of the protein.

PEPSTATS of GST-αB30.2 from 1 to 416

Molecular weight = 48203.91 Residues = 416
Average Residue Weight = 115.875 Charge = 3.0
Isoelectric Point = 6.8822
Improbability of expression in inclusion bodies = 0.663

Residue	Number	Mole%	DayhoffStat
A = Ala	19	4.567	0.531
B = Asx	0	0.000	0.000
C = Cys	6	1.442	0.497
D = Asp	29	6.971	1.267
E = Glu	27	6.490	1.082
F = Phe	21	5.048	1.402
G = Gly	30	7.212	0.859
H = His	14	3.365	1.683
I = Ile	27	6.490	1.442
K = Lys	31	7.452	1.129
L = Leu	38	9.135	1.234
M = Met	10	2.404	1.414
N = Asn	17	4.087	0.950
P = Pro	23	5.529	1.063
Q = Gln	7	1.683	0.431
R = Arg	21	5.048	1.030
S = Ser	26	6.250	0.893
T = Thr	14	3.365	0.552
V = Val	21	5.048	0.765
W = Trp	9	2.163	1.664
X = Xaa	0	0.000	0.000
Y = Tyr	26	6.250	1.838
Z = Glx	0	0.000	0.000

Property	Residues	Number	Mole%
Tiny	(A+C+G+S+T)	95	22.837
Small	(A+B+C+D+G+N+P+S+T+V)	185	44.471
Aliphatic	(I+L+V)	86	20.673
Aromatic	(F+H+W+Y)	70	16.827
Non-polar	(A+C+F+G+I+L+M+P+V+W+Y)	230	55.288
Polar	(D+E+H+K+N+Q+R+S+T+Z)	186	44.712
Charged	(B+D+E+H+K+R+Z)	122	29.327

Figure 34. PRETTYSEQ result showing nucleotide and amino acid sequence of GST-βB30.2. The thrombin cleavage site that separates that GST domain and the βB30.2 domain is underlined and the 5'-pGEX sequencing primer binding site is highlighted in blue.

```
    ---------|---------|---------|---------|---------|---------|
  1 atgtcccctatactaggttattggaaaattaagggccttgtgcaacccactcgacttctt 60
  1 M  S  P  I  L  G  Y  W  K  I  K  G  L  V  Q  P  T  R  L  L   20

    ---------|---------|---------|---------|---------|---------|
 61 ttggaatatcttgaagaaaaatatgaagagcatttgtatgagcgcgatgaaggtgataaa 120
 21 L  E  Y  L  E  E  K  Y  E  E  H  L  Y  E  R  D  E  G  D  K   40

    ---------|---------|---------|---------|---------|---------|
121 tggcgaaacaaaaagtttgaattgggtttggagtttcccaatcttccttattatattgat 180
 41 W  R  N  K  K  F  E  L  G  L  E  F  P  N  L  P  Y  Y  I  D   60

    ---------|---------|---------|---------|---------|---------|
181 ggtgatgttaaattaacacagtctatggccatcatacgttatatagctgacaagcacaac 240
 61 G  D  V  K  L  T  Q  S  M  A  I  I  R  Y  I  A  D  K  H  N   80

    ---------|---------|---------|---------|---------|---------|
241 atgttgggtggttgtccaaaagagcgtgcagagatttcaatgcttgaaggagcggttttg 300
 81 M  L  G  G  C  P  K  E  R  A  E  I  S  M  L  E  G  A  V  L   100

    ---------|---------|---------|---------|---------|---------|
301 gatattagatacggtgtttcgagaattgcatatagtaaagactttgaaactctcaaagtt 360
101 D  I  R  Y  G  V  S  R  I  A  Y  S  K  D  F  E  T  L  K  V   120

    ---------|---------|---------|---------|---------|---------|
361 gattttcttagcaagctacctgaaatgctgaaaatgttcgaagatcgtttatgtcataaa 420
121 D  F  L  S  K  L  P  E  M  L  K  M  F  E  D  R  L  C  H  K   140

    ---------|---------|---------|---------|---------|---------|
421 acatatttaaatggtgatcatgtaacccatcctgacttcatgttgtatgacgctcttgat 480
141 T  Y  L  N  G  D  H  V  T  H  P  D  F  M  L  Y  D  A  L  D   160

    ---------|---------|---------|---------|---------|---------|
481 gttgttttatacatggacccaatgtgcctggatgcgttcccaaaattagtttgttttaaa 540
161 V  V  L  Y  M  D  P  M  C  L  D  A  F  P  K  L  V  C  F  K   180

    ---------|---------|---------|---------|---------|---------|
541 aaacgtattgaagctatcccacaaattgataagtacttgaaatccagcaagtatatagca 600
181 K  R  I  E  A  I  P  Q  I  D  K  Y  L  K  S  S  K  Y  I  A   200

    ---------|---------|---------|---------|---------|---------|
601 tggcctttgcagggctggcaagccacgtttggtggtggcgaccatcctccaaaatcggat 660
201 W  P  L  Q  G  W  Q  A  T  F  G  G  G  D  H  P  P  K  S  D   220

    ---------|---------|---------|---------|---------|---------|
661 ctgatcgaaggtcgtgggatctcactggttccgcgtggatcttgtgagctcaccctggac 720
221 L  I  E  G  R  G  I  S  L  V  P  R  G  S  C  E  L  T  L  D   240

    ---------|---------|---------|---------|---------|---------|
721 ccagaaacagcacaccaggtcctgactctgtccgagggcaacaaaaaggcagtttcaggg 780
241 P  E  T  A  H  Q  V  L  T  L  S  E  G  N  K  K  A  V  S  G   260

    ---------|---------|---------|---------|---------|---------|
781 aatacgaagtcacccaccgatcacctagagaagttcagccactttcagcaggtgatgtgc 840
261 N  T  K  S  P  T  D  H  L  E  K  F  S  H  F  Q  Q  V  M  C   280
```

```
    ---------|---------|---------|---------|---------|---------|
 841 accaaggggctgagtgggcgccattactgggagttagagtggtctggttacgttggtgca 900
 281 T  K  G  L  S  G  R  H  Y  W  E  L  E  W  S  G  Y  V  G  A   300

    ---------|---------|---------|---------|---------|---------|
 901 ggtgtcacatataaaggaatcggtaggaaaacatctacctcagattcctcccttggaaaa 960
 301 G  V  T  Y  K  G  I  G  R  K  T  S  T  S  D  S  S  L  G  K   320

    ---------|---------|---------|---------|---------|---------|
 961 aatgagaagtcctggctttttgaatattctacaaaatcaggctaccaacaaattcataat 1020
 321 N  E  K  S  W  L  F  E  Y  S  T  K  S  G  Y  Q  Q  I  H  N   340

    ---------|---------|---------|---------|---------|---------|
1021 agtaaaaagactcgtgtcactgtgtcctccactggctttaaacttttaggagtgtatctg 1080
 341 S  K  K  T  R  V  T  V  S  S  T  G  F  K  L  L  G  V  Y  L   360

    ---------|---------|---------|---------|---------|---------|
1081 gactggcctgctggcactctgtccttctacatggtcaacaaagcctgggttactcatctc 1140
 361 D  W  P  A  G  T  L  S  F  Y  M  V  N  K  A  W  V  T  H  L   380

    ---------|---------|---------|---------|---------|---------|
1141 cacactttccacaccaaatttaatgaagctgtttatccagccttcttgattggggatgca 1200
 381 H  T  F  H  T  K  F  N  E  A  V  Y  P  A  F  L  I  G  D  A   400

    ---------|---------|---------|---------|---------|-
1201 caacagaaagtcaatgatgtcgactcgagcggccgcatcgtgactgactga 1251
 401 Q  Q  K  V  N  D  V  D  S  S  G  R  I  V  T  D  *   416
```

Figure 35. Pepstat analysis of GST-βB30.2 showing the predicted molecular weight, isoelectric point and other properties of the protein.

PEPSTATS of GST-βB30.2 from 1 to 416

Molecular weight = 47452.20 Residues = 416
Average Residue Weight = 114.068 Charge = 7.0
Isoelectric Point = 7.6474
Improbability of expression in inclusion bodies = 0.692

Residue	Number	Mole%	DayhoffStat
A = Ala	18	4.327	0.503
B = Asx	0	0.000	0.000
C = Cys	6	1.442	0.497
D = Asp	26	6.250	1.136
E = Glu	26	6.250	1.042
F = Phe	17	4.087	1.135
G = Gly	33	7.933	0.944
H = His	14	3.365	1.683
I = Ile	19	4.567	1.015
K = Lys	37	8.894	1.348
L = Leu	44	10.577	1.429
M = Met	11	2.644	1.555
N = Asn	11	2.644	0.615
P = Pro	18	4.327	0.832
Q = Gln	12	2.885	0.740
R = Arg	15	3.606	0.736
S = Ser	30	7.212	1.030
T = Thr	24	5.769	0.946
V = Val	24	5.769	0.874
W = Trp	9	2.163	1.664
X = Xaa	0	0.000	0.000
Y = Tyr	22	5.288	1.555
Z = Glx	0	0.000	0.000

Property	Residues	Number	Mole%
Tiny	(A+C+G+S+T)	111	26.683
Small	(A+B+C+D+G+N+P+S+T+V)	190	45.673
Aliphatic	(I+L+V)	87	20.913
Aromatic	(F+H+W+Y)	62	14.904
Non-polar	(A+C+F+G+I+L+M+P+V+W+Y)	221	53.125
Polar	(D+E+H+K+N+Q+R+S+T+Z)	195	46.875
Charged	(B+D+E+H+K+R+Z)	118	28.365

Figure 36. Pepstat analysis of GST-βB30.2 (mutated – refer to section 3.8.2) showing the predicted molecular weight, isoelectric point and other properties of the protein.

PEPSTATS of GST-βB30.2 1 from 1 to 416

Molecular weight = 47464.20 Residues = 416
Average Residue Weight = 114.097 Charge = 6.5
Isoelectric Point = 7.6291
Improbability of expression in inclusion bodies = 0.700

Residue	Number	Mole%	DayhoffStat
A = Ala	18	4.327	0.503
B = Asx	0	0.000	0.000
C = Cys	6	1.442	0.497
D = Asp	26	6.250	1.136
E = Glu	26	6.250	1.042
F = Phe	17	4.087	1.135
G = Gly	33	7.933	0.944
H = His	13	3.125	1.562
I = Ile	19	4.567	1.015
K = Lys	37	8.894	1.348
L = Leu	44	10.577	1.429
M = Met	11	2.644	1.555
N = Asn	11	2.644	0.615
P = Pro	18	4.327	0.832
Q = Gln	12	2.885	0.740
R = Arg	15	3.606	0.736
S = Ser	31	7.452	1.065
T = Thr	23	5.529	0.906
V = Val	24	5.769	0.874
W = Trp	9	2.163	1.664
X = Xaa	0	0.000	0.000
Y = Tyr	23	5.529	1.626
Z = Glx	0	0.000	0.000

Property	Residues	Number	Mole%
Tiny	(A+C+G+S+T)	111	26.683
Small	(A+B+C+D+G+N+P+S+T+V)	190	45.673
Aliphatic	(I+L+V)	87	20.913
Aromatic	(F+H+W+Y)	62	14.904
Non-polar	(A+C+F+G+I+L+M+P+V+W+Y)	222	53.365
Polar	(D+E+H+K+N+Q+R+S+T+Z)	194	46.635
Charged	(B+D+E+H+K+R+Z)	117	28.125
Basic	(H+K+R)	65	15.625
Acidic	(B+D+E+Z)	52	12.500

3.10 PURIFICATION OF GST, GST-αB30.2 AND GST-βB30.2 PROTEINS

3.10.1 AFFINITY PURIFICATION OF SOLUBLE GST, GST-αB30.2 OR GST-βB30.2

Soluble GST-αB30.2 (~48kDa) and GST-βB30.2 (~47kDa) in bacterial supernatant produced under the conditions of protein expression described in Section 2.4.2.1 were co-purified with a 57kDa protein under the native conditions of protein purification described in Section 2.4.2.3 (Figure 37). The 57kDa protein was found to be GroEL through N-terminal sequencing. Pure GST (~28kDa) without GroEL was purified under the same conditions. The yield of soluble GST-αB30.2 (+ GroEL) and GST-βB30.2 (+GroEL) purified from 1*l* bacterial culture is low, i.e. 0.2535mg and 0.2571mg respectively. Conversely, the yield of affinity purified soluble GST is high, i.e. 27mg/*l* bacterial culture.

Figure 37. Purification of soluble GST-αB30.2, GST-βB30.2 and GST: (a) GST-αB30.2 (~48kDa) + GroEL (57kDa), (b) GST-βB30.2 (~47kDa) + GroEL (57kDa) and (c) GST (26kDa). Fractions (1, 2) collected from FPLC were analyzed by 12% SDS-PAGE. Note the conditions of bacterial growth, protein expression and non-denaturing protein purification described in Sections 2.4.2.1 and 2.4.2.3. M represents Bio-Rad broad-range molecular weight marker.

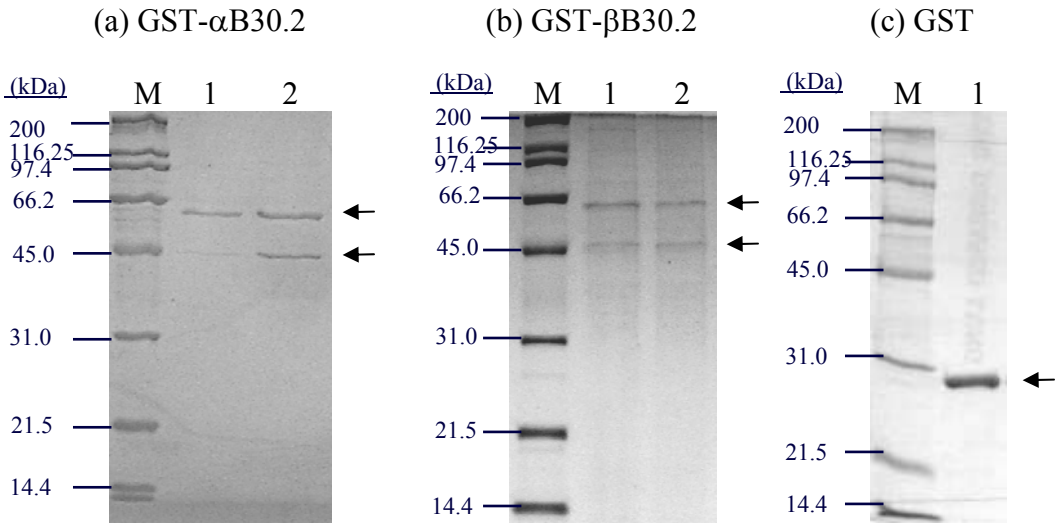

3.10.2 ATTEMPTED REMOVAL OF GRO-EL FROM SOLUBLE GST-αB30.2 AND GST-βB30.2 USING AN ATP WASH BUFFER

As an attempt to separate co-purifying GroEL from GST-αB30.2 and GST-βB30.2 (refer to Section above), an additional ATP washing step was included into the purification process (see Section 2.4.2.4). GroEL has been postulated to function together with GroES in the presence of ATP to facilitate the correct folding of proteins and their subsequent release from the GroEL-GroES complex (Fenton & Horwich, 2003 and references therein). The inclusion of the ATP washing step resulted in the purification of pure GST-βB30.2 without GroEL (Figure 38). GST-αB30.2 however was still purified together with GroEL.

Figure 38. Attempted removal of GroEL from GST-αB30.2 and GST-βB30.2 using an ATP wash buffer. (a) Successful removal of GroEL (57kDa) from GST-βB30.2 (~47kDa) and (b) copurification of GroEL (57kDa) with GST-αB30.2 (~48kDa). M represents Bio-Rad broad-range molecular weight marker. Fraction 1 collected from FPLC were analyzed by 12% SDS-PAGE.

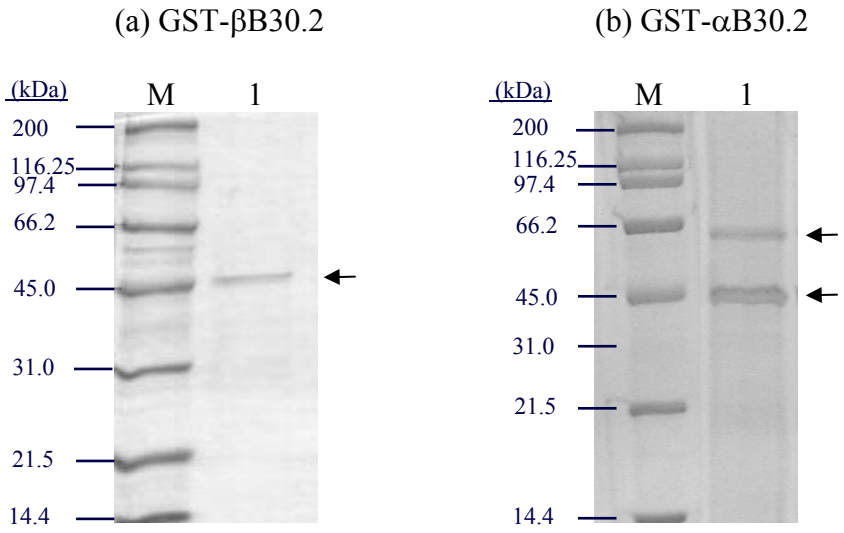

3.10.3 ATTEMPTED REMOVAL OF GRO-EL FROM SOLUBLE GST-αB30.2 USING AN ATP WASH BUFFER AND GRO-ES

Since there have been reports of successful removal of contaminating GroEL from GST-fusion proteins using a combination of an ATP wash buffer and GroES (Thain *et al*., 1996, Vandenbroeck & Billiau, 1998), this method was used as a further attempt to remove GroEL from GST-αB30.2. However, contaminating GroEL was still co-purified with GST-αB30.2 (Figure 39).

Figure 37. Attempted removal of GroEL from GST-αB30.2 using a combination of an ATP wash buffer and GroES. GroEL (57kDa) is still copurified with GST-αB30.2 (~48kDa). M represents Bio-Rad broad-range molecular weight marker. Fraction 1 collected from FPLC were analyzed by 12% SDS-PAGE.

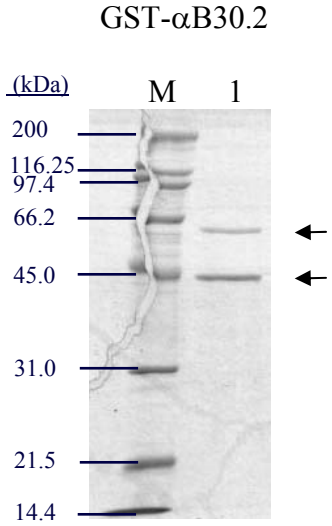

3.10.4 PURIFICATION OF GST-αB30.2 AND GST-βB30.2 FROM INCLUSION BODIES

3.10.4.1 METHOD 1

Pure GST-αB30.2 and GST-βB30.2 was purified without Gro-EL from inclusion bodies solubilized with N-lauroylsarcosine (Figure 40, refer to Section 2.4.2.6.1). The amount of GST-αB30.2 and GST-βB30.2 purified from the inclusion bodies (21.3 and 18.9 mg/*l* bacterial culture respectively) was much higher compared to that purified from the bacterial supernatant (i.e. 0.254 and 0.257 mg/*l* bacterial culture respectively).

Figure 40. Purification of GST-αB30.2 and GST-βB30.2 from inclusion bodies solubilized with N-lauroylsarcosine. (a) GST-αB30.2 (~48kDa) and (b) GST-βB30.2 (~47kDa) purified from inclusion bodies. M represents Bio-Rad broad-range molecular weight marker. Fractions (1,2) collected from FPLC were analyzed by 12% SDS-PAGE.

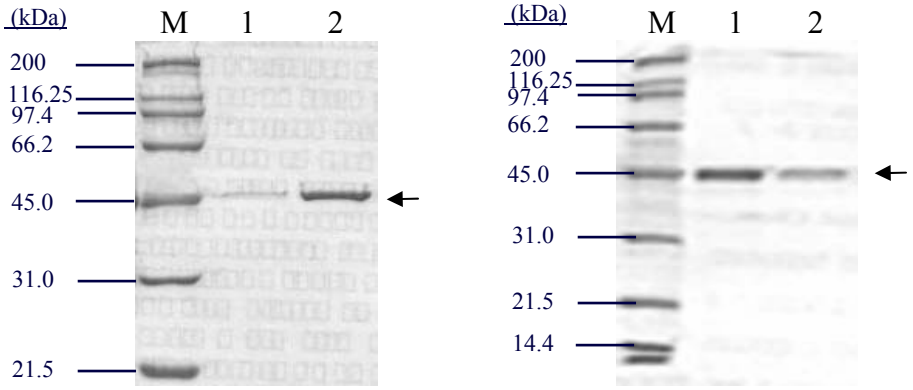

3.10.4.2 METHOD 2

Inclusion bodies containing GST-αB30.2 or GST-βB30.2 were obtained and prepared as described in section 2.4.2.6.2. The inclusion bodies solubilized in urea were refolded and analysed by SDS-PAGE (Figure 41). Large amounts of pure GST-αB30.2 and GST-βB30.2 were found to be in the inclusion bodies preparation. As determined by Bradford assay, the amount of GST-αB30.2 and GST-βB30.2 from 1 liter of bacterial culture are 16 mg and 12.1 mg respectively.

Figure 41. Solubilization and refolding of inclusion bodies containing recombinant GST-αB30.2 or GST-βB30.2. Inclusion bodies preparation obtained for GST-αB30.2 (lane 1) and GST-βB30.2 (lane 2) purified according to the method described in section 2.2.4.6.2 M represents Bio-Rad broad-range molecular weight marker.

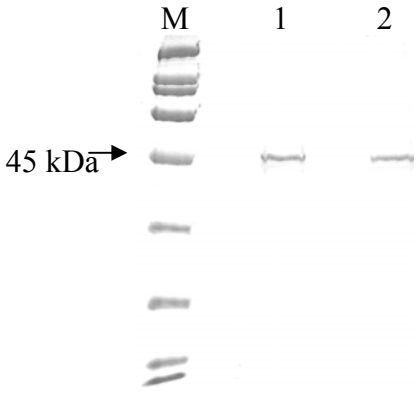

3.10.5 WESTERN BLOTTING: IMMUNORECOGNITION OF GST-αB30.2 AND GST-βB30.2 BY POLYCLONAL ANTIBODIES DIRECTED AGAINST SNTX

GST-αB30.2 (+ GroEL) and GST-βB30.2 (- GroEL) both purified from the bacterial supernatant (see Section 3.10.2) were recognized by polyclonal anti-SNTX antibodies obtained from rabbits subcutaneously injected with native SNTX (120μg) emulsified in complete Freund's adjuvant. (Figure 42). In addition, pure GST-αB30.2 and GST-βB30.2 purified from inclusion bodies (see Section 3.10.4.2 and Section 2.4.2.6.2) were also detectable by the polyclonal anti-SNTX antibodies (Figure 43).

Figure 42. Immunodetection of SNTX and affinity purified GST-αB30.2 (+GroEL) and GST-βB30.2. SNTX, GST-αB30.2 (+ GroEL) and GST-βB30.2 (- GroEL) were loaded into lane 1, 2 and 3 respectively.

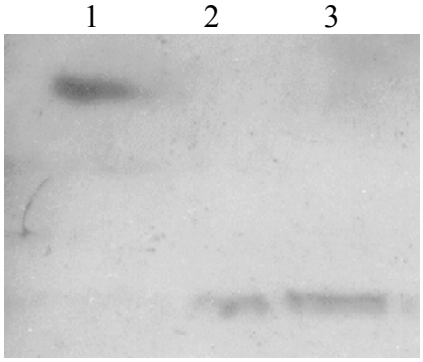

Figure 43. Immunodetection of pure GST-αB30.2 and GST-βB30.2 purified from inclusion bodies preparation (see Section 3.10.4.2 and Section 2.2.4.6.2). Lane 1 in both (a) and (b) contains SNTX. Similarly lane 2 in (a) and (b) contains proteins purified from inclusion bodies.

3.11 ORGAN BATH STUDIES WITH PURIFIED RECOMBINANT PROTEINS

Organ bath studies with cumulative concentrations of SNTX led to progressive vasorelaxation of 0.32μM PE-precontracted, 2mm thoracic rat aortic rings (Figure 21). Using equimolar of GST-αB30.2 (+GroEL), GST-βB30.2 or GST-αB30.2 (+GroEL) + GST-βB30.2 affinity purified according to Section 2.4.2.4 and Section 3.10.2 from the soluble fraction of IPTG induced *E. coli BL21* bacterial cells did not lead to the vasorelaxation of the PE-precontracted aortic rings. The use of equimolar of GST-αB30.2, GST-βB30.2 or GST-αB30.2 + GST-βB30.2 that was purified from N-lauroylsarcosine solubilized inclusion bodies also did not lead to the vasorelaxation of the PE-precontracted aortic rings. The use of control did not cause any vasorelaxation as well. These results suggest that the B30.2 domains in SNTX may not be responsible for the vasorelaxing effect of SNXT on precontracted rat aorta. The domains may possibly be involved in other biological effects of SNTX.

CHAPTER FOUR

DISCUSSION

DISCUSSION

Sto*nus*toxin (SNTX), a lethal protein factor isolated from the venom of the stonefish *Synanceja horrida* (Poh *et al*., 1991) causes a number of biological activities including species-specific haemolysis and platelet aggregation, edema-induction, hypotension, endothelium-dependent vasorelaxation, and inhibition of neuromuscular function in the mouse hemidiaphragm and chick biventer cervicis muscle (Low *et al*., 1993; Khoo *et al*., 1995; Chen *et al*., 1997; Sung *et al*., 2002). Lethality arising from SNTX is due to the marked hypotension that results from the potent vasorelaxation it causes (Low *et al*., 1993).

The focus of this thesis is to find out the potential involvement of hydrogen sulfide (H_2S) acting in synergy with nitric oxide (NO) in SNTX-induced vasorelaxation of endothelium-intact, precontracted rat thoracic aortic rings. H_2S is a novel endogenous smooth muscle relaxant discovered by Hosoki *et al*., 1997. As SNTX causes vasorelaxation, H_2S could possibly be a gaseous mediator of SNTX's vasorelaxing effect. In addition, H_2S may also possibly work with NO in causing vasorelaxation. Low *et al*., 1993 through the use of inhibitors in organ bath studies found that NO is a component of SNTX-induced vasorelaxation of endothelium-intact, precontracted rat aorta.

The other aim of this thesis is to find out whether if the B30.2 domains present in each of the SNTX subunit possess any vasorelaxing effects. The B30.2 domain is present in a rapidly growing family of proteins with diverse functions and cellular locations (refer to

Section 1.2.6.4). Currently not much is known about the function and structure of this domain. An attempt was made to express the SNTX B30.2 domains as a fusion with Glutathione S-Transferase (GST) in *E. coli* for subsequent purification and functional studies.

4.1 PURIFICATION OF SNTX FOR PHARMACOLOGICAL STUDIES

As a first step to the series of experiments to be done, SNTX was purified from *S. horrida* venom using Sephacryl S-200 High Resolution (HR) gel filtration chromatography and DEAE Bio-Gel A anion exchange chromatography, according to the method of Poh *et al.*, 1991 with some modifications. A decrease in total purification time resulted from a change to the column size and flow rate used for DEAE Bio-Gel A anion exchange chromatography. Using the method described in Section 2.4.1.3, anion-exchange chromatography took 1 day compared to 4 days when the method described for Poh *et al*., 1991 for this part of the purification was used.

The purification was able to yield a protein that is made up of two subunits (71 and 79kDa) linked via non-disulfide bonds (Section 3.1.3). SNTX has been shown to have a molecular weight of 148kDa and is made up of two subunits SNTX-α and SNTX-β with molecular weights of 71 and 79kDa respectively (Poh *et al.*, 1991). The subunits have been shown to be linked via non-disulfide linkages (Ghadessey *et al*., 1996). To confirm that the purified protein described in Section 3.1.3 was indeed SNTX, organ bath studies with endothelium-intact, 0.32μM L-phenylephrine-precontracted, 2mm rat thoracic aortic

rings was done to check whether if the protein possesses any vasorelaxation effects (see Section 3.3). Stonustoxin has been found to cause vasorelaxation of endothelium-intact, precontracted rat aorta or rat thoracic aortic rings by previous studies in our laboratory (Low *et al.*, 1993; Sung *et al.*, 2002).

4.2 PRELIMINARY ORGAN BATH STUDIES

Low *et al.*, 1993 demonstrated that SNTX (20-160ng/ml) causes vasorelaxation of endothelium-intact rat aortic strips (from the descending aortae) precontracted with 25nM noradrenaline (NA). Sung *et al*., 2002 also demonstrated that progressive addition of SNTX (5-640ng/ml) causes cumulative vasorelaxation of 4mm, endothelium-intact rat thoracic aortic rings precontracted with 7.5 X 10^{-5} M L-phenylephrine hydrochloride (PE). In my experiments, 2mm rat thoracic aortic rings were used and preliminary experiments were done to check their response to PE and acetylcholine chloride (Ach). 2mm aortic rings were used instead of aortic strips and 4mm aortic rings so that more experiments can be conducted with one strip of thoracic aortae, and comparisons can be made for different drug treatment on sections of one thoracic aortae.

4.2.1 Effect of L-phenylephrine Hydrochloride on 2mm Rat Thoracic Aortic Rings

PE like NA used by Low *et al*., 1993 causes vasoconstriction by binding to alpha 1-adrenoceptors on vascular smooth muscle (Rang *et al.*, 1994). This binding lead to the activation of the polyphosphoinositide cascade which leads to the sequestration of Ca^{2+}

from intracellular stores; as well as the influx of Ca^{2+} through nifedipine-sensitive Ca^{2+} channels to mediate the contraction of vascular smooth muscle (Nishimura *et al*., 1991). However, PE unlike NA is not a catechol derivative that is inactivated by Catechol-O-methyltransferase (COMT). As PE is not readily broken down, it produces a more easily monitored, stable contractile response of the aorta than NA. The vasorelaxant effect produced by SNTX on PE-precontracted aortic rings should also theoretically show less variation than NA-precontracted aortic rings and hence were used in my experiments. The results obtained from the cumulative addition of PE to 2mm rat thoracic aortic rings showed progressive vasoconstriction of the aortic rings, with a cumulative dose-vasoconstriction curve with an IC_{50} of 0.0390 μM and an EC_{85} of 0.32μM. 0.32μM PE was used to precontract 2mm rat thoracic aortic rings prior to any vasorelaxation experiments.

4.2.2 Effect of Acetylcholine Chloride on 2mm Rat Thoracic Aortic Rings

Before using an aortic ring for experimentation, it was tested with 0.32μM PE to check for the response of its vascular smooth muscle. In addition, it was also tested with Ach to check for the integrity and the responsiveness of its single layer of endothelial cells, to check whether if it has been denuded during the isolation and processing of the thoracic aortae. Ach acts on muscarinic M3 receptors on the endothelium to cause the release of nitric oxide, which diffuses to the vascular smooth muscle to activate guanylyl cyclase, cause an increase in cGMP and the subsequent vasorelaxation of the vascular smooth muscle (Furchgott & Zawadzki, 1980). To determine the concentration of Ach to use to

test for the integrity and responsiveness of the endothelial cells, 0.32μM PE-precontracted aortic rings were tested with cumulative amounts of Ach. The results showed that cumulative addition of Ach to 0.32μM PE-precontracted aortic rings led to progressive vasorelaxation with IC_{50} of 0.0824uM and EC_{85} of 2.56μM. 2.56μM Ach corresponding to EC_{85} was used to check for the integrity of the endothelial cells. 0.32μM PE-precontracted aortic rings that exhibit greater or equal to 70% vasorelaxation with 2.56μM Ach (refer to Figure 14) were termed as endothelium-intact aortic rings and were used for further experimentation, with SNTX or purified B30.2 recombinant proteins.

4.3 VASORELAXATION BY SNTX

To confirm that the purified protein described in Section 4.1 was indeed SNTX, it was added cumulatively to 2mm, endothelium-intact, 0.32μM PE-precontracted rat thoracic aortic rings in organ bath studies to check whether if it causes vasorelaxation (Section 3.3). The protein progressively causes vasorelaxation of the aortic rings. In addition, the vasorelaxation was inhibited by L-NAME which indicates a role of nitric oxide (NO) as a mediator of SNTX's effects. This is consistent with what has been determined by Low *et al*., 1993 and Julia *et al*., 2002, that NO is responsible for SNTX-induced vasorelaxation of precontracted aorta or aortic rings. Together with the PAGE studies, the organ bath studies confirmed that the purified protein in Section 3.1.3 was SNTX. The purified SNTX was used for further tests in inhibitor studies to check for other mediators of SNTX's vasorelaxing effect.

4.4 INVOLVEMENT OF HYDROGEN SULFIDE (H_2S) ON SNTX-INDUCED VASORELAXATION

Gases such as nitric oxide (NO) and carbon monoxide play important roles in both normal physiology and in disease. In recent years, efforts have been directed towards detecting the endogenous biological production of other naturally occurring gases such as hydrogen sulfide (H_2S), and elucidating their potential physiological roles.

In 1997, H_2S which is a well known toxic gas associated with many industrial fatalities (Burnett *et al.*, 1977; Guidotti, 1994; Synder *et al.*, 1995), was found to be an endogenously generated smooth muscle relaxant that may work in synergy with NO (Hosoki *et al.*, 1997). As the stonefish toxin of interest SNTX relaxes precontracted aorta (Low *et al*., 1993 and Sung *et al*., 2002), H_2S could possibly be a mediator of SNTX's vasorelaxing effect beside NO. NO is a well-known smooth muscle relaxant (Furchgott *et al*., 1980; Ignarro *et al*., 1984; Palmer *et al*., 1987 and 1988) and has been determined by Low *et al.*, 1993 and Sung *et al*., 2002 to play a part in SNTX-induced vasorelaxation of precontracted rat aorta. Hence, a series of RT-PCR and organ bath studies were conducted to investigate the role of H_2S in SNTX-induced vasorelaxation of precontracted rat thoracic aortic rings.

4.4.1 RT-PCR DETECTION OF CSE BUT NOT CBS IN RAT'S THORACIC AORTA

To date, CSE is the only H_2S-generating enzyme that has been identified in vascular tissues (Hosoki *et al.*, 1997; Zhao *et al*., 2001). Northern blot hybridization using a BamHI fragment of CSE cDNA (from Erickson *et al*., 1990) showed that CSE is present in rat's thoracic aorta and portal vein (Hosoki *et al*., 1997). With an Eco RI fragment of CBS (from Swaroop *et al*., 1992), CBS was not detected in the same vascular tissues (Hosoki *et al*., 1997). Subsequently, Zhao *et al*., 2001 cloned and sequenced the CSE isoform in rat mesenteric artery (Pubmed ID: AB052882) and other vascular tissues (Pubmed ID: AY032872).

Preliminarily to using CSE inhibitors for organ bath studies to see their effect on SNTX-induced vasorelaxation of PE-precontracted thoracic aortic rings, reverse-transcription polymerase chain reaction i.e. RT-PCR was conducted and the results showed that CSE but not CBS was detected in the thoracic aorta of Sprague Dawley rats.

4.4.2 INHIBITION OF SNTX-INDUCED VASORELAXATION BY CSE-INHIBITORS

Cystathionine γ-lyase (CSE) mRNA expression and H_2S production have been detected in the thoracic aorta (Hosoki *et al*, 1997). To determine if H_2S, a novel endogenous gasotransmitter is involved in vasorelaxation by Stonustoxin, D, L-proparglyglycine (PAG) and β-cyano-L-alanine (BCA) were used in organ bath studies to see if

vasorelaxation of 0.32μM PE-precontracted rat aortic rings by Stonustoxin is inhibited. PAG is an irreversible inhibitor of CSE ($IC_{50} = 10^{-4}$M, Stipanuk *et al.*, 1982; Uren *et al*., 1978) while BCA, a structural analogue of PAG, is a competitive inhibitor of CSE ($IC_{50} = 10^{-5}$M, Uren *et al*., 1978; Pfeffer, 1967).

The results obtained indicate that H_2S could be a gaseous mediator of SNTX's vasorelaxing effect. Preincubation of 2mm, endothelium-intact, 0.32μM PE-precontracted thoracic aortic rings with 1mM PAG or 1mM BCA for 1h prior to SNTX vasorelaxation of PE-precontracted aortic tissues resulted in an inhibition of the vasorelaxant effect of SNTX, with an increase in the IC_{50} of SNTX and a decrease in maximum vasorelaxation induced by SNTX (Figure 24).

4.5 SYNERGISTIC EFFECT OF HYDROGEN SULFIDE (H_2S) AND NITRIC OXIDE (NO) ON VASORELAXATION BY SNTX

Since H_2S is possibly a mediator of SNTX's vasorelaxing effect, we would like to see whether does it work together with NO to bring about vasorelaxation. Previous experiments in our laboratory has showed that NO is responsible for SNTX-induced vasorelaxation of rat aorta or aortic rings (Low *et al*., 1997; Sung *et al*., 2002). In addition, Hosoki *et al*., 1997 showed that H_2S acts in synergy to bring about smooth muscle (such as the thoracic aorta) vasorelaxation. A combination of CSE-inhibitor and nitric oxide synthase inhibitor was used in organ bath studies and the results showed that preincubation of the aortic rings with L-NAME in conjuction with PAG or BCA led to an

inhibition of SNTX-induced vasorelaxation (Section 3.6). The inhibitory effect is much greater than when each inhibitor is used individually and hence suggests that H_2S and NO work together to bring about SNTX-mediated vasorelaxation of precontracted aortic rings.

4.6 EFFECT OF L-CYSTEINE ON THORACIC AORTIC RINGS

Teague *et al.*, 2001 showed that 1mM L-Cysteine was able to cause a slowly developing decline in the size of BCA-augmented twitch response of guinea pig ileum. Cheng *et al*., 2004 also showed that 1mM L-cysteine increased endogenous H_2S production by 6-fold in rat mesenteric artery tissues and decreased contractility of mesenteric artery beds. As a result, 1mM L-cysteine was used to see whether the inhibition by BCA on SNTX-induced vasorelaxation of 2mm, endothelium-intact, 0.32μM PE-precontracted thoracic aortic rings was reversed. However, when 1mM L-Cysteine was added to endothelium-intact, resting thoracic aortic rings preincubated for 30mins with BCA or control saline, a transient increase in tone of the thoracic aortic rings was observed in all cases (Figure 26). The transient increase in tone of the thoracic aortic rings caused by L-cysteine is unexpected and cannot be explained by pH changes as Krebs solution is an effective buffer. Currently, this observation by L-cysteine has not been reported in the literature. Theoretically speaking, L-cysteine is a substrate for H_2S biosynthesis and since H_2S causes vasorelaxation, this phenomenon should not be observed. Further work with regards to the effect of L-cysteine and cystine on vascular tone could possibly be done.

4.7 FUNCTIONAL DOMAINS INVOLVED IN SNTX-INDUCED VASORELAXATION

4.7.1 THE B30.2 DOMAIN OF SNTX-α AND SNTX-β

(Bacterial clones confirmation, Bioinformatics Analysis and Purification)

The cDNA of SNTX-α and SNTX-β, the two subunits that make up SNTX have been isolated, characterized and cloned from a *Synanceja horrida* venom gland cDNA library (Ghadessey *et al*., 1996). SNTX shows no significant homology to other proteins except that it possess a small stretch of amino acids (in each of its subunit) that make up a B30.2 domain that is present in a rapidly growing family of proteins with diverse functions and cellular locations (Henry *et al.*, 1998). Currently, there is little information regarding the function of the B30.2 domain, except that it was shown that the B30.2 domain in mouse butyrophilin is able to interact with xanthine oxidase of mammary epithelial cells and milk fat globule membrane (Ishii *et al*., 1995). The structure of a protein with this domain has also not been solved. Hence, in this project, we hope to produce the B30.2 domain in SNTX for functional and crystallographic studies. In particular, we would like to see whether the domains are responsible for SNTX-induced vasorelaxation.

4.7.1.1 BACTERIAL CLONES CONFIRMATION

The B30.2 domain in each of the α- and β- subunits of SNTX have been amplified by PCR and cloned into various bacterial expression systems (Sung, 2001; Chapter 3). The

use of bacterial cells offers certain advantages such as simplicity, short generation times, and large yields of products with low costs. More importantly, functional SNTX-subunits and domains could possibly be produced in prokaryotic expression systems because the venom-secreting cells of *S. horrida* that secretes SNTX were found to be different from other venom-secreting cells in scorpions, spiders and snakes in that they do not possess the features of a typical eukaryotic protein secreting cell (Gopalakrishnakone and Gwee, 1993). The venom-secreting cells do not possess golgi apparatus nor rough endoplasmic reticulum. In addition, Ghadessey *et al*. (1996) also found that SNTX lack typical leader sequences and post-translational modifications that are characteristics of eukaryotic secretary proteins associated with the endoplasmic reticulum-golgi apparatus. These findings suggest that SNTX can be cloned into prokaryotes that do not possess the membranous organelles required for post-transcriptional and translational modifications.

In my experiments, I used the bacterial clones *E. coli BL21*-pGEX-5X-1-αB30.2 and *E. coli BL21*-pGEX-5X-1-βB30.2 for the purification of GST-αB30.2 and GST-βB30.2 proteins respectively. *E. coli BL21*-pGEX-5X-1 was used for the purification of control GST. Before purifying recombinant GST-αB30.2 and GST-βB30.2 fusion proteins for functional studies, PCR amplification and DNA sequencing were done to confirm that the B30.2 domains of SNTX-α and SNTX-β have been cloned-in-frame into *E. coli BL21*-pGEX-5X-1-αB30.2 and *E. coli BL21*-pGEX-5X-1-βB30.2 respectively and that no mutations of the clones had occurred. PCR amplification of the B30.2 domains in the clones produced PCR products of the appropriate size. DNA sequencing of the amplified PCR products showed that the B30.2 domains had been cloned in frame, at the correct

orientation. No mutation of *E. coli BL21*-pGEX-5X-1-αB30.2 had occurred. However, *E. coli BL21*-pGEX-5X-1-βB30.2 showed 4 point mutations. 3 are conserved mutations where the amino acid encoded by the codon is not changed. The other mutation CAT (His) was replaced by TAT (Tyr). Tyr is hydrophobic whereas His is basic. However, the clone was still used for purification of GST-βB30.2.

4.7.1.2 AFFINITY PURIFICATION OF SOLUBLE GST, GST-αB30.2 OR GST-βB30.2

Sung (2001) found that GST-αB30.2 and GST-βB30.2 were expressed both in the soluble fraction and as insoluble protein aggregates known as inclusion bodies within the cytoplasm of *E. coli BL21*-pGEX-5X-1-αB30.2 and *E. coli BL21*-pGEX-5X-1-βB30.2 respectively during bacterial induction with IPTG. Affinity purification of GST-αB30.2 and GST-βB30.2 from the soluble fraction of IPTG induced bacterial cells using a 5ml GSTrapFF column resulted in the purification of the fusion proteins together with a bacterial chaperonin GroEL. This is consistent with the results obtained by Sung JML. Affinity purification of GST using the same method as GST-αB30.2 and GST-βB30.2 resulted in large amounts of pure GST, i.e. 27mg/*l* bacterial culture in comparison with the low quantities of GST-αB30.2 (+ GroEL) and GST-βB30.2 (+ GroEL), i.e. 0.254 and 0.257mg/*l* bacterial culture respectively that was purified.

4.7.1.3 ATTEMPTED REMOVAL OF GRO-EL FROM SOLUBLE GST-αB30.2 AND GST-βB30.2

GroEL is a tetradecamer of identical 57 kDa subunits, arranged in two heptameric rings stacked back-to-back with a central cavity in each ring (Fenton & Horwich, 2003). Each subunit comprises three domains: equatorial which binds ADP or ATP and provides the inter-ring contacts that hold the rings together; apical which contains the hydrophobic surface at the entrance to the cavity that binds non-native polypeptides and interacts with the co-chaperonin, GroES; and intermediate, which links the other domains together and has flexible hinges at each end that permit the large-scale domain movements that occur during a folding cycle in which non-native polypeptides are aided to fold correctly into their correct conformations. GroES, a co-chaperonin, is a single-ring heptamer of identical 10 kDa subunits that binds to GroEL in the presence of ADP or ATP, capping one cavity to form an asymmetric complex. GroES is dynamic during the reaction cycle, binding to and releasing from one GroEL ring and then the other.

Since GroEL has been postulated to function together with GroES in the presence of ATP to aid in the proper folding of proteins into their native, functional conformation and their subsequent release from the GroEL-Gro-ES machinery (Fenton & Horwich, 2003 and references therein) and successful removal of GroEL from GST fusion proteins using an ATP wash buffer during purification has been reported (Thain *et al*., 1996), an ATP washing step was included into the purification of soluble GST-αB30.2 and GST-βB30.2. The use of the ATP wash buffer resulted in the successful removal of

contaminating GroEL from GST-βB30.2 but not GST-αB30.2. As a further attempt to purify pure GST-αB30.2 for functional studies, GroES was added to the ATP wash buffer and the buffer was applied to the GSTrapFF column in which GST-αB30.2 was bound. This did not help in removing GroEL form GST-αB30.2 which possibly indicates a different mechanism (i.e. kinetics and strength) of interaction between the GroEL-GroES machinery and GST-αB30.2. As GST-αB30.2 could still be purified using a GSTrapFF column, this suggests that the GST part of GST-αB30.2 is possibly not enclosed within the chaperonin molecule and can interact with glutathione in the GSTrapFF column. Interaction of GroEL with GST-αB30.2 is thus possibly at the B30.2 domain. The purification results obtained is generally similar to that obtained by Sung, 2001.

4.7.1.4 PURIFICATION OF GST-αB30.2 AND GST-βB30.2 FROM INCLUSION BODIES

High level protein biosynthesis in prokaryotes may lead to the accumulation of rapidly synthesized heterologous proteins as light-refractile aggregates known as inclusion bodies. The extent of intracellular protein aggregation depends on the protein itself, the *E. Coli* strain, the rate of protein synthesis and the growth conditions. If the protein of interest could be refolded adequately so that biological activity can be obtained, the formation of inclusion bodies is desirable because proteolysis decreases, and purification can be facilitated. When the protein cannot be refolded from inclusion bodies, it must be produced in soluble form, which may not be so simple to achieve in *E. coli*.

Sung (2001) reported that GST-αB30.2 and GST-βB30.2 were expressed as inclusion bodies, i.e. insoluble protein aggregates in the cytoplasm of *E. coli BL21*-pGEX-5X-1-αB30.2 and *E. coli BL21*-pGEX-5X-1-βB30.2 despite using a low bacterial growth temperature of 30°C and a low IPTG concentration of 0.1mM. Therefore, an attempt was made to purify more GST-αB30.2 and GST-βB30.2 proteins for pharmacological experiments from the inclusion bodies, in particular to verify whether they have any vasorelaxing effect on precontracted aorta. In addition, if more GST-αB30.2 and GST-βB30.2 fusion proteins are purified, they can be used to screen for other biological activities that SNTX possesses.

Solubilization of inclusion bodies with N-lauroylsarcosine or urea and their subsequent purification was done. Large amounts of pure GST-αB30.2 and GST-βB30.2 without the GroEL contaminant was obtained from the inclusion bodies as compared to the low amounts of GST-αB30.2 (+ GroEL) and GST-βB30.2 (+ GroEL) purified from the soluble fraction. Purification of GST-αB30.2 and GST-βB30.2 (for functional and structural studies) from inclusion bodies rather than from the soluble fraction could therefore be a better alternative as large amounts of pure recombinant fusion proteins could be obtained. However, the protein has to be tested to be functionally active as they could be denatured by the detergents and may not be properly refolded into their functional conformation. This aside, bioinformatics analysis in Section 3.9 to predict the properties of the recombinant proteins were done and may be incorporated in the purification of the recombinant fusion proteins.

4.7.1.5 IMMUNOLOGICAL DETECTION OF GST-αB30.2 AND GST-βB30.2 BY POLYCLONAL ANTI-SNTX ANTIBODIES

Soluble GST-αB30.2 (+ Gro EL) and GST-βB30.2 purified from the cytoplasm of IPTG induced bacterial cells *E. coli BL21*-pGEX-5X-1-αB30.2 and *E. coli BL21*-pGEX-5X-1-βB30.2 respectively by affinity chromatography was detected by polyclonal anti-SNTX antibodies obtained from rabbits by the subcutaneous injection of native SNTX (120μg) emulsified in complete Freund's adjuvant. Pure GST-αB30.2 and GST-βB30.2 from urea-solubilized inclusion bodies of *E. coli BL21*-pGEX-5X-1-αB30.2 and *E. coli BL21*-pGEX-5X-1-βB30.2 were also similarly detected by the polyclonal anti-SNTX antibodies. Previously, SNTX subunits had also been expressed in *E. coli* as cleavable maltose-binding fusion proteins that cross-react with antibodies raised against the native toxin (Ghadessey *et al*., 1996). The B30.2 domains can possibly be used as immunogen to produce antibodies to counteract the particular biological effect(s) that it produces.

4.7.1.6 ORGAN BATH STUDIES

Organ bath studies with cumulative concentrations of SNTX led to progressive vasorelaxation of 2mm, endothelium-intact, 0.32μM PE-precontracted rat thoracic aortic rings. Equimolar of GST-αB30.2 (+GroEL), GST-βB30.2 or GST-αB30.2 (+GroEL) + GST-βB30.2 affinity purified according to Section 2.4.2.4 from the soluble fraction of IPTG induced *E. coli BL21* bacterial clones did not lead to the vasorelaxation of the precontracted aortic rings. Similarly, control GST purified under the same conditions also

did not possess any vasorelaxing effect. This could mean that the B30.2 domains in SNTX do not possess vasorelaxing effects. However, this may not be the case since successful purification of the B30.2 domains without the GST domain and GroEL have not been done. Cleavage of the GST domain from the B30.2 domain and subsequent B30.2 domain purification is not possible and detectable because of the low yield of starting fusion proteins purified under non-denaturing conditions.

The use of equimolar of GST-αB30.2, GST-βB30.2 or GST-αB30.2 + GST-βB30.2 that was purified from N-lauroylsarcosine solubilized inclusion bodies also did not lead to vasorelaxation of the PE-precontracted thoracic aortic rings. Control GST was also unable to elicit any vasorelaxing effects. This indicates that the B30.2 domains of SNTX-α and SNTX-β are possibly not involved in SNTX-induced vasorelaxation of precontracted aortic rings. However, since the fusion proteins are purified in the presence of detergents, they may have been denatured and not refolded into their functionally active conformation.

In conclusion, if the SNTX B30.2 domains are not involved in the vasorelaxing properties of SNTX, it may possibly be involved in other biological effects of SNTX. Presently, SNTX has been shown to cause species-specific haemolysis and platelet aggregation, edema-induction, hypotension, endothelium-dependent vasorelaxation, and inhibition of neuromuscular function in the mouse hemidiaphragm and chick biventer cervicis muscle (Low *et al*., 1993; Khoo *et al*., 1995; Chen *et al*., 1997; Sung *et al*., 2002). However, the use of more suitable protein expression systems may need to be

considered to obtain better protein yield. The use of eukaryotic expression systems may also be considered because even though it was reported that the venom-secreting cells of *S. horrida* do not have the typical features of a eukaryotic protein-secreting cell such as Golgi apparatus and rough endoplasmic reticulum (Gopalakrishnakone and Gwee, 1993), they do possess cisternae and secretory vacuoles. Currently, not many studies have been done to elucidate the halocrine mechanism of protein secretion exhibited by cells such as the venom-secreting cells of *S. horrida*.

CHAPTER FIVE

CONCLUSION

CONCLUSION

Stonustoxin (SNTX), a 148kDa, dimeric protein from the stonefish *Synanceja horrida* was successfully purified according to the method of Poh *et al*. (1991) with some minor changes to the anion-exchange chromatography part of the purification process, leading to a decrease in the purification time. SNTX (10-640ng/ml) lead to vasorelaxation of 2mm, endothelium-intact, 0.32μM L-phenylephrine-precontracted rat thoracic aortic rings. The use of inhibitors in organ bath studies showed that hydrogen sulfide (H_2S) is a gaseous mediator of SNTX's effect and that it work together with nitric oxide (NO) to bring about vasorelaxation. In addition, an unexpected transient increase in tone of resting thoracic aortic rings was observed with 1mM L-cysteine.

SNTX possesses a B30.2 domain in each of its subunit SNTX-α and SNTX-β. Expression of GST-αB30.2 and GST-βB30.2 fusion proteins using the bacterial clones *E. coli-BL21*-pGEX-5X-1-αB30.2 or *E. coli-BL21*-pGEX-5X-1-βB30.2 at a low culturing temperature of 30°C and a low IPTG concentration of 0.1mM was unable to prevent the aggregation of the fusion proteins as inclusion bodies. Low yields of GST-αB30.2 and GST-βB30.2 was copurified with a bacterial chaperonin GroEL from fusion proteins expressed and distributed in the soluble fraction. The inclusion of an ATP wash buffer into the purification process as an attempt to facilitate the refolding and subsequent release of the fusion proteins from the GroEL-GroES complex was effective only for GST-βB30.2 but not GST-αB30.2. With the

use of an ATP wash buffer together with GroES, GroEl was still not removed from GST-αB30.2. The fusion proteins were used in organ bath studies on precontracted aortic rings. Equimolar SNTX concentrations of the fusion proteins and control GST was unable to elicit vasorelaxation indicating that the B30.2 domains in SNTX may not be responsible for SNTX's vasorelaxing effects. However, this may not be very conclusive. For the case of GST-αB30.2, it is not removed from GroEL. Since GroEL has been found to be a bulky tetradecamer (Fenton & Horwich, 2003; refer to Section 4.7.1.3), the B30.2 domain of GST-αB30.2 may be stearically hindered and unable to produce any biological effects. For the case of GST-βB30.2, it possesses a non-conserved point mutation where CAT (His) was replaced by TAT (Tyr). Tyr is hydrophobic whereas His is basic. The point mutation may have affected any vasorelaxing function that the βB30.2 possesses. Otherwise, the GST portion may have affected its functional activity. The low yield of fusion proteins obtained under native, non-denaturing conditions was unable to allow the enzymatic cleavage of the βB30.2 domain from the GST portion and its subsequent purification and detection. Since GST-αB30.2 and GST-βB30.2 were expressed in majority as inclusion bodies, an attempt to purifiy the fusion proteins after solubilization with N-lauroylsarcosine was made. A high yield of pure GST-αB30.2 and GST-βB30.2 was obtained. However, equimolar SNTX concentrations of the fusion proteins were unable to elicit any vasorelaxing effects. A combination of equimolar SNTX concentrations of GST-αB30.2 + GST-βB30.2 was also unable to elicit any vasorelaxing effect similarly to the GST control. This implies that the B30.2 domains in SNTX may not be responsible for its vasorelaxing effect. As SNTX is a relatively large molecule of

148kDa, the active moiety leading to SNTX-induced vasorelaxation of precontracted aorta may reside at another site instead of the B30.2 domain. Otherwise, if the B30.2 domain is the functionally active moiety, it may need to be expressed in more suitable expression systems such as eukaryotic expression systems before it can be conformationally correct to elicit its biological activity. The change of protein expression systems to obtain higher yields of fusion proteins to study the effect of the B30.2 domains on other biological effects that SNTX possesses may also be interesting.

CHAPTER SIX

FUTURE WORK

FUTURE WORK

Hydrogen sulfide (H_2S) was found to work in synergy with nitric oxide (NO) to mediate SNTX-induced vasorelaxation of rat thoracic aortic rings. This conjecture was based on the use of Cystathionine-γ-lyase (CSE) inhibitors (D, L-proparglyglycine and β-cyano-L-alanine) in organ bath studies. In future, the measurement of H_2S and NO production in response to SNTX could possibly be done as more sensitive assays are developed. This will be able to give direct evidence that the gases are produced in response to SNTX. In addition, the use of more potent and selective CSE inhibitors would also confirm the biologic significance of H_2S on vasorelaxation of precontracted aorta. The use of other blood vessels such as mesenteric artery beds (MAB) that exhibits 5-fold higher sensitivity to H_2S as compared to the aorta (Cheng *et al*., 2004) can also be done to confirm SNTX's vasorelaxing effects. As a representative peripheral resistance blood pressure, MAB makes more contribution in determining systemic blood pressure than aorta, a conduit artery. Therefore, the MAB may be a better choice for the study of the marked hypotension that SNTX causes.

Other cellular components and mediators of SNTX's vasorelaxing effect may also be studied. H_2S has been found to relax blood vessels by opening K^+_{ATP} channels (Zhao *et al*., 2001; Cheng *et al*., 2004). Therefore, since H_2S is involved in SNTX-induced vasorelaxation, K^+_{ATP} channels may also be a mediator of SNTX's effect. The effect of L-cysteine and low molecular weight S-nitrosothiol intermediates on SNTX's vasorelaxing effect can also be looked into. In addition, besides H_2S, the involvement of

other gases such as carbon monoxide as mediators of SNTX's effect and their interaction with H_2S and NO can also be investigated. Sulfur dioxide (SO_2) for example, has been found to be a vasodepressor in the rat (Meng *et al*., 2003).

Besides its effect on the vascular system, the effect of toxins such as SNTX on other smooth muscles of the gastrointestinal and respiratory systems etc would also be interesting as H_2S has been shown to reduce spontaneous contractility of the rabbit ileum and inhibit electrically evoked contractions of the guinea-pig ileum and rat vas deferens (Teague *et al*., 2002). In addition, since the venom of *S. horrida* has been reported to cause inhibition of the uptake of choline and aminobutyric acid into rat brain synaptosomes and a concentration-dependent release of acetylcholine from rat brain synaptosomes, it may be worthwhile to study whether SNTX is responsible for this interference of the synthesis and release of neurotransmitters from their storage sites, and whether H_2S and NO are involved as well. H_2S has been found to be an endogenous neuromodulator in the brain (Abe & Kimuara, 1996).

REFERENCES

Abe K & Kimura H. The possible role of hydrogen sulfide as an endogenous neuromodulator. J Neurosci (1996) 16(3): 1066-1071.

Akagi R. Purification and characterization of cysteine aminotransferase from rat liver cytosol. Acta Med Okayama (1982) 36: 187–197.

Armstrong KM. Interaction of tetraethylammonium ion derivatives with the potassium channels of giant axons. J Gen Physiol (1971) 58: 413-437.

Arnon SS. Human tetanus and human botulism. In: Rood JI, McClane BA, Songer JG, Titball RW, editors. The clostridia: molecular biology and pathogenesis. San Diego: Academic Press; 1997. p. 95-115.

Averbuch-Heller L & Leigh RJ. Medical treatments for abnormal eye movements: pharmacological, optical and immunological strategies. Aust N Z J Ophthalmol (1997) 25: 7-13.

Banghart LR, Chamberlain CW, Velardde J, Koroko IV, Ogg SL, Jack LJW, Vakharia VN & Mather IH. Butyrophilin is expressed in mammary epithelial cells from a single-sized messenger RNA as a type I membrane glycoprotein. J Biol Chem (1998) 273: 4171-4179.

Bao L, Vlcek C, Paces V & Kraus JP. Identification and tissue distribution of human cystathionine beta-synthase mRNA isoforms. Arch Biochem Biophys (1998) 350, 95–103.

Bartholomew TC, Powell GM, Dodgson KS & Curtis CG. Oxidation of sodium sulphide by rat liver, lungs and kidney. Biochem Pharmacol (1980) 29: 2431–2433.

Beauchamp RO Jr, Bus JS, Popp JA, Boreiko CJ & Andjelkovitch DA. A critical review of the literature on hydrogen sulfide toxicity. CRC Crit Rev Toxicol (1984) 13: 25–97.

Bellini M, Lacroix J-C, Gall GG. A putative zinc-binding protein on lampbrush chromosome loops. EMBO J (1993) 12: 107-114.

Bokoch GM, Katada T, Northup JK, Hewlett EL & Gilman AG. Identification of the predominant substrate for ADP-ribosylation by islet activating protein. J Biol Chem (1983) 258: 2072-2075.

Braunwaldy E. Effects of Digitalis on the Normal and Failing Heart. Journal of American College of Cardiology (1985) 5(suppl): 51A-59A.

Burnett WW, King EG, Grace M & Hall WF. Hydrogen sulfide poisoning: review of 5 years' experience. Can Med Assoc J (1977) 117(11): 1277-80.

Carter SR & Seiff SR. Cosmetic botulinum toxin injections. Int Ophthalmol Clin (1997) 37: 69-79.

Chen D, Kini RM, Yuen R, Khoo HE. Haemolytic activity of stonustoxin from stonefish (*Synanceja horrida*) venom: pore formation and the role of cationic amino acid residues. Biochem J (1997) 325: 685-691.

Chen P, Poddar R., Tipa EV, Dibello PM, Moravec CD, Robinson K, Green R, Kruger WD, Garrow TA & Jacobsen DW. Homocysteine metabolism in cardiovascular cells and tissues: implications for hyperhomocysteinemia and cardiovascular disease. Adv Enzyme Regul (1999) 39, 93–109.

Cheng Y, Ndisang JF, Tang G, Cao K & Wang R. Hydrogen sulfide induced relaxation of resistence mesenteric artery beds of rats. Am J Physiol Heart Circ Physiol (2004).

Cohen HJ, Betcher-Lange S, Kessler DL & Rajagopalan KV. Hepatic sulfite oxidase.

Congruency in mitochondria of prosthetic groups and activity. J Biol Chem (1972) 247: 7759–7766.

Colosante C, Meunier FA, Kreger AS, Molgo J. Selective depletion of clear synaptic vesicles and enhanced quantal transmitter release at frog motor nerve endings by trachynilysin, a protein toxin isolated from stonefish (*Synanceia trachynis*) venom. Eur J Neurosci (1996) 8: 2149-2156.

Coloso RM & Stipanuk MH. Metabolism of cyst(e)ine in rat enterocytes. J Nutr (1989) 119: 1914–1924.

De La Rosa J, Drake MR, Stipanuk MH. Metabolism of cysteine and cysteine sulfinate in rat and cat hepatocytes. J Nutr (1987) 117: 549–558.

Duhig JV & Jones G. Haemotoxin of the stonefish *Synanceja horrida*. Aust J Exp Biol (1928) 5: 173-179.

El-Hodiri HM, Che S, Nelman-Gonzalez M, Kuang J & Etkin LD. Mitogen-activated protein kinase and cyclin B/Cdc2 phosphorylate Xenopus nuclear factor7 (xnf7) in extracts from mature oocytes. Implications for regulation of xnf7 subcellular localization. J Biol Chem (1997) 272: 20463-20470.

Endean R. A study of the distribution, habitat, behaviour, venom apparatus and venom of the stonefish. Aust J Marine and Freshwater Res (1961) 12(2): 177-190.

Frankel AE Oncology (Huntington - 1993), 7(5): 69-78; discussion 79-80, 83-6. Immunotoxin Therapy of Cancer.

Gallagher SR. Current Protocols in Molecular Biology (1999) 10.2.1. Electrophoretic separation of proteins.

Garnier P, Goudeyperriere F, Breton P, Dewulf C, Petek F, Perriere C. Enzymatic-

properties of the stonefish (*Synanceja verrucosa* Bloch and Schneider, 1801) venom and purification of a lethal, hypotensive and cytolytic factor. Toxicon (1995) 33: 143-155.

Garnier P, Grosclaude JM, GoudeyPerriere C. Presence of norepinephrine and other biogenic amines in stonefish venom. J Chrom B Biomed Appl (1996) 685: 364-369.

Garnier P, Sauviet MP, GoudeyPerriere F, Perriere C. Cardiotoxicity of verrucotoxin, a protein isolated from the venom of *Synanceia verrucosa*. Toxicon (1997) 35: 47-55.

Geng B, Chang L, Pan CS, Qi YF, Zhao J, Pang YZ, Du JB & Tang CS. Endogenous hydrogen sulfide regulation of myocardial injury by isoproterenol. Biochem & Biophysic Comms (2004) 318: 756-763.

Ghadessey FJ, Chen D & Kini RM. Stonustoxin is a novel lethal factor from stonefish (*Synanceja horrida*) venom. cDNA cloning and characterization. J Biol Chem (1996) 271: 25575-25581.

Ghadessey FJ, Jeyaseelan K, Chung MC & Khoo HE. A genomic region encoding stonefish (*Synanceja horrida*) stonustoxin beta-subunit contains an intron.Toxicon. 1994 Dec;32(12):1684-8. Toxicon (1994) 32: 1684-1688.

Goodwin LR, Francom D, Dieken FP, Taylor JD, Warenycia MW, Reiffenstein RJ & Dowling G. Determination of sulfide in brain tissue by gas dialysis/ion chromatography: postmortem studies and two case reports. J Analyt Toxicol (1989) 13: 105-109.

Gopalakrishnakone P & Gwee MCE. The structure of the venom gland of stonefish *Synanceja horrida*. Toxicon (1993) 31(8): 979-988.

Gopalakrishnakone P & Kochva E. Venom glands and some associated muscles in sea snakes. J Morph (USA) (1990) 205: 85-96.

Gopalakrishnakone P. Light and electron microscopic study of the venom apparatus of

the saw-scaled viper *Echis carinatus*. Snake (J Jpn Snake Inst) (1985a) 17, 10-14.

Gopalakrishnakone P. Structure of the venom gland of the Malayan banded coral snake (*Maticora intestinalis*). Snake (J Jpn Snake Inst) (1986)18: 19-26.

Gopalakrishnakone P. Structure of the venom apparatus of the scorpion *Heterometrus Longimanus.*Toxicon (1985b) 23: 570.

Gopalakrishnakone P. Sturcture of the venom glands of the three species of theraphosids. Toxicon (1987) 26: 22-23.

Griffith OW. Mammalian sulfur aminoacid metabolism: an overview. Method Enzymol (1987) 143: 366–376.

Gruetter CA, Gruetter DY, Lyon JE, Kadowitz PJ, Ignarro EF. Relationship between cyclic guanosine 3',5'-monophospahte formation and relaxation of coronary arterial smooth muscle by glyceryl trinitrate, nitroprusside, nitrite and nitric oxide: effects of methylene blue and methemoglobin. J. Pharmac. Exp. Ther. (1981) 219, 181-186.

Guidotti TL. Occupational exposure to hydrogen sulfide in the sour gas industry: some unresolved issues. Int Arch Occup Environ Health (1994) 66(3): 153-160.

Gwee MC, Gopalakrishnakone P, Yuen R, Khoo HE & Low KS. A review of stonefish venoms and toxins. Pharmaco Ther (1994) 64: 509-528.

Hainut K & Desmedt JE. Effect of dantrolene sodium on calcium movements in single muscle fibres. Nature (1974) 252: 728-730.

Halpern JL & Neale EA. Neurospecific binding, internalization and retrograde axonal transport. Curr Top Microbiol Immunol (1995) 195: 221-41.

Harnett MM. Analysis of G-proteins regulating signal transduction pathways. Methods Mol Biol (1994) 27: 199-211.

Henry J, Mather IH, McDermott MF, Pontarotti P. B30.2-like domain proteins: Update and new insights into a rapidly expanding family of proteins. Mol Biol Evol (1998) 15(12): 1696-1705.

Henry J, Ribouchon M-T & Pontarotti P. B30.2-like domain proteins: A growing family. Biochem & Biophysiol Res Comms (1997) 235: 162-162.

Hoffman BF & Bigger T Jr: Digitalis and allied cardiac glycosides. In: Gilman AG, Rall TW, Nies AS, Taylor P, eds. Goodman and Gilman's The Pharmacological Basis of Therapeutics. 8th ed. New York, NY: Pergamon Press; 1990:814-39.

Holmgren J, Lycke N & Czerkinsky C. Cholera toxin and cholera-B subunit as oral mucosal adjuvant and antigen vector systems. Vaccine (1993) 11: 1179-1184.

Hosoki R., Matsiki N & Kimura H. Biochem. The possible role of hydrogen sulfide as an endogenous smooth muscle relaxant in synergy with nitric oxide. Biophysic Res Commun (1997) 237: 527–531.

Huang J, Khan S & O'Brien PJ. The glutathione dependence of inorganic sulfate formation from L-or D-cysteine in isolated rat hepatocytes. Chem Biol Interact (1998) 110: 189–202.

Ignarro LJ, Byrns RE, Buga GM and Wood KS. Endothelium-derived relaxing factor from pulmonary artery and vein possess pharmacological and chemical properties identical to those of nitric oxide radical. Circ Res (1987) 61, 866-879.

Inoue S, Orimo A, Hosoi T. Genomic binding-site cloning reveals an estrogen-responsive gene that encodes a RING finger protein. Proc Natl Acad Sci USA (1993) 90: 11117-11121.

Ishii T, Aoki N, Noda A, Adachi T, Nakamura R & Matsutada T. Carboxy-terminal

cytoplasmic domain of mouse butyrophilin specifically associates with a 150-kDa protein of mammary epithelial cells and milk fat globule membrane. Biochim Biophys Acta (1995) 1245: 285-292.

Itoh K, Itoh Y & Frank MB. Protein heterogeneity in the human Ro/SSA ribonucleoproteins. The 52- and 60-kD Ro/SSA auntoantigens are encoded by separate genes. J Clin Invest (1991) 87: 177-186.

Kamoun P. Endogenous production of hydrogen sulfide in mammals. Amino acids (2004) 26: 243-254.

Katzung BG. Basic & Clinical Pharmacology (1998, 7th edition).

Kessler KR & Benecke R. Botulinum toxin: from poison to remedy. Neurotoxicology (1997) 18:761-70.

Khoo HE, Chen D & Yuen R. The role of cationic amino acid residues in the lethal activity of stonustoxin from stonefish (*Synanceja horrida*) venom. Biochem & Mol Biol Int (1998a) 44(3): 643-646.

Khoo HE, Chen D & Yuen R. Role of thiol groups in the biological activities of stonustoxin, a lethal factor from stonefish (*Synanceja horrida*) venom. Toxicon (1998b) 36(3): 469-476.

Khoo HE, Hon WM, Lee SH, Yuen R. Effects of stonustoxin (lethal factor from *Synanceja horrida* venom) on platelet aggregation. Toxicon (1995) Aug;33(8):1033-41.

Khoo HE, Yuen R, Poh CH & Tan CH. Biological activities of *Synanceja horrida* (stonefish) venom. Nat Toxins (1992) 1(1): 54-60.

Khoo HE. Bioactive proteins from stonefish venom. Clin Exp Pharmacol Physiol (2002) 29(9): 802-6.

Knight B. Ricin-a potent homicidal poison. Br Med J (1979) 278: 350-351.

Kreger AS, Molgo J, Comella JX, Hansson B & Thesleff S. Effects of stonefish (*Synanceja trachynis*) venom on murine and frog neuromuscular junction. Toxicon (1993) 31: 301-317.

Kreger AS. Detection of a cytolytic toxin in the venom of the stonefish (*Synanceja trachynis*). Toxicon (1991) 29: 733.

Liu H-L, Golder-Novoselsky E, Seto MH, Webster L, McClary J & Zajchowski DA. The novel estrogen-responsive B box protein (EBBP) gene is tamoxifen-regulated in cells expressing an estrogen receptor. Mol Endo(1998).

Low KSY, Gwee MCE, Yuen R, Gopalakrishnakone P & Khoo HE. Stonustoxin: Effects on Neuromuscular function in vitro and in vivo. Toxicon (1994) 32(5): 573-581.

Low KSY, Gwee MCE, Yuen R, Gopalakrishnakone P, Khoo HE. Stonustoxin: a highly potent endothelium-dependent vasorelaxant in the rat. Toxicon (1993) 31: 1471-1478.

Low KSY. Some Pharmacological Actions of Stonustoxin - Thesis (1995).

Martin W, Villani GM, Jothianandan D and Furchgott RF. Selective block of endothelium-dependent and glyceryl nitrate-induced relaxation by hemoglobin and by methylene blue in the rabbit aorta. J Pharmac Exp Ther (1985) 232, 708-716.

Mattei C, Pompa C, Thieffry M, Kreger AS, Molgo J. Trachynilysin, a toxin isolated from stonefish Cynanceia *trachynis venom*, forms pores in planar lipid bilayers. Cybium (2000) 24: 141-148.

McKay R. A guide to common venomous fishes. Toxic Plants and Animals - A guide for Australia (1987).

Meunier FA, Mattei C, Chameau P. Trachynilysin mediates SNARE-dependent release

of catecholamines from chromaffin cells via external and stored Ca2+. J Cell Sci (2000) 113: 1119-1125.

Miyagawa S, Okada N, Inagaki Y, Kitano Y, Ueki H, Sakamoto K & Steinberg ML. SSA/Ro antigen expression in simian virus 40-transformed human keratinocytes. J Invest Dermatol (1998) 90: 342-345.

Nagahara N, Ito T, Kitamura H, Nishino T. Tissue and subcellular distribution of mercaptopyruvate sulfurtransferase in the rat: confocal laser fluorescence and immunoelectron microscopic studies combined with biochemical analysis. Histochem Cell Biol (1998) 110: 243–250.

Nakane M, Klinghofer V, Kuk JE, Donnelly JL, Budzik GP, Pollock JS, Basha F, Carter GW. Novel potent and selective inhibitors of inducible nitric oxide synthase. Mol Pharmacol (1995) Apr; 47(4):831-4.

Neer EJ. Heterotrimeric G proteins: organizers of transmembrane signals. Cell (1995) 80: 249-57.

Ouanounou G, Mattei C, Meunier FA, Kreger AS, Molgo J. Trachynilysin, a protein neurotoxin isolated from stonefish (*Synanceja trachynis*) venom, on frog atrial muscle. Cybium (2000) 24: 149-156.

Phoon WO & Alfred ER. A study of stonefish (*Synanceja horrida*) stings in Singapore with a review of the venomous fishes of Malaysia. Sing Med J (1965) 6: 158-63.

Poh CH, Yuen R, Chung MC & Khoo HE. Purification and partial characterization of hyaluronidase from stonefish (*Synanceja horrida*) venom. Comp Biochem Physiol (1992) 101B(1/2): 159-163.

Poh CH, Yuen R, Khoo HE, Chung M, Gwee M & Gopalakrishnakone P. Purification

and partial characterization of stonustoxin from *Synanceja horrida* venom. Comp Biochem Physiol (1991) 99B(4): 793-798.

Rapoport RM and Murad F. Agonist-induced endothelium-dependent relaxation in rat thoracic aorta may be mediated through cGMP. Circ Res (1983) 52, 352-357.

Reddy BA, Kloc M, Etkin L. The cloning and characterization of a maternally expressed novel zinc finger nuclear phosphoprotein (xnf7) in Xenopus laevis. Dev Biol (1991) 148: 107-116.

Robertus JD. The structure and action of ricin, a cytotoxic N-glycosidase. Sem in Cell Biol (1991) 2: 23-30.

Saunders PR, Rothman S. Medrano VA & Chin HP. Cardiovascular actions of venom of the stonefish *Synanceja horrida.* Am J Physiol (1962) 203: 429-32.

Sauviat MP, Meunier FA, Kreger A, Molgo J. Effects of trachynilysin, a protein isolated from stonefish (*Synanceia trachynis*) venom, on frog atrial heart muscle. Toxicon (2000) 38: 945-959.

Savage JC & Gould DH. Determination of sulfide in brain tissue and rumen fluid by ion interaction, reversedphase high-performance liquid chromatography. J Chromatogr 526: 540–545.

Schiavo G & Montecucco C. The structure and mode of action of botulinum and tetanus toxins. In: Rood JI, McClane BA, Songer JG, Titball RW, editors. The clostridia: molecular biology and pathogenesis. San Diego: Academic Press; 1997. p. 295-322.

Seto MH, Liu HL, Zajchowski DA, Whitlow M. Protein fold analysis of the B30.2-like domain. PROTEINS: Structure, Function, and Genetics (1999) 35: 235-249.

Singh BR, Li B & Read D. Botulinum versus tetanus neurotoxins: why is botulinum

neurotoxin but not tetanus neurotoxin a food poison? Toxicon (1995) 33: 1541-1547.

Smith TW, Antman EM & Friedman PL: Digitalis glycosides: mechanisms and manifestations of toxicity. Part I. Prog Cardiovasc Dis 1984 Mar-Apr; 26(5): 413-58

Snider DP. The mucosal adjuvant activities of ADP-ribosylating bacterial enterotoxins. Crit Rev Immunol (1995)15: 317-48.

Snyder JW, Safir EF, Summerville GP & Middleberg RA. Occupational fatality and persistent neurological sequelae after mass exposure to hydrogen sulfide. Am J Emerg Med (1995) 13(2): 199-203.

Snyder JW, Safir EF, Summerville GP & Middleberg RA. Occupational fatality and persistent neurological sequelae after mass exposure to hydrogen sulfide. Am J Emerg Med (1995) 13(2): 199-203.

Sorbo B & Ohman S. Determination of thiosulphate in urine. Scand J Clin Lab Invest (1978) 38: 521–527.

Stipanuk MH & Beck PW. Characterization of the enzymatic capacity for cysteine desulphhydration in liver and kidney of the rat. Biochem J (1982) 206: 267-277.

Stipanuk MH. Metabolism of sulfur-containing aminoacids. Ann (1986) Rev Nutr 6: 179–209.

Stipanuk MH. Sulfur amino acid metabolism: Pathways for production and removal of homocysteine and cysteine. Annu Rev Nutr (2004) 24: 539-577.

Sugahara K, Yamada S, Sugiura M, Takeda K, Yuen R, Khoo HE & Poh CH. Identification of the reaction products of the purified hyaluronidase from stonefish (*Synanceja horrida*) venom. Biochem J (1992) 283: 99-104.

Sung JML, Low KSY & Khoo HE. Characterization of the mechanism underlying

stonustoxin-mediated relaxant response in the rat aorta in vitro. Biochemical Pharmacology (2002) 7149: 1-6.

Sung JML. Cloning, expression and structure-function relationship of stonustoxin (2001).

Swaroop M, Bradley K, Ohura T, Tahara T, Roper MD, Rosenberg LE & Kraus JP. Rat cystathionine-synthase. J Biol Chem (1992) 267: 11455–11461.

Taylor MR, Peterson JA, ceriani RL & Couto JR. Cloning and sequence analysis of human butyrophilin reveals a potential receptor function. Biochim Biophys Acta (1996) 1306: 1-4.

Teague B, Asiedu S & Moore PK. The smooth muscle relaxant effect of hydrogen sulphide in vitro: evidence for a physiological role to control intestinal contractility. British Journal of Pharmacology (2002) 137, 139-145.

Tissot C, Mechti N. Molecular cloning of a new interferon-induced factor that represses human immunodeficiency virus type I long terminal repeat expression. J Biol Chem (1995) 270: 14891-14898.

Ubuka T, Ohta J, Yao WB, Abe T, Teraoka T & Kurozumi Y. L-cysteine metabolism in a 3-mercaptopyruvate pathway and sulfate formation in rat liver mitochondria. Amino Acids (1992) 2: 143–155.

Ubuka T, Umemura S, Yuasa S, Kimuta M & Watanabe K. Purification and characterization of mitochondrial cysteine aminotransferase from rat liver. Physiol Chem Phys (1978) 10: 483–500.

Ubuka T, Yuasa S, Ohta J, Masuoka N, Yao K & KinutaM. Formation of sulfate from L-cysteine in rat liver mitochondria. Acta Med Okayama (1990) 44: 55–64.

US Environmental Protection Agency - Public health statement for H_2S, 1999.

Vitetta ES & Thorpe PE. Sem in Cell Biol (1991) 2: 47-58. Immunotoxins containing ricin or its A chain.

Wang R. Two's company, three's a crowd: can H_2S be the third endogenous gaseous transmitter? FASEB J (2002) 16, 1792–1798.

Warenycia MW, Goodwin LR, Benishin CG, Reiffenstein RJ, Francom DM, Taylor JD & Dieken FP. Acute hydrogen sulfide poisoning: demonstration of selective uptake of sulfide by the brainstem by measurement of brain sulfide levels. Biochem Pharmacol (1989) 38: 973-981.

Westley J. Rhodanese and the sulfane pool. Enzymatic basis of detoxication vol II, chapter 13. Academic Press, New York, pp 245–262 (1980).

Wheeler AH. Therapeutic uses of botulinum toxin. Am Fam Physician (1997) 55: 541-8.

Wiley RG & Oeltmann TN (1991) Ricin and Related Plant Toxins: Mechanisms of Action and Neurobiological Applications; In, Handbook of Natural Toxins, Vol.6, ed. R.F.Keeler and A.T.Tu, Marcel Dekker, Inc., New York.

Yamanashi T & Tuboi S. The mechanism of the L-cystine cleavage reaction catalyzed by rat liver gamma-cystathionase. J Biochem (1981) 89: 1913–1921.

Yan H, Du JB, Tang CS, Bin G, Jiang HF. Changes in arterial hydrogen sulfide (H_2S) content during septic shock and endotoxin shock in rats. J Infec (2003) 47: 155-160.

Yan H, Du JB, Tang CS. The possible role of hydrogen sulfide on the pathogenesis of spontaneous hypertension in rats. Biochem & Biophysic Comms (2003).

Yew WS & Khoo HE. The role of tryptophan residues in the hemolytic activity of stonustoxin a lethal factor from stonefish (*Synanceja horrida*) venom. Biochimie (2000) 82: 251-257.

Yew WS, Kolatkar PR, Kuhn Peter & Khoo HE. Crystallization and preliminary crystallographic study of Stonustoxin, a protein lethal factor isolated from the stonefish (*Synanceja horrida*) venom. J Struct Biol (1999) 128(2): 216-218.

Yuen R, Cai B & Khoo HE. Production and characterization of monoclonal antibodies against stonustoxin from *Synanceja horrida*. Toxicon (1995) 33(12): 1557-1564.

Zhang CY, Du JB, Bu DF, Yan H, Tang XY& Tang CS. The regulatory effect of hydrogen sulfide on hypoxic pulmonary hypertension in rats. Biochem & Biophysic Comms (2003) 302: 810-816.

Zhang QY, Du JB, Zhao WJ, Yan H, Tang CS & Zhang CY. Impact of hydrogen sulfide on carbon monoxide/heme oxygenase pathway in the pathogenesis of hypoxic pulmonary hypertension. Biochem & Biophysic Comms (2004) 317: 30-37.

Zhao G, Meier T, Hoskins J & Jaskunas SR. Penicillin-binding protein 2a of *Streptococcus pneumoniae*: Expression in *Escherichia coli* and purification and refolding of inclusion bodies into a soluble and enzymatically active enzyme. Protein Expression & Purification (1999) 16: 331-339.

Zhao W & Wang R. H_2S-induced vasorelaxation and underlying cellular and molecular mechanisms. Am J Physiol Heart Circ Physiol (2002) 283: H474-H480.

Zhao W, Zhang J, Lu Y & Wang R. The vasorelaxant effect of H_2S as a novel endogenous K_{ATP} channel opener. EMBO J (2001) 20: 6008-6016.

APPENDIX

SNTX-α and SNTX-β are two subunits in SNTX that have been isolated, characterized and cloned from a *Synanceja horrida* venom gland cDNA library (Ghadessey *et al*., 1996). The B30.2 domain of both SNTX-α and SNTX-β have been amplified by PCR using the appropriate primers in Table 18, and cloned into pGEX-5X-1 (Figure 44), producing pGEX-5X-1-αB30.2, pGEX-5X-1-βB30.2 respectively. The restriction enzymes used for the amplified B30.2 PCR products are *Bgl* II and *Sal* I while the pGEX-5x-1 vector is cleaved with *BamH* I and *Sal* I. The recombinant vectors were transformed into *E. coli* BL21 (DE3). The use of αB30.2F-pGEX-5X-1 and βB30.2F-pGEX-5X-1 primers with a thrombin cleavage site is an added attempt to cleave GST-αB30.2 and GST-βB30.2 fusion proteins more efficiently, as the Factor Xa cleavage site provided within the pGEX-5X-1 vector was unable to allow efficient cleavage of the fusion proteins.

Table 17. Primers used in the amplification of the B30.2 domain of SNTX-α and SNTX-β, to produce inserts which are then cloned into pGEX-5X-1. The additional thrombin cleavage site in αB30.2F-pGEX-5X-1 and βB30.2F-pGEX-5X-1 primers are underlined.

Primers	**Sequences**
αB30.2F-pGEX-5X-1	5'-GCG CAG ATC TCA TGT GAC CTC ACC TTT GA-3'
αB30.2F-pGEX-5X-1 (with incorporation of thrombin cleavage site)	5'-GCG CAG ATC TCA <u>CTG GTT CCG CGT GGA TCT</u> TGT GAC CTC ACC TTT GA-3'
αB30.2R-pGEX-5X-1	5'-GCG CGT CGA CAT CGT GGT TAC CGG CAG GCC-3'
βB30.2F-pGEX-5X-1	5'-GCG CAG ATC TCA TGT GAG CTC ACC CTG GA-3'
βB30.2F-pGEX-5X-1 (with incorporation of thrombin cleavage site)	5'-GCG CAG ATC TCA <u>CTG GTT CCG CGT GGA TCT</u> TGT GAG CTC ACC CTG GA-3'
βB30.2R-pGEX-5X-1	5'-GCG CGT CGA CAT CAT TGA CTT TCT GTT GTG-3'

Figure 44. Vector map of pGEX-5X-1.